AD-A181 401 INVESTIGATION OF THE ELECTRIC AND MAGNETIC PROPERTIES OF INTERCALATED GRAPHITES(U) BOSTON UNIV MA DEPT OF PHYSICS G O ZIMMERMAN 1987 AFOSR-TR-87-0410 1/2

UNCLASSIFIED AFOSR-82-0206 F/G 11/4 NL

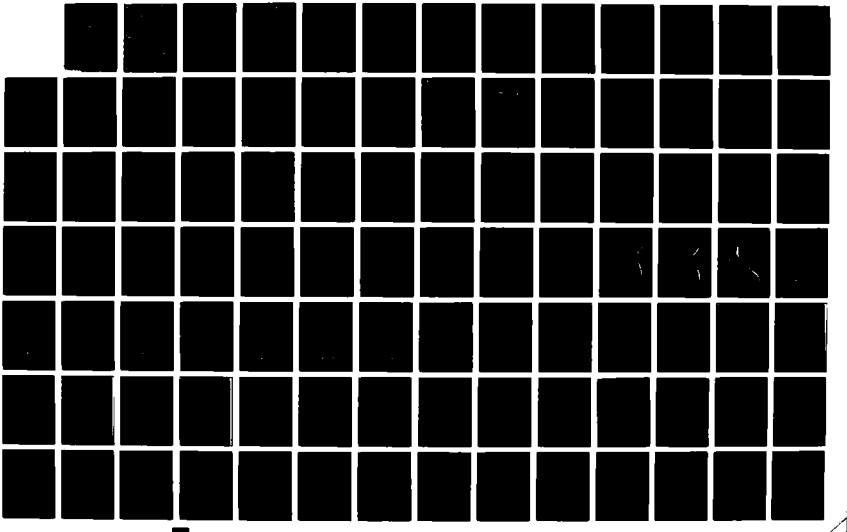

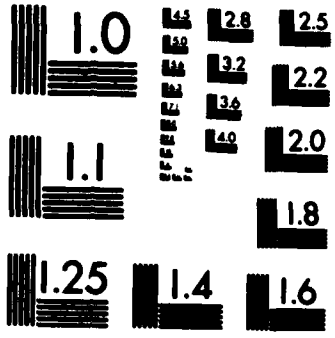

SECURITY CLASSIFICATION OF THIS PAGE

DTIC FILE COPY (2)

REPORT DOCUMENTATION PAGE

1a. REPORT SECURITY CLASSIFICATION: UNCLASSIFIED	1b. RESTRICTIVE MARKINGS
2a. SECURITY CLASSIFICATION AUTHORITY	3. DISTRIBUTION/AVAILABILITY OF REPORT: Distribution is unlimited
AD-A181 481	5. MONITORING ORGANIZATION REPORT NUMBER(S): AFOSR-TR- 87-0418
6a. NAME OF PERFORMING ORGANIZATION: Boston University; 6b. OFFICE SYMBOL (If applicable):	7a. NAME OF MONITORING ORGANIZATION: AFOSR
6c. ADDRESS (City, State and ZIP Code): Department of Physics, Boston MA 02215	7b. ADDRESS (City, State and ZIP Code): Bolling AFB Wash DC 20332
8a. NAME OF FUNDING/SPONSORING ORGANIZATION: same as 7a; 8b. OFFICE SYMBOL (If applicable): NE	9. PROCUREMENT INSTRUMENT IDENTIFICATION NUMBER: AFOSR 82 0286
8c. ADDRESS (City, State and ZIP Code): same as 7b	10. SOURCE OF FUNDING NOS.

PROGRAM ELEMENT NO.	PROJECT NO.	TASK NO.	WORK UNIT NO.
61102F	2306	C3	

11. TITLE (Include Security Classification): Investigation of the Electric and Magnetic Properties of Intercalated Graphites

12. PERSONAL AUTHOR(S): Zimmerman

13a. TYPE OF REPORT	13b. TIME COVERED	14. DATE OF REPORT (Yr., Mo., Day)	15. PAGE COUNT
Final	FROM 9/30/82 TO 9/29/86		

16. SUPPLEMENTARY NOTATION

17. COSATI CODES			18. SUBJECT TERMS (Continue on reverse if necessary and identify by block number)
FIELD	GROUP	SUB. GR.	

19. ABSTRACT (Continue on reverse if necessary and identify by block number)

SEE ABSTRACT ON BACK

DTIC ELECTE JUN 17 1987 S D

20. DISTRIBUTION/AVAILABILITY OF ABSTRACT: UNCLASSIFIED/UNLIMITED ☒ SAME AS RPT. ☐ DTIC USERS ☐	21. ABSTRACT SECURITY CLASSIFICATION: UUUUU
22a. NAME OF RESPONSIBLE INDIVIDUAL: Dr. Harold Weinstock	22b. TELEPHONE NUMBER (Include Area Code): 767-4933; 22c. OFFICE SYMBOL: NE

DD FORM 1473, 83 APR EDITION OF 1 JAN 73 IS OBSOLETE.

87 6 5 092

SECURITY CLASSIFICATION OF THIS PAGE

Progress:

NARR. --- PROG. - FROM U)
9/30/82 to 9/29/86

The picture which emerges from our investigations is that we are indeed observing the behavior of a two dimensional magnetic system. The low demensionality is brought about by the shielding of the intercalant layers by the intervening graphite layers. The shielding also depends on the charge transfer between the intercalant and the graphite. In graphite there is a band near K = 0 about half filled with electrons (10). The intercalation of an acceptor compound will draw off those electrons so that the electrical conduction is hole like. Thus low stages exhibit a positive Hall coefficient. The shielding of the intercalant layers is due to electromagnetic shielding analogous to the skin effect, where the skin depth is a function of the electrical conductivity, which in turn is a function of the number of charge carriers. Stages 1 to 5 almost empty the band of electrons and thus the graphite layers have maximum conductivity. Above stage 5, the quantity of acceptors is not large enough to absorb all the electrons which can be donated by the graphite, and the conductivity of the graphite layers decreases. Moreover, the conductivity, according to our Hall measurements, is due to both positive and negative carriers. This gives rise to decreased magnetic shielding of the intercalant layers, with a corresponding decrease in the peak height in the susceptibility at 1.7K. Thus, the transition at 1.7K can become a very sensitive probe of the internal magnetic field, the charge transfer, and the electrical conductivity of the graphite layers.

AFOSR-TR- 87-0418

FINAL REPORT

AIR FORCE OFFICE OF SCIENTIFIC RESEARCH

Grant number AFOSR-82-0286

entitled

INVESTIGATION OF THE ELECTRIC AND MAGNETIC PROPERTIES OF INTERCALATED GRAPHITES

Awarded to

BOSTON UNIVERSITY

DEPARTMENT OF PHYSICS

G.O. Zimmerman, Principal Investigator

9/30/82–9/29/86

Review of Accomplished Work and Work in Progress

I. Introduction

Most of the work to date was performed on $FeCl_3$ intercalated graphite, where the $FeCl_3$ is the magnetic substance. Work on $FeCl_3$ intercalated graphite at Boston University was begun in the late 1970's and was initially confined to Mössbauer investigation of the compound [1]. In those investigations it was shown that the $FeCl_3$ had a magnetic phase transition with long range order in stage 1 and stage 2 compounds, while no such transition took place in stages 4 and 6. Subsequent measurements of the magnetic susceptibility, which are described in more detail in Appendix I, have shown that besides the susceptibility maxima which denote a ferromagnetic transition in the out of plane direction and an antiferromagnetic transition in the in-plane direction in stage 1 and an antiferromagnetic transition both in the in-plane and out-of-plane directions in stage 2 [2,3] There exists an anomaly in the magnetic susceptibility which occurs in all stages at about the same temperature, 1.7K to 1.8K.

Graphite intercalation compounds (GIC) are naturally layered [4] and are of interest because it was believed that electronically, only the graphite layers next to the intercalant change significantly upon intercalation [5]. From our measurements we now have evidence that the charge transfer affects layers other than those next to the intercalant. The intercalant forms a monomolecular layer which is boarded by graphite. Fig.1 of appendix II shows a schematic of stage 2 intercalated graphite compound, where the striped layers represent the intercalant, (stage index refers to the number of graphite layers between two consecutive intercalant layers). For a magnetic intercalant, the graphite layers can be a controlling factor in the magnetic interactions between different magnetic intercalant layers. The graphite layers can control the magnetic interaction by separating successive intercalant layers from each other. Increasing the distance will generally decrease the ex-

change and dipolar interactions. They can also actively shield the intercalant layers from each other because the graphite planes are good electrical conductors. Thus there will be electromagnetic shielding. The systematic change of the number of graphite layers between two adjecent intercalant magnetic layers can provide two-dimensional magnetic systems by shielding the intercalant layers from each other until their magnetic interaction is insignificant. In our investigations we found that in low stages this shielding increased exponentially with stage. Thus intercalation of magnetic species into graphite provides us with very useful model systems in which to study two dimensional magnetism.

Magnetic compounds have been widely used in the intercalation of highly ordered pyrolytic graphite (HOPG) and generally one observes magnetic anomalies in the GIC's, even in high stages. The structure of the intercalant is similar to that of the bulk material and generally magnetic compounds intercalated into graphite also undergo a phase transition in the intercalated state, but the nature of the transition is altered by the enviroment. Additional transitions due to the magnetic two dimensionality of the systems were also reported [6,7].

We have performed a systematic study of the magnetic phase transitions of $FeCl_3$ intercalated graphite compounds and their behavior as a function of the stage of the sample, (see appendices). We also investigated the dependence of these transitions on an external dc magnetic field.

The crystal structure of $FeCl_3$ is a repeated sequence of chlorine, iron, and chlorine hexagonally arranged atoms [8], such that every iron atom is surrounded by an octahedron of chlorine atoms. The iron atoms in subsequent layers are displaced with respect to each other by 1/3 of the unit cell and thus three $FeCl_3$ layers are encompassed by the cell vector in the $\vec{C}$ direction. Upon intercalation of $FeCl_3$ into the graphite, one electron is donated by the graphite host for every four iron atoms [9]. It is not yet clear what site these donated

electrons occupy. At room temperatures, Mössbauer data [10,11] and Raman spectroscopy [12] do not support the existence of $FeCl_2$ as a result of the acceptance by $FeCl_3$ of the donated electron [13]. However, in the low temperature Mössbauer data for $FeCl_3$, Millman and Kirczenow [14], at Boston University, have seen Fe^{2+} ions at temperatures as high as 100K.

II. Magnetic Susceptibility (Appendix I, II and III)

In its pristine state, $FeCl_3$ undergoes a magnetic phase transition at 8K [15]. Measurements of the magnetic properties of stages 1 and 2 [1a,3], prepared from HOPG, revealed that the samples undergo a magnetic phase transition with long range order, however the transition temparatures are depressed from those of the pristine $FeCl_3$. The measurement of Millman et al [1a] was performed by means of the Mössbauer effect, while Millman et al [3] (see appendix I) measured the magnetic susceptibility of the system, the latter method has a better temperature resolution. Both measurements found that stage 1 undergoes a phase transition at 4.3K while stage 2 undergoes a transition at 1.3K. Moreover, the Curie-Weiss θ indicated that stage 1 orders antiferromagnetically in-plane and ferromagnetically between planes while stage 2 orders antiferromagnetically both in-plane and between planes.

A Mössbauer investigation of higher stages [1] revealed that no long-range order existed in stages 4 and 6 down to temperatures of 65mK. Subsequent susceptibility measurements on those samples and others revealed a magnetic susceptibility maximum which occured in all the samples at a temperature between 1.7K and 1.8K, depending on stage [2a]. Although the maxima occured seemingly at the same temperature for all stages, the size of the maximum varied widely from stage to stage becoming generally greater as the stage increased. In fact our measurements reveal that the size of the maximum increases by a factor of 55 from stage 1 to stage 5, (see appendix II). Moreover the susceptibility

maximum was supressed by relatively low magnetic fields, of the order of 10G. Since the maximum increased in intensity with stage, we assume that it is a consequence of the two-dimensionality of the system. Within the same stage, the height of the susceptibility peak increased with the number of iron atoms next to iron vacancies [16],(see appendix III).

Phase transitions in other GIC such as $CoCl_2$, and $NiCl_2$ were also reported by Karimov et al [17], recently these transitions were also confirmed by Elahy et al [2b]. The authors of reference 2b have concluded that the magnetic intercalants exhibit a very general type of magnetic behavior, independent of species or of stage. More recently low temperature magnetic phase transitions were reported for $MnCl_2$ [18], and also for stage 1 C_6Eu [19]. Qualitatively most of the reported phase transitions have shown similarties in both magnetic field and temperature dependence, differences exist only in the location of the transition points and the dc magnetic field needed to quench the peaks in the measured magnetic susceptibility. Most of the reported experimental data have been analysed on the basis of a two-dimensional XY model with a low temperature transition to a two-dimensional antiferromagnetic phase [19,20].

Although the details are given in appendix II, the highlights of our measurements were:

1) The size of the magnetic susceptibility peak increases exponentially with stage up to stage 5.

2) The temperature of the maxima decrease from stage 1 to stage 4 and then increase after that. All the maxima occur between 1.7K and 1.8K.

3) At any stage the size of the maximum in the susceptibility decreases with the application of a small magnetic field, the size of the decrease depends on the direction of the field.

4) The magnetic field shifts the temperature at which the maximum occurs to a higher temperature.

5) At high fields, the susceptibility starts to increase.

6) The susceptibility as a function of temperature obeys the general power law of a second order phase transition.

•

III. Spin-lattice Relaxation (Appendix IV)

The technique used to measure the magnetic susceptibility allowed us to measure both the inphase and out-of-phase components of the susceptibility. The relation of the in-phase to the out-of-phase component at various frequencies is related to the spin lattice relaxation time of the system. Appendix IV gives the details of the measurement and their analysis. The main conclusion is that the maximum in the magnetic susceptibility is accompanied by a corresponding maximum in the relaxation times and in the specific heat. The maxima in the relaxation times come at a temperature which is lower than that of the susceptibility maximum by as much as 25mK. Although we first suspected the electrical conductivity to be the culprit in the relaxation maximum, direct measurements of the conductivity revealed a smooth and continuous behavior with no evidence of anomalous behavior in the temperature region of the susceptibility maximum, (see following section).

IV. Electrical Resistivity (Appendix V)

We have measured the c-axis electrical resistivity of the various stages of $FeCl_3$ GIC. Appendix V gives the details of the measurements. We have measured the electrical resistivity by means of the conventional four probe technique. The temperature range of these measurements was between 1K and 300K. At room temperature stage 5 has the highest resistivity. Stage 5 is also the pivotal stage where in stages higher than that the c-axis resistivity decreases with temperature (this includes unintercalated HOPG), while in the lower stages it increases. Thus stage 5 seems to be the dividing stage between the metalic behavior, low stages, and activated behavior, high stages. The behavior of the c-

axis resistivity is in qualitative agreement with the theory of Sugihara[21] which attributes the c-axis conductivity to a phonon assisted hopping mechanism. We have also measured the in-plane resistivity of selected samples of $FeCl_3$ GIC's at selected temperatures in connection with our galvanomagnetic measurements, (see following section).

V. Galvanomagnetic Measurements, (Hall Effect, Magnetoresistance and the Shubnikov-de Haas Effect) (Appendix VI and VII)

Again, the details of these measurements are given in Appendix VI and VII. The main results of these measurements are:

1) The conduction in stage 2 and 5 is dominated by hole carriers, while stage 9 and HOPG exhibit both electron and hole conduction with the dominant mechanism depending on temperature and field.

2) The magnetoresistance is positive in all stages and at low temperatures exhibits quantum oscillations.

3) The quantum oscillations in the magnetoresistance persist up to temperatures as high as 30K.

4) The Fourier analysis of the data indicates that the oscillation instage 5 is dominated by a single frequency contributed by holes, while in stage 9 several frequencies were observed.

VI. Theoretical Calculations (Appendix VIII and IX)

A theoretical effort was started after the experimental investigation had yielded interesting results. At the beginning it was aimed at the explanation of some of our results. After a while, however, this investigation became of interest in itself. The model explored was that of a two dimensional array of dipoles situated on a honeycomb lattice. A classical dipolar potential was assumed, and an exact ground-state energy was calculated. A mean-field calculation was performed to determine the dependence of the system on temperature. So far only the planar lattice was considered and calculations of the influence of

boundaries and defects in the array are currently in progress.

The details of the calculations and their results are given in Appendix VIII and IX. The major results of the calculations are:

1) There is an infinitely degenerate ground state.

2) If one uses the spacing and the dipole moments measured for the iron ions in $FeCl_3$ the energy of the ground state becomes -0.98K.

3) There is a critical point near 1K in zero field.

4) We are able to map out a phase diagram in the magnetic field - temperature plane with three phases. At low temperature and field there is the ordered phase, at low temperature and high field there is a field induced ferromagnetic phase, and at high temperature we obtain a paramagnetic phase.

5) In the low and moderate field region, and below the transition temperature, the magnetic isothermal susceptibility increases with an applied external field.

6) From our calculation we can determine the exact orientation of the dipoles as a function the applied magnetic field and the angle of the field with respect to the lattice.

Further calculations to determine the interaction of this lattice with similar lattices in three dimensions above and below it are in progress. We also propose to calculate the influence of defects, and superlattices on the behavior of the system. As shown in Appendix IX, some of this work has already been started.

VII. Instrumentation (Appendix X)

In connection with our experimental work, we have developed a self-balancing resistance bridge which uses a novel feedback system. The bridge is appropriate for low temperature measurements because of its low power dissipation. The details of the bridge are given in appendix X. We intend to develop more self balancing instrumentd, applying this feedback system. This system is fully compatible with computer usage.

Characterization of Samples

The samples which were used in the above measurements were characterized for staging by means of 00l x-ray analysis and mixed stage samples were not considered. In many cases the samples were also examined by means of the Mössbauer effect which could shed light on the in-plane density of the intercalant and the ratio of Fe^{2+} to Fe^{3+}.

Summary

The picture which emerges from our investigations is that we are indeed observing the behavior of a two dimensional magnetic system. The low dimensionality is brought about by the shielding of the intercalant layers by the intervening graphite layers. The shielding also depends on the charge transfer between the intercalant and the graphite. In graphite there is a band near $\vec{k} = 0$ about half filled with electrons[10]. The intercalation of an acceptor compound will draw off those electrons so that the electrical conduction is hole like. Thus low stages exhibit a positive Hall coefficient. The shielding of the intercalant layers is due to electromagnetic shielding analogous to the skin effect, where the skin depth is a function of the electrical conductivity, which in turn is a function of the number of charge carriers. Stages 1 to 5 almost empty the band of electrons and thus the graphite layers have maximum conductivity. Above stage 5, the quantity of acceptors is not large enough to absorb all the electrons which can be donated by the graphite, and the conductivity of the graphite layers decreases. Moreover, the conductivity, according to our Hall measurements, is due to both positive and negative carriers. This gives rise to decreased magnetic shielding of the intercalant layers, with a corresponding decrease in the peak height in the susceptibility at 1.7K. Thus, the transition at 1.7K can become a very sensitive probe of the internal magnetic field, the charge transfer, and the electrical conductivity of the graphite layers.

The nature of the magnetic phase transition is still not definitely determined, although

some facts have been established: 1) The transition is definitely due to the two dimensional nature of the system; 2) Dipolar interactions play a significant role in the transition. Our theoretical efforts are directed towards the explanation of the nature of the low temperature phase and so far we have managed to theoretically reproduce some of the effects observed experimentally. Those effects are the increase of the susceptibility in the magnetic field at fields above 40G, which agrees with our measurements which are given in appendix II and calculated in appendix VIII, and the decrease at extremely low fields when defects are present as seen in appendix II and calculated in appendix IX. It is evident that dipolar interactions do not tell the whole story, and that exchange interactions will also play a role. However, the degeneracy in the ground state of our dipolar model as well as the extreme sensitivity of the dipole configuration to the direction of the magnetic field give us a hint that the material may resemble a two dimensional spin-glass. This will be the subject of further investigations.

REFERENCES

1- a) Millman S.E., Corson M.R. and Hoy G.R., Phys. Rev. B25, 6595, (1982)

– b) Corson M.R., Millman S.E., Hoy G.R. and Mazurek H., Sol. St. Comm. 42, 667,(1982)

2- a) Zimmerman G.O., Holmes B.W. and Dresselhaus G., Extended Abstracts, Fifteenth Biannial Conference on Carbon, University of Pennsylvania, (1981), Ubbelohe and Drummond Eds. p42

– b) Elahy M., Nicolini C., Dresselhaus G. and Zimmerman G.O., Sol. St. Comm. 41, 289, (1982)

– c) For further references see Extended Abstracts-GRAPHITE INTERCALATION COMPOUNDS, Eklund, Dresselhaus and Dresselhaus Eds., Materials Research Society, Pittsburgh, 1984 and Dresswlhaus, Dresselhaus and Solin Eds., Materials Research Society, Pittburgh, 1986

3- Millman S.E., Holmes B.W. and Zimmerman G.O., Sol. St. Comm. 43, 903, (1982)

4- a) Herold A., Intercalated Layered Materials, Levy F.A. Ed., Reidel Dortrecht, Holland (1979)

– b) Stumpp E., Mater. Sci. Eng. 31, 53, (1977)

5- Dresselhaus M.S. and Dresselhaus G., Adv. Phys. 30, 139, (1981)

6- Karimov Y.S., Sov. Phys. JETP 41, 772, (1976)

7- Erbil A., Birgenau R.J. and Dresselhaus M.S., Phys. Rev. Latters 49, 1427, (1982)

8- Blairs S. and Shelton R.A.J., J. Inorg. Nucl. Chem. 28, 1855, (1966)

9- Wertheim G.K., Von Attekum P.M., Guggenheim H.J. and Clements K.E., Sol. St. Comm. 33, 809, (1980)

10- Liegme B.V., Bartelett M.W., Hooley J.G. and Sams J.R., Phys. Lett. 25, 127, (1967)

11- Ohhashi K. and Tsujikawa I., J. Phys. Soc. Jap. 36, 422, (1974)

12- Caswell N. and Solin S.A., Sol. St. Comm. 27, 961, (1978)

13- Dzurus M.L. and Henning G.R., J. Amer. Chem. Soc. 79, 1051, (1957)

14- Millman S.E. and Kirczenow G., Phys. Rev. B28, 5019, (1983)

15- Stamfel J.P., Oosterhuis W.T., Window B. and deS. Barros S., Phys. Rev. B8, 4371, (1973)

16- Millman S.E. and Zimmerman G.O., J. Phys. C Solid State Phys. 16, 289, (1983)

17- a) Karimov Y.S., Sov. Phys. JETP 38, 129, (1974)

— b) Karimov Y.S., Sov. Phys. JETP Lett. 79, 159, (1974)

18- Kimishima Y., Furukawa A., Koga K., Nagona H. and Suzuki M., see Ref. 6c 1984 p.88

19- a) Sugihara K., Chen S.T. and Dresselhaus G., Bull. Amer. Phys. Soc. 30, 331, (1985)

— b) Boolchand P., Lemon G., Bresser W., McDaniel D., Heinz R.E., Eklund P.C. and Nietsfeld G., Intercalated Graphite, Dresselhaus, Dresselhaus, Fischer and Moran Eds., North Holland Elsevere (1983) p.393

— c) Hwang D.M., Solin S.A. and Guerard D., Physics of Intercalation Compounds, Pietronero and Tosatti Eds., Springer SSS-38, Berlin (1981), p.187

— d) Date M., High Field Magnetism, Date Ed., North Holland (1983), p.401

— e) Suematsu H., see 6c 1984 p.85

20- a) Suzuki M., Oguro I. and Jinzaki Y., see Ref. 2c 1984 p.91

— b) Zabel H., Suzuki M. and Chow P.C., Bull. Amer. Phys. Soc. 30, 332, (1985)

21- Sugihara K., Phys. Rev. B29, 5872, (1984)

PUBLICATION LIST UNDER THIS GRANT:

RESUBMITTED FOR PUBLICATION IN THE PHYSICAL REVIEW:

G.O.Zimmerman, A.K. Ibrahim and F.Y. Wu, "A Planar Dipolar System on a Honeycomb Lattice"

IN PREPARATION

R. Powers, A.K. Ibrahim, M. Tahar and G.O. Zimmerman, "C-Axis Resistivity of $FeCl_3$ Intercalated Graphite"

A.K. Ibrahim, R. Powers, M. Tahar and G.O. Zimmerman, "Magnetoresistance Hall Effect and Shubnikov-deHaas Oscillations in Graphite and Acceptor Intercalated Graphite Compounds."

PUBLICATIONS

A.K. Ibrahim and G.O. Zimmerman, "Magnetic Properties of Graphite Intercalation Compounds", Physical Review B35,Feb.1, (1987)

G.O.Zimmerman, A.K. Ibrahim and F.Y. Wu, "The Effect of Defects on a Two Dimensional Dipolar System on a Honeycomb Lattice", Journal of Applied Physics, April (1987)

A.K. Ibrahim, R. Powers, M. Tahar and G.O. Zimmerman, "Hall Effect and Magnetoresistance in Low Dimensional Magnetic Systems", Journal of Applied Physics, April (1987)

A.K. Ibrahim, R. Powers and G.O.Zimmerman, "Galvanomagnetic Effects in Graphite and Graphite Intercalation Compounds", Extended Abstracts Graphite Intercalati

Solin, Dresselhaus and Dresselhaus EDS. MRS society Dec. (1986) p.140

A. Kaplan G.O. Zimmerman and D.S. Edmonds Jr., "Self-Balancing Resistance Bridges," Review of Scientific Instruments, 57, 2895, (1986)

A.K. Ibrahim and G.O. Zimmerman, "Relaxation Effects in Graphite Intercalation Compounds" Physical Review B34, 4224, (1986)

G.O.Zimmerman and A.K. Ibrahim, "Two Dimensional Dipolar System on a Honeycomb Lattice" Bulletin of the American Physical Society 31, 508, (1986)

A.K. Ibrahim, R. Powers, M. Tahar and G.O. Zimmerman "C-Axis Resistivity of F_eCL_3 Intercalated Graphite" ibid p. 664

A.K. Ibrahim and G.O. Zimmerman, "Spin Lattice Relaxation In Stage-6 F_eCL_3 Intercalated Graphite Near the 1.75K Magnetic Anomaly" ibid p. 664

A.K. Ibrahim and K. Galuszewski and G.O. Zimmerman, "Electronic and Magnetic Properties of Stage-3 F_eCL_3 IGC", Bulletin of the American Physical Society 30, 284, (1985)

A.K. Ibrahim G.O.Zimmerman and K. Galuszewski, "Electrical Conductivity of $FeCl_3$ Intercalated Graphite" **Extended Abstracts Graphite Intercalation compounds** Ecklund, Dresselhaus and Dresselhaus edts., (Materials Research Society, Pittsburgh 1984) p. 63.

G.O. Zimmerman,C. Nicolini, D. Solenberger, D. Gata and B. Holmes, "Critical Exponent γ of the Magnetic Anomaly of Stage-6 $FeCl_3$ Intercalated Graphite" ibid. p. 101.

S.E. Millman and G.O. Zimmerman, "Observation of Spin Glass State in $FeCl_3$ Intercalated Graphite," J. Phys. C: Solid State Phys., **16**, L89 (1983).

S.E.Millman, " Are Ferric Chloride Intercalated Graphite Compounds Air Stable?", Synthetic Metals **5**, 147, (1983)

S.E. Millman and G. Kirczenow, "Study of the Phase Diagrams of Graphite Intercalation Compounds", Phys. Rev. **B28**, 3482, (1983)

S.E. Millman and G. Kirczenow, "Mössbauer Analysis of the Acceptor Site for the Donated Electrons in $FeCl_3$-intercalated Graphite Compounds", Phys. Rev. **B28**, 5019, (1983)

S.E. Millman, "Mössbauer Study of Magnetic Properties in Low Stage $FeCl_3$ Intercalated Graphite", Solid St. Comm. **44**, 23, (1982).

S.E. Millman, B.W. Holmes and G.O.Zimmerman, "Magnetic Susceptibility Study of Magnetic Properties in Low Stage $FeCl_3$ Intercalated Graphite", Solid State Communications **43**, 903, (1982).

M. Elahy, C. Nicolini, G. Dresselhaus and G.O. Zimmerman, "Magnetic Phases in Transition Metal Chloride Intercalation Compounds of Graphite." Solid State Communications **41**, 289 (1982).

G.O.Zimmerman,B.W. Holmes and G. Dresselhaus, "Low Field Magnetic Susceptibility of Graphite $FeCl_3$." Extended Abstracts and Program of the 15th Biennial Conference on Carbon, University of Pennsylvania, p. 42 (1981).

PERSONELL WORKING ON THIS PROJECT

G.O.ZIMMERMAN, PRINCIPAL INVESTIGATOR, PROFESSOR OF PHYSICS

C. NICOLINI, POST-DOCTORAL ASSOCIATE

A.K. IBRAHIM, POST-DOCTORAL ASSOCIATE

S.E. MILLMAN, GRADUATE STUDENT AND POST DOCTORAL ASSOCIATE

B.W. HOLMES, POST-DOCTORAL ASSOCIATE

R.J. SAMARATUNGA, GRADUATE STUDENT

K. GALUSZEWSKI, GRADUATE STUDENT

R. POWERS, GRADUATE STUDENT

M. TAHAR, GRADUATE STUDENT

D. SOLENBERGER, GRADUATE STUDENT

D. GATA, GRADUATE STUDENT

A. KAPLAN, UNDERGRADUATE STUDENT

DISSERTATION

"MAGNETIC, ELECTRONIC AND STRUCTURAL PROPERTIES OF FERRIC CHLORIDE INTERCALATED GRAPHITE", S.E. MILLMAN, BOSTON UNIVERSITY, 1983

APPENDIX I

Solid State Communications, Vol.43,No.12, pp.903-906, 1982. 0038-1098/82/360903-04$03.00/0
Printed in Great Britain. Pergamon Press Ltd.

MAGNETIC SUSCEPTIBILITY STUDY OF MAGNETIC PROPERTIES IN LOW STAGE $FECL_3$ INTERCALATED GRAPHITE

S.E. Millman, B.W. Holmes, and G.O. Zimmerman
Department of Physics, Boston University, Boston Massachusetts 02215

(Received April 19, 1982, in revised form June 7, 1982 by R.H. Silsbee)

Measurement of the ac susceptibility of well characterized ferric chloride intercalated graphite compounds both parallel and perpendicular to the basal plane, shows that the stage 1 and 2 compounds undergo a magnetic phase transition at 4.3 ± 0.2 K and 1.3 ± 0.2K respectively.

1. INTRODUCTION

The structure of graphite intercalation compounds indicates that both the graphitic and intercalate layers retain the identity of their parent materials.[1] For magnetic intercalants this observation suggests that these compounds should show magnetic phase transitions. Thus, intercalation can be used to separate the magnetic layers by a controlled number of diamagnetic layers. By comparing the magnetic properties of the parent magnetic material and the different stage compounds, one can investigate the influence of interlayer interactions on the magnetic properties of the system.

Magnetic susceptibility, neutron diffraction, and Mössbauer spectroscopy data show that pristine anhydrous $FeCl_3$ undergoes a magnetic phase transition at about 8.8 K. However, the reported magnetic properties in graphite-$FeCl_3$ have shown discrepancies which may possibly be sample dependent.[5-11] For the magnetic susceptibility measurements, there are discrepancies not only in the transition temperature and character of a magnetic phase transition,[6-10] but also in the very existence of a magnetic state. However, it is not surprising to find such discrepancies in the literature due to the uncharacterized differences in iron vacancies, chlorine vacancies, $FeCl_3$ vacancies, and $FeCl_2$ impurities which are likely to vary from sample to sample.

In this work, we find a susceptibility peak in both the stage 1 and 2 graphite-$FeCl_3$ compounds similar in functional form to that observed in pristine anhydrous $FeCl_3$.[2] We show that the stage 1 and 2 compounds undergo a magnetic phase transition at 4.3 ± 0.2 K and 1.3 ± 0.2 K respectively. Thus the interactions between magnetic planes seem to strongly influence the magnetic order observed in these compounds. In addition to x-ray analysis we have also characterized our samples by Mössbauer spectroscopy to determine the amount of iron vacancies, chlorine vacancies, $FeCl_3$ vacancies, and $FeCl_2$ impurities.

2. EXPERIMENTAL

The samples studied were prepared by intercalating anhydrous $FeCl_3$ into highly ordered pyrolytic graphite (HOPG) using the two-zone vapor transport method. Employing this growth process, the graphite temperature was maintained at 350°C while the temperature of the ferric chloride was varied to achieve different stages. The intercalated compounds were characterized for identity and uniformity of staging using (00ℓ) x-ray diffraction both before and after our magnetic susceptibility measurements. Both samples were essentially single staged, and showed less than 20% and 5% of secondary diffraction peaks from both other stages and free graphite in the stage 1 and 2 compounds respectively.

These samples[12] were further checked for fidelity of in-plane density by taking their Mössbauer spectra at 100 K. For the stage 1 sample at this temperature the Mössbauer peak can be fit with only a single Lorentzian line whose linewidth, 0.38 mm/sec, and isomer shift, 0.56 mm/sec, are essentially the same as those of pristine anhydrous $FeCl_3$[13]. This indicates that there is neither a change in site symmetry at the iron ions nor is there any appreciable formation, i.e. less than 4%, of either iron vacancies, chlorine vacancies, $FeCl_3$ vacancies, or $FeCl_2$ impurities in this sample. An analysis of the Mössbauer spectrum of the stage 2 sample indicates that 9% of the sites are nearest neighbors to iron vacancies. This identification will be discussed in detail elsewhere.[14] Assuming these vacancies are randomly situated, this implies that only approximately 3% of the iron lattice sites contain vacancies.

The susceptibility measurements were made by a standard ac bridge method[15] operating at about 40 hz. The amplitude of the magnetic field at the sample was kept below 1 Oe. The coils were kept at a constant temperature while the temperature of the samples was varied inside an isolated chamber. The temperatures above 4.2 K were measured by a calibrated carbon resistor and a calibrated metal resistance thermometer. Below 4.2 K the sample was in direct contact with the helium bath and temperatures were determined from the vapor pressure of the helium bath.

3. RESULTS

In Figure 1, we show the susceptibility curves of the stage 1 and 2 samples with the

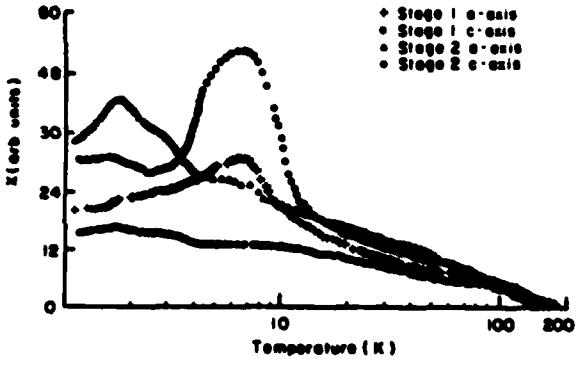

Figure 1. susceptibility (χ) versus temperature (T), plotted on a semi-logarithmic scale, for the stage 1 and 2 compounds. The measuring field was fixed both parallel (a-axis) and perpendicular (c-axis) to the basal plane. Notice the small amount of stage 1 (undetectable in the x-ray diffractograms) which can be detected in the stage 2 curve.

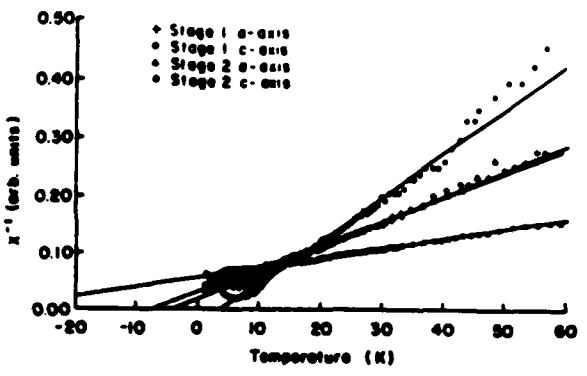

Figure 2. Inverse susceptibility (χ^{-1}) versus temperature (T) for the curves shown in Figure 1. The solid lines represent least squares fits to the data.

measuring field both parallel (a-axis) and perpendicular (c-axis) to the basal plane over the temperature range of 1 K to 200 K. The susceptibility is given in arbitrary units which have been normalized for the amount of iron in each sample by assuming the stoichiometry $C_{6.6n}$ $FeCl_3$. However, we note that a comparison of areas under the Mössbauer curves implies that as much as 50% of the bulk stage 1 sample may have consisted of unintercalated regions. This estimate could be made to within 15%. Coupled with Mossbauer information that the electronic spins for both stages are pointing in the basal plane.[12] several important results can be deduced from the data. For the stage 1 compound an antiferromagnetic susceptibility peak is observed whose maximum occurs at 6.5 K in both the parallel and perpendicular susceptibilities. As expected for the electronic spins pointing in the basal plane, the susceptibility is greater in the direction perpendicular to the planes. Also, at temperatures less than 3K, the parallel susceptibility is clearly decreasing while the perpendicular susceptibility is approximately constant. For the stage 2 compound the maximum of the antiferromagnetic peak has shifted down to 1.72 K and the peak in the perpendicular direction is drastically reduced. This indicates that the magnetic moments are more strongly bound in the basal plane in stage 2 than in stage 1. A comparison of the parallel susceptibility of both stages, plotted on a logarithmic scale in Figure 1 shows that the curves are qualitatively similar in reduced units, T/T_N.

The Néel temperature, T_N, for zero field susceptibility, is given by a maximum in $|d(T\chi)/dT|$.[13] The value of T_N, obtained for the stage 1 compound is 4.3 ± 0.2 K for orientations both parallel and perpendicular to the basal plane. For the stage 2 compound, we obtain 1.3 ± 0.2 K for both parallel and perpendicular to the basal plane. Thus the transition temperature decreases by approximately a factor of three when the interplanar spacing is increased from 9.4 Å (stage 1) to 12.6 Å (stage 2).

As shown in Figure 2, the stage 1 compound obeys the Curie-Weiss law in the temperature region above 15 K. We obtain the values of $\theta = -3.8 \pm 0.5$ K for the direction parallel to the planes and $\theta = +3.8 \pm 0.5$ K for the direction perpendicular to the planes. Although, because of the large anisotropy energies it is difficult to relate θ to the exchanged interactions, these results are consistent with the transition temperature. The values of the Curie-Weiss constants, θ, may indicate that the dominant exchange interaction is antiferromagnetic within the layers while it is ferromagnetic between the layers. Previous results have indicated that the interlayer interaction was antiferromagnetic.[5,8] For the stage 2 compound, we obtain the result $\theta = -7.6 \pm 1.0$ K and $\theta = -33 \pm 2.0$ K in the direction parallel and perpendicular to the layers respectively, and the Curie-Weiss law is followed above 5 K as shown in Figure 2. These values of θ are markedly different from the T_N values obtained by finding the maximum in $|d(T\chi)/dT|$. The transition temperatures, T_N, values of θ and the Curie constants are listed in Table 1.

In order to corroborate our results for the stage 2 compound, we measured the a-axis susceptibility of two other stage 2 compounds. The susceptibility of one of the samples exhibited the same qualitative behavior as the stage 2 compound reported here. Its Mössbauer spectrum was also essentially the same as the stage 2 compound reported here, except that slightly more, 11%, of the sites were nearest neighbors to iron vacancies. The susceptibility curve of the other stage 2 sample had both a peak at the same temperature, 7.1 K, and the same qualitative behavior as the stage 2 compound of Karimov et al.[8] However, its Mössbauer spectrum indicated that at least most, and probably all of this sample was composed of $FeCl_2$. We note that this sample was produced in the same apparatus and under the same growth conditions as all the other samples. These results underscore the need for both a structural and chemical characterization of these compounds in addition to the standard

REFERENCES

1. M.S. Dresselhaus and G. Dresselhaus, Physics and Chemistry of Materials with Layered Structures, Vol. 6, edited by F. Levy (Dordrecht:Teidel), 423 (1979); Advances in Physics. 30, 139 (1981).
2. P.B. Johnson, S.A. Friedberg and J.A. Rayne, Phys. Rev. B, to be published.
3. J W. Cable, M.K. Wilkinson, E.O Woolan, and W.C. Koehler, Phys. Rev. 127, 714 (1962).
4. J.P Stampfel, W.T. Oosterhuis, B. Window, and F. deS. Barros, Phys. Rev. B8 4171, (1973).
5. K. Ohhashi and I. Tsujikawa, J. Phys. Soc. Japan 36 422 (1974).
6. K. Ohhashi and I Tsujikawa, J. Phys. Soc. Japan 36 980 (1974).
7. D. Hohlwein, P.W. Readman, A. Chamberod, and J.M.D. Coey, Phys. Status Solidi B64, 305 (1974).
8. Yu. S. Karimov, A.V. Zvarykina, and Yu. N. Novikov, Sov. Phys --Solid State 13, 2388 (1972).
9. G.O. Zimmerman, B.W. Holmes, and G. Dresselhaus, Extended Abstracts of the 15th Biennial Conference on Carbon, University of Pennsylvania 42 (1981).
10. D.G. Onn, M.G. Alexander, J.J. Ritsko, and S. Flandrois, Extended Abstracts of the 15th Biennial Conference on Carbon, University of Pennsylvania 44 (1981).
11. J.D. Axe, C.F. Majkrzak, L. Passell, S.K. Satija, G. Dresselhaus and H. Mazurek, Extended Abstracts of the 15th Biennial Conference on Carbon, University of Pennsylvania 52 (1981).
12. More extensive Mössbauer measurements were made on different samples and are reported by S.E. Millman, this issue.
13. J.G. Hooley, M.W. Bartlett, B.V. Liengme and J.R. Sams, Carbon 6 681 (1968).
14. S.E. Millman and G. Kirczenow, to be published.
15. E. Maxwell, Rev. Sci. Inst. 36 553 (1965).
16. M.E. Fisher, Phil. Mag. 7, 1731 (1962).
17. M. Elahy, C. Nicolini, G. Dresselhaus and G.O. Zimmerman, Solid State Commun. 41 289 (1982).

TABLE 1 This table lists the magnetic properties of the compounds.

STAGE	DIRECTION	TRANSITION TEMPERATURE	SUSCEPTIBILITY MAXIMUM	θ	CURIE CONSTANT (ARBITRARY UNITS)	NEAREST NEIGHBORS TO IRON VACANCIES
1	a-axis	4.3	6.5	-3.8	222	≤4%
1	c-axis	4.3	6.5	+3.8	132	≤4%
2	a-axis	1.3	1.72	-7.6	242	9%
2	c-axis	1.3	1.72	-33.0	575	9%

characterization by (00ℓ) x-ray diffractograms.

The data at temperatures below 2.2 K, in the curves of Figure 1, were all measured in a dc field of 80 Oe. As seen in Fig. 3, a small narrow peak is observed at 1.7 K when no external dc field is applied. This peak also appears at this temperature in higher stages but is reduced by approximately a factor of 50 in the low stages (stage 1 and 2) relative to the high stages (stage 4 and 6).[9] It can be almost completely quenched by fields as small as 20 Oe. Similar behavior was observed in both $NiCl_2$ and $CoCl_2$ intercalated graphite compounds.[17] Because of the coincidence of this peak and that due to antiferromagnetism in the stage 2 compound, we suppressed it in an 80 Oe field in order to observe the full features of the antiferromagnetic transition. The occurence of the small peak at a lower temperature in the stage 1 sample than the three-dimensional magnetic transition indicates that it may be caused by high stage impurities in the predominately low stage samples.

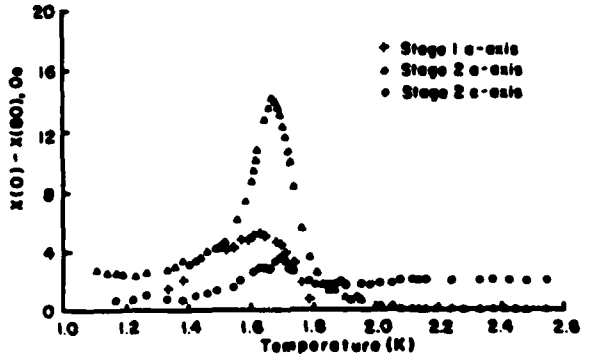

Figure 3. Subtraction of the susceptibility at 80 Oe from that at zero field. For clarity, the susceptibility scale has been expanded by a factor of 3 from that of Figure 1. Note, within the accuracy of our experiment the stage 1 c-axis susceptibility was the same both at zero field and at 80 Oe and is therefore not plotted.

4. DISCUSSION

Previous susceptibility results have been interpreted as showing that even for stage 1 graphite-$FeCl_3$ the interlayer interactions are negligible compared with the intralayer interactions.[6-8] However, our results indicate that the magnetic order seen, at least in the stage 1 compound, is strongly influenced by the interlayer interactions. In fact, we have shown that the transition temperature decreases by a factor of 2 in going from pristine anhydrous $FeCl_3$, $T_N = 8.8$ K[2-4] to stage 1 and by an additional factor of 3 in going from stage 1 to stage 2. Both the parallel and perpendicular susceptibilities follow the Curie-Weiss law, and an increase in either the ac measuring frequency or the amplitude of the ac field by about an order of magnitude, or an applied dc field of 160 Oe causes no change in the transition temperature.

The small susceptibility and the quite large value of θ in the direction perpendicular to the basal plane in the stage 2 compound may be due to the presence of iron vacancies in this compound. Iron vacancies would create an electric field gradient in the basal plane which would cause anisotropy between the in-plane and out-of-plane directions.

We are happy to acknowledge many helpful discussions with Professors G. Kirczenow, and S. Redner. Our deep gratitude is expressed to Dr. R.B. Frankel and Dr. G. Papaefthymiou for the use of their Mössbauer equipment, to Dr. A.W. Moore of Union Carbide for donating the HOPG, and to Dr. H. Mazurek, Dr. C. Nicolini, and A. Thompson for growing and characterizing one of the samples. This work was supported in part by AFOSR contract #F49620-81-0006.

To BE PUBLISHED PHYS. REV. B. Feb. 1987

APPENDIX II

MAGNETIC PROPERTIES OF GRAPHITE INTERCALATION COMPOUNDS*

A.K. Ibrahim and George O. Zimmerman

Physics Department, Boston University

Boston, MA 02215

Comprehensive measurements of the magnetic properties of $FeCl_3$ graphite intercalation compounds are presented with an emphasis on the low temperature region where a susceptibility maximum is observed in all stages. This maximum, which varies in size according to stage, occurs in a very narrow temperature range and is attributed to the two-dimensionality of the intercalate system. It obeys the power law of a second order phase transition with an exponent γ which has a value between 1.8 and 2.0. The maximum occurs only in the in-plane direction with no corresponding c-axis susceptibility response. The application of an external magnetic field drastically supresses the susceptibility maximum and shifts it to higher temperatures. Both in plane and out of plane measurements are presented and the magnetic properties of stages 1 through 6 as well as stage 9 are compared.

* Supported by Air Force Office of Scientific Research Grant AFOSR 82-0286.

INTRODUCTION

Graphite intercalation compounds (GIC) are naturally layered [1] and are of interest because electronically, only the graphite layers next to the intercalant change significantly upon intercalation [2]. For a magnetic intercalant, the inner layers can be a controlling factor in the magnetic interactions between different magnetic intercalant layers. The systematic change of the number of graphite layers between two adjecent intercalant magnetic layers can provide two-dimensional magnetic systems by shielding the intercalant layers from each other until their interaction is insignificant.

Magnetic compounds have been widely used in the intercalation of highly ordered pyrolytic graphite (HOPG) and generally one observes magnetic anomalies in the GIC, even in high stages (stage index refers to the number of graphite layers between two consecutive intercalant layers). It has been reported [3] that for all the magnetic compounds which have a low temperature phase transition there exists a corresponding transition when these compounds are intercalated into graphite. Additional transitions due to the magnetic two dimensionality of the systems were also reported [4,5]. Thus intercalation of magnetic species into graphite provides very useful model systems for the study of two-dimensional magnetism.

In this work we present a systematic study of the low temperature phase transition of $FeCl_3$ intercalated graphite compounds and its behavior as a function of the stage of the sample. We also investigate the dependence of these transitions on an external dc magnetic field. Our data for $FeCl_3$ GIC are compared with reported data for similar GIC sytems. The standard low frequency ac susceptibility bridge technique [6] is used to obtain the experimental data .

The crystal structure of $FeCl_3$ is a repeated sequence of chlorine, iron, and chlorine hexagonally arranged atoms [7], such that every iron atom is surrounded by an octa-

hedron of chlorine atoms. The iron atoms in subsequent layers are displaced with respect to each other by 1/3 of the unit cell and thus three $FeCl_3$ layers are encompossed by the cell vector in the $\vec{C}$ direction. Upon intercalation of $FeCl_3$ into the graphite, one electron is donated by the graphite host for every four iron atoms [8]. It is not yet clear what site these donated electrons occupy, room temperatures Mössbauer data [9,10] and Raman spectroscopy [11] do not support the existence of $FeCl_2$ as a result of the acceptance by $FeCl_3$ of the donated electron [12]. However, there is a discrepancy in the low temperature Mössbauer data for $FeCl_3$. Millman and Kirczenow [13] have reported the existence of Fe^{++} ions at temperatures as high as 100K which is contradictory to the work of Ohhashi et al [10].

Magnetic susceptibility measurements on $FeCl_3$ graphite intercalated compound were performed by Karimov et al [14] and Hohlwein et al [15] in the 70's. The interest there was the nature of magnetic behavior of the $FeCl_3$ which in pristine state undergoes a magnetic phase transition at 8K [16]. Those measurements concentrated mainly on the properties of stages 1 and 2. Although the results of those measurements disagreed on the details the authors reported a phase transition in the temperature region of their measurements . The method used in those measurements was the Faraday-ballance supplemented by an ac method, the samples consisted of small crystallites. More recent measurements of the magnetic properties of stages 1 and 2 [17,18], prepared from HOPG, revealed that the samples undergo a magnetic phase transition with long range order, however the transition temparatures are depressed from those of the pristine $FeCl_3$. The measurement of Millman et al [17] was performed by means of the Mössbauer effect, while Millman et al [18] measured the magnetic susceptibility of the system, the latter method has a better temperature resolution. Both measurements found that stage 1 undergoes a phase transition at 4.3K while stage 2 undergoes a transition at 1.3K. Moreover, the Curie-Weiss θ indicated that stage 1 orders antiferromag-

netically in-plane and ferromagnetically between planes while stage 2 orders antiferromagnetically both in-plane and between planes.

A Mössbauer investigation of higher stages [19] revealed that no long-range order existed in stages 4 and 6 down to temperatures of 65mK. Subsequent susceptibility measurements on those samples and others revealed a magnetic susceptibility maximum which occured in all the samples at a temperature between 1.7K and 1.8K, depending on stage [20]. Although the maxima occured seemingly at the same tamperature for all stages, the size of the maximum varied widely from stage to stage becoming generally greater as the stage increased. In fact this investigation reveals that the size of the maximum increases by a factor of 55 from stage 1 to stage 5. Moreover the susceptibility maximum was supressed by relatively low magnetic fields, of the order of 10G, which may have accounted for the fact that it was not seen by other investigators prior to that time. Since the maximum increased in intensity with stage, it was assumed that it was a consequence of the two-dimensionality of the system. Within the same stage, the height of the susceptibility peak increased with the number of iron atoms next to iron vacancies [21].

Phase transitions in other GIC such as $CoCl_2$, and $NiCl_2$ were also reported by Karimov et al [22,23], recently these transitions were also confirmed by Elahy et al [24]. The authors of [24] have concluded that the magnetic intercalants exhibit a very general type of magnetic behavior, independent of species or of stage. More recently low temperature magnetic phase transitions were reported for $MnCl_2$ [25], and also for stage 1 C_6Eu [26]. Qualitatively most of the reported phase transitions have shown similarties in both magnetic field and temperature dependence, differences exist only in the location of the transition points and the dc magnetic field needed to quench the peaks in the measured magnetic susceptibility. Most of the reported experimental data have been analysed on the basis of a two-dimensional XY model with a low temperature transition

to a two-dimensional antiferromagnetic phase [24-25].

EXPERIMENTAL

a) Characterisation of samples

The $FeCl_3$-GIC samples were prepared using a standard two-zone furnace technique where stage index was controlled by the temperature difference between the graphite host (HOPG) and the $FeCl_3$ powder. The samples were in the form of thin rectangular plates of dimensions 1.5x0.5x0.1 cm^3. Well-staged samples were achieved by controlling the pressure of Cl_2 gas inside the intercalation tube, as well as the partial pressure of $FeCl_3$ through rigid temperature controll. After intercalation, the samples were characterized for identity and uniformity of staging using x-ray (00l) diffraction. Only single stage, well staged samples were used in the magnetic measurements. The x-ray diffractograms were also used to determine the c-axis repeat distance I_c after cycling the samples from room to liquid helium temperature, and showed that the cycling did not affect this staging distance.

Most of the samples measured were characterized by means of the Mössbauer effect, which can reveal the ratio of iron atoms next to iron vacancies to that of the total number of iron atoms in the intercalant layer as well as that of Fe^{2+} to that of Fe^{3+} [17,19]. The initial measurements were performed on the same samples used in the Mössbauer investigations. The same measured samples were characterized periodically, before and after the measurements, over a time span of over a year, having been stored at room temperature in a dry nitrogen enviroment. No deterioration was observed in the samples during the period of measurements [27]. Once deterioration was obeserved the samples were discarded. In higher stage samples, where stage-disorder is expected [28], the Hendricks-Teller [29], and Metz and Hohlwein [30] analysis technique were used to calculate the intensity, width and location of the x-ray reflections. We find that our experimental x-ray data on the stage 9 samples reported in this article are in good agreement

with that calculated for the pure and well-staged stage 9. Although a small admixture of stage 10 can not be excluded, this stage serves as an example of a high stage sample.

As shown in Table I of reference [19], the Mössbauer analysis of our initial samples showed that 17±3% of the iron sites were next to vacancies (ISNV) in stages 1 and 2 while this number was 19±3% and 13±3% for stages 4 and 6, respectively. The Fe^{2+} sites comprised 23±3% in stages 1 and 2 at low temperatures while only 3±1% in stages 4 and 6. In a similar set of measurements it was also shown that the amount of Fe^{2+} increased systematically with a decrease in temperature from about 100K to 10K, and was constant below that temperature [13]. In some of the subsequent samples the percentage of iron atoms next to vacancies was reduced to 7% or lower.

If one assumes that most of the sites near to vacancies come from the atoms at the boundary of the intercalate islands, one can calculate the minimum average diameter of an island to be 64Å for a 19% ISNV and 175Å for 7% ISNV corresponding to clusters of 200 and 1500 atoms respectively. If, however, most of the ISNV's were to come from the island boundaries, one would observe two ISNV sites. One would come from the ISNV next to one vacancy and another next to two vacancies. Only the ISNV next to one vacancy was observed [31]. It is therefore argued that since only one kind of ISNV was observed, the ISNV's were within the islands. Because on a honeycomb lattice there would be three ISNV's near to one vacancy, the vacancy percentage would be 1/3 that of the ISVN percentage and the island size would be much bigger than the above limits. On the whole, there was consistency in the magnetic measurements between the samples within one stage. This is true with the exception of several samples which significantly deviated from the norm and upon further examination turned out to be $FeCl_2$ intercalated compounds. In each case, more than one sample was used in our magnetic measurements, and in some cases as many as 5 or 6.

b) Measurement techniques

A standard ac bridge technique [6] was employed to probe the magnetic susceptibility(χ') of the system. The signal was picked-up by a two-phase lock-in analyzer which can detect signals down to 1 μ volt. The data were taken at several frequencies ranging between 40 Hz to 1000 Hz.

A computer-controlled system, via A/D and D/A converters, was used to operate the apparatus at all desirable conditions. The temperatures of the samples above 2K were measured by a calibrated silicon diode thermometer, while temperatures below 2K were determined by means of the He^4 vapor pressure. This allowed for an accuracy of $\pm$1mK at 2K. When greater resolution was required, a carbon resistor was employed. The resistance of certain carbon resistors, in our case an IRC brand, is very temperature sensitive at low temperatures. This method enabled us to detect temperature changes of less than 0.1mK

The susceptibility coils were always kept in a cryogenic bath, thus changing the the temperature of the sample did not change the temperature of the coils. At high temperatures (nitrogen to room temperature), the coils were immersed in liquid nitrogen.

An ac current in the primary circuit, of magnitude 4 mA and below, was used to keep the amplitude of the exciting ac field below 0.1G, thus non-linear susceptibility effects were excluded. To investigate the susceptibility as a function of the magnetic field, a dc magentic field in the range of (0-150G) was applied to the samples. Fig(1) shows schematically several layers of GIC with the intercalant (striped layers). Generally the probing ac and the external dc magnetic fields are parallel to the a-b plane, thus the in-plane magnetic susceptibility component was measured in this configuration. Other configurations were used in the various measurements and will be mentioned as appropriate. Our sample holder was designed so that the orientation of the sample can be adjusted to

any desired configuration relative to the exciting field direction. The c-axis susceptibility data were taken when the a-b plane aligned perpendicular to the exciting field. Configurations where the dc field was perpendicular to the measuring ac field, either along the c-axis or along the a-b plane were also used.

Mechanical vibrations can cause serious problems in this kind of experiment, thus careful attention has been paid to ensure that the sample was firmly attached to the sample holder and in a rigid configuration with the susceptibility coils. A special computer program was made to transfer the data from a MACSYM-350, ANALOG DEVICES, Inc., computer, which monitors the apparatus and collects the data, to a Digital Equipment Corporation VAX11 minicomputer for routine analysis.

RESULTS AND ANALYSIS

a) In-Plane Susceptibility

The susceptibility results in zero external dc magnetic field of stage 1 through 6, and 9 samples are presented in Fig.(2). In this configuration the measuring ac field was perpendicular to the c-axis, thus in-plane susceptibility data are shown in the figure. The susceptibility is given in arbitrary units, however it is normalized for the amount of iron in each sample and at a frequency of 40 Hz. Also, all the susceptibility data are subtracted from the value at the lowest measured temperature 1.1K. At low frequencies and away from the transition, (at the transition the relaxation times can be very long, $\tau = 6 \times 10^{-3} s$ [32]) the arbitrary unit is equal to 1.0 emu/mole of iron. However, the susceptibility varies with the measuring frequency and thus we give our data in "arbitrary" units. For a more detailed analysis of this we refer the reader to reference 32. As shown in the figure, all the stages have low temperature susceptibility maxima at about the same temperature but the relative size of the peaks is different, stage 5 has the largest peak.

As shown in the insert to figure 2, where the logarithm of the peak size, χ_m, is plotted as a function of stage, n, the peak size for stages 1 through 5 follows an exponential law. More exactly,

$$\chi_m = 0.028 exp(n) \tag{1}$$

for $1 \leq n \leq 5$. This suggests that the graphite layers shield the intercalant layer interaction exponentially, similar to the shielding of electromagnetic radiation from the interior of a conductor due to the skin depth. The conducting graphite layers between the intercalant layers shield the interplanar intercalant interaction, and thus controll the dimensionality of the magnetic system. In stage 5 the magnetic intercalant layers are 22.7Å apart. The sharp increase of the peak size from stage 1 to stage 5 indicates that five

stages of the graphite layers between the intercalant layers are sufficient to completely reduce the interlayer interactions and produce a two-dimensional magnetic system. As shown in Fig.(2), the peak sizes started to decrease for samples of stages higher than stage 5.

We surmise that the decrease in the relative peak size beyound stage 5 is related to the in-plane density of the magnetic ions, because the in-plane intercalant density of graphite-$FeCl_3$ compounds decreases as the stage is increased [31]. As shown in reference 31, the in-plane density varies within stage at low stages from 100% to 95%. This variation was not observed in our susceptibility measurements. The variation of the in-plane density can be attributed to the existence of large islands [33,34] in the intercalant compound, a decrease in the number of iron ions in these islands is expected when the stage index is increased. Therefore we suggest that the maximum in the relative peak size of the susceptibility versus the stage index, presented in Table I, is due to the competition between the dimensionality of the system and the intercalant in-plane density. Moreover it is interesting to note that, as shown in Table I, the transition temperatures also vary with the stage index and stage 4 has the lowest transition temperature. This indicates an additional aspect of the competition between dimensionality and in plane density, since otherwise all the transitions would have occured at the same temperature for all the stages.

The magnetic anomaly in this system depends strogly on the external applied dc magnetic field. The susceptibility data versus the external applied dc magnetic field for stage 6 and stage 3, as examples, are presented in Fig.(3) and Fig.(4) respectively. Note that the scales of Fig.(3) and Fig.(4) are different from those of Fig.(2) at the maximum. The reason is that, because of the relaxation times [32] the susceptibility varies with frequency. Fig.(2) represents the peak sizes at 397Hz while Fig.(3) is at 39Hz and Fig.(4) is at 197Hz. In these figures the exciting field is perpendicular to the c-axis, thus the

in-plane susceptibilities are the measured data. In this paper we have adopted the convention that B stands for the enternal exciting ac magnetic field and H stands for the external applied dc magnetic field. In this case H is applied parallel to B. As shown in the figures, the peak size is drastically reduced when a magnetic field of the order of 5G is applied to the sample. One would expect that in three dimensions a phase transition would be quenched by a magnetic filed at least in the order of $k_B T$ or 1.6KG. Therefore we suspect that the increase in the number of graphite layers between two successive intercalant layers, which reduce the intercalant interaction, contribute to the strong field dependence. Spin glasses also exhibit strong low field dependence and there may be a relation of our system to that of a two-dimensional spin glass.

In Fig.(5) and Fig.(6) the in-plane susceptibility at constant temperature, normalized to the zero field value, is shown as a function of the external applied dc magnetic field H for different temperatures for stage 6 and stage 3 respectively. Here H is again parallel to B. The remarkable features in these figures are the low field local minima in the susceptibility, more pronounced for stage 3, which steeply decrease on the left shoulder near the transition temperature. This rapid turnover of the susceptibility at a very small magnetic fields and its subsequent increase is in qualitative agreement with the results of mean field calculations for two dimensional dipoles on a honeycomb lattice [35].

In these mean field calculations, we considered a system of dipoles on a two-dimensional honeycomb lattice. Dipolar interactions are inherently anisotropic since they depend on both $\vec{\mu}_i \cdot \vec{\mu}_j$ and $\vec{\mu}_i \cdot \vec{r}_{ij}$, where $\vec{\mu}_i$ denotes the magnetic moment of the dipole and $\vec{r}_{ij}$ is the distance between the two interacting dipoles. The dipoles were constrained to rotate about an axis normal to the plane and thus to point along the plane. That system has a continuously degenerate ground state whose energy is -1.95K per dipole if the dipole moment and separation of the dipoles is that of the iron in $FeCl_3$. There is a phase transition in zero field which takes place at 1K and is lowered in an

applied field. In a perfect lattice, the magnetic susceptibility increases with an applied magnetic field at low fields. If, however, defects are taken into account, the susceptibility has a minimum with the application of an external field at a constant temperature. Since the results calculated for this model system are of the same order of magnitude and qualitatively similar to those measured for $FeCl_3$ IGC, we assume that in-plane dipolar interactions play a significant role in the behavior of our measured systems. As will be seen below, in the c-axis measurements at low temperatures, the spins tend to rotate in the plane, thus approximating the configuration of the model system above.

It is of interest to note the relative large increase in the susceptibiliy on the high field side of the minima for stage 3, compared with that for stage 6, where the susceptibility exceeds the zero field value. This emphasizes the still existing interplanar interactions in the lower stages. Stage 2 exhibits similar behaviour to that of stage 3 [18]. As we have shown the interplanar interactions decrease as the stages increase, thus the in-plane magnetic phase of stage 3, where 3-dimensional effects are still significant, is effected by the applied field in a way as to reduce the interplanar interaction and increase the in-plane interactions of the system. In stage 6 the interplanar interactions are already quenched by the graphite layers and the external field is not expected to increase the in-plane magnetization significantly in this low magnetic field.

The explanations of other susceptibility peaks [24] were based on a two-dimensional XY model [36], however the existence of a spin glass transition was also suggested [21]. The model calculations mentioned above [35] have the XY symmetry. Lundgren et al [37] have suggested a three dimensional spin glass model to relate the in-phase and out-of-phase parts of the magnetic susceptibility. We have tried their approach to the analysis of the magnetic anomaly in our system in the frequency range of our data and found no quantitave agreement between the suggested model and our data. Therefore we again conclude that the magnetic anomaly in this system is two dimensional in nature. The

spins are locally locked in layered planes and contibute to the two-dimensional anomaly. The fact that the spins are confined to the the a-b plane is confirmed by our c-axis susceptibility measurements.

b) C-Axis Susceptibility

The c-axis susceptibility was measured over wide temperature range. For stage 3 and stage 6 we did not observe any magnetic anomaly at low temperatures, however the susceptibility showed a steep decline as the temperature decreased thus indicating that the spins are locked in the planes as temperature is lowered. Appearently the Curie law is not applicable for these data in any temperature range.

The low temperature data are presented in Fig.(7). The figure shows the c-axis susceptibility of stage 6 versus the temperature at different external dc magnetic fields. As shown in the figure, the susceptibility in this direction is down by a factor of 100 from the in-plane value. No significant anomaly exists in this direction. Experimentally, perfect orientation of the sample is very difficult and in addition the graphite planes may be out of parallel by as much as a few degrees, thus we expect a small contribution from the in-plane anomaly to the c-axis data. This contribution due to misorientation appears as a small peak in the c-axis susceptibility data near the transition temperature.

As shown in Fig.(7), the applied dc magnetic field does not change the the c-axis susceptibility significantly as it does in the in-plane case which is shown in Fig.(3). In this high stage low temperature limit the spins are expected to be confined to a plane parallel to the graphite layers, and thus are free to realign themselves along the applied field only in the in-plane directions. Therefore, in this small magnetic field limit and for the higher stage samples, the c-axis susceptibility is less sensitive to the applied magnetic field than the in-plane data.

Since the c-axis susceptibility data at low temperature were continously increasing as a function of temperature, we decided to extend our measurements to higher temperatures where a high temperature magnetic susceptibility maximum might exist. As shown in Fig.(8), the stage 3 susceptibility increases monotonically while the stage 6 susceptibility has a shoulder at about 65K and a small maximum at a temperature of about 140K. At 65K the c-axis susceptibility of stage 6 is a factor of 200 greater than that at 2K and below. We take this as evidence that the spins are locked in the plane at low temperatures. This is contrasted with stages 1 and 2 where above 15K the magneti susceptibility obeys the Curie-Weiss law both along the a-b and along the c-direction.

The large size of stage 6 c-axis susceptibility versus the temperatures relative to that for stage 3, shown in Fig.(8), is another manifestation of the two dimensionality at low temperatures. In stage 6 the spins are locked in the plane at low temperatures and as the temperature is raised the spins are released from the planar orientation and are free to respond to the field in the $\vec{c}$ direction. In stage 3, the interaction between planes hinders the response of the spins in the $\vec{c}$ direction, and thus the susceptibility is smaller. Stage 3 is not completely two dimensional, and interplane interactions play a role in this stage.

c) Critical Behavior

A maximum in the magnetic susceptibility often denotes a magnetic phase transition which, if it is a second order transition, can be analyzed in terms of critical exponents [38]. As mentioned above, similar transitions were anlyzed in terms of the Kosterlitz and Thoules XY model [39,40] and thus we decided to subject our data to a similar analysis. Before this analysis, however, the measured susceptibility has to be modified so as to account for the shape of the sample [41].

Because of the high susceptibility at the maximum, each spin does not see the externally applied field, but a field which is modified by the field of the surrounding dipoles. This modification or shielding depends on the shape of the sample. In what follows we designate the externally measured susceptibility by χ_{ext}, and the actual susceptibility of the spin as χ_{int}. The relation between the two susceptibilities is

$$\chi_{int} = \chi_{ext}/(1 - \epsilon\chi_{ext}) \tag{2}$$

where ϵ is the shape factor. The shape factor can be exactly calculated only for homogenious substances of ellipsoidal shape. Neither of these conditions applies to our substance since it is an inhomogenous substance in the form of thin rectangular plates. Because of that one has to resort to experiment.

If one assumes that at the maximum the χ_{int} is infinite then

$$\epsilon = 1/\chi_{ext} \tag{3}$$

at that point. A finite but very large susceptibility does not change this result significantly.

If one uses the value obtained for ϵ from equation 2 and applies it to our data by use of Eq.(2) one obtains susceptibility values shown in Fig.(9). This figure shows the

natural logarithm of χ_{int} as a function of the reduced temperature $t = (T - T_c)/T_c$ where T_c is the temperature at the susceptibility maximum. Although this procedure introduces an infinity where only rounded maxima exist, it is justified by the fact that our data agree well with equation (4), below, over a wide range of temperature. Moreover, the best fit was found with χ_{int} being finite and of the order of 400 rather than infinity.

Figure (10) shows the natural logarithm of the susceptibility as a function of the natural logarithm of the absolute value of the reduced temparature for stage 6. Similar data reduction was performed on stages 4, 5 and 9 with similar results. Stages 1 , 2 and 3 were not suited for this analysis because of interference from the high susceptibility due to 3-dimensional interactions [18] which necessitated the subtraction of the field sensitive component from the total susceptibility, with an accompanying loss in accuracy. The squares are for $T > T_c$ while X represent data for $T < T_c$. This graph suggests the usual power law behavior of the susceptibility

$$\chi \propto |(T - T_c)/T_c|^{\gamma} \tag{4}$$

with $\gamma = 1.97$ for $T > T_c$ and $\gamma = 1.85$ for $T < T_c$. The error in γ is ± 0.1. The slopes of the drawn lines denote γ. The value for γ is unusually large. For a three dimensional system γ has the value between 1 and 1.25 while the calculated value for the two dimensional Ising model is 1.75 (see reference 38 p. 47). Our values appear to be higher than that and thus it appears that we are dealing wih a somewhat different phenomenon. Our data were also fitted to an equation derived by Kosterlitz [40]

$$\chi \propto exp(bt^{-.5}) \tag{5}$$

where b is a constant. Our data fit Eq.(5) only in a very limited temperature region. The data shown in Fig.(10) are well within the accuracy of our experiment since $ln|(T - T_c)/T_c| = -7.5$ represents a temperature difference of one millidegree.

Figures (11) and (12) show the magnetic field dependence of the susceptibility. Two configurations were used. The measuring field was along the a-b plane while the applied dc magnetic field was normal to the measuring field either along the a-b, in plane direction H_a, or along the c-axis direction H_c. Both the temperature shift of the maximum and the size show a high field and low field behavior. The horizontal axis is calibrated in terms of H_o where H_o has a value of 17G for H_c and 7.5G for H_a.

Figure (11) shows the temperature at which the peak occurs, in terms of the reduced temperature $(T-T_c)/T_c$ as a function of the applied field. Here T_c is the trasition temperature at zero field. One sees that the maximum is shifted to higher temperatures as the magnetic field is applied. Moreover, two straight lines can be drawn through the points. One at low field with a steep slope and one at high field with a shallower slope. The slope at low field is a factor of 3 greater than that at high field. In addition, H_a is more effective in shifting the temperature of the maximum than H_c by a factor of 17/7.5, the ratio of H_o in the respective directions. A similar low and high field behavior is seen if one plots the logarithm of the susceptibility peak size as a function of the applied magnetic field normalized to H_o, as shown in Fig.(12). One can fit the data in Fig.(12) with the expression

$$\chi_{max}(H) = \chi_{max}(0)exp(-\phi H/H_o) \tag{6}$$

with χ_{max} denoting the susceptibility at the maximum. For H_a the value of $\phi = 1.3$ for the low field and $\phi = 0.6$ at high field, while for H_c the value of $\phi = 1$ for low field and $\phi = 0.4$ for high field. Similar behavior was observed in other GIC samples [24].

To summarise, our data obey the power law behavior of general second order phase transitions, with an exponent γ greater than that expected for a two-dimensional Ising model. In an externally applied magnetic field the susceptibility maximum exhibits a distinct low field and high field behavior.

CONCLUSION

The in-plane magnetic susceptibility data of $FeCl_3$ GIC indicate that all the stages of this intercalant compound possess a low temperature magnetic phase transition at temperature between 1.7K and 1.8K. This transition obeys the power law dependence of second order transitions. The data suggest that the transition is two-dimensional in nature. Similarities in the behavior of the transition and calculations of the behavior of a two-dimensional dipolar system on a honeycomb lattice suggest that dipolar interactions play a significant role. The relative size of the anomaly in the magnetic susceptibility is maximum for stage 5. If the size of the low temperature susceptibility maximum is taken as an indication of two-dimensionality, then the shielding of the magnetic interaction by graphite layers is exponential. The variation in the size of the maximum is described as a competition between the staging mechanism which contributes to the two-dimensionality and the in-plane density.

As shown in GIC, the graphite layers between the intercalant layers screen the intercalant interplane interactions in a way as to provide a two-dimensional magnetic system. The low dimensional nature of this phase trasition is supported by the dependence of the susceptibility peaks on the magnetic field, the application of a small dc magnetic field in the order of 10G smears out the peak completly, whereas one would expect this to happen at fields of the order of 1.6kG in three dimensions. The c-axis susceptibility does not show any anomaly at low temperature. Moreover, the susceptibility in this direction is not senstive to the small dc external magnetic fields which implies the confinement of the intercalant magnetic spins to the planes parallel to the graphite layers.

Acknowledgment

We would like to acknowledge with thanks Dr. A.W. Moore for donating the HOPG, Dr. G. Dresselhaus and Dr. M.S. Dresselhaus for many helpful discussion and

preperation of initial samples, Dr. S.E. Millman and Dr. B.W. Holmes who participated in the initial measurements and Dr. R.B. Frankel and Dr. G. Papaefthymiou for their help in the Mössbauer analysis.

REFERENCES

1- A. Hérold, in Physics and Chemistry of Materials with Layered Structures, edited by F. Levy (Dordrechet, Reidel,1979),p.323.

2- M.S. Dresselhaus and G. Dresselhaus, Adv. Phys. 30,139(1981).

3- M. Elahy and G.Dresselhaus, MRS, Sympos. Proc. 20,207(1983).

4- Yu.S. Karimov, Sov. Phys. JETP 41,772(1976).

5- A. Erbil, R.J. Birgeneau and M.S. Dresselhaus, Phys. Rev. Lett. 49,1427 (1982).

6- M.D. Daybell, Rev. Sc. Inst. 38,1412(1967).

7- S. Blairs and R.A.J. Shelton, J. Inorg. Nucl. Chem. 28, 1855(1966).

8- G.K. Wertheim, P.M. von Attekum, H.J. Guggenheim, and K.E. Clements Solid State Commun. 33, 809(1980).

9- B.V. Liengme, M.W. Bartlett,J.G. Hooley, J.R. Sams, Phys. Lett. 25,127 (1967).

10- K. Ohhashi and I. Tsujikawa, J. Phys. Soc. Jpn. 36, 422(1974).

11- N. Caswell and S.A. Solin, Solid State Commun. 27, 961(1978).

12- M.L. Dzurus and G.R. Hennig, J. Am. Chem. Soc. 79, 1051(1957).

13- S.E. Millman, and G. Kirczenow, Phys Rev. B28,5019(1983).

14- Yu.S. Karimov, A.V. Zvarykina and Yu.N. Novikov, Sov. Phys.-Solid State 13,2388(1972).

15- D. Hohlwein, P.W. Readman, A. Chamberod, And J.M.B. Coey, Phys. Stat. Sol. B64,305(1974).

16- J.P. Stampfel, W.T. Oosterhuis, B. Window, and F. deS. Barros, Phys. Rev. B8,4371(1973).

17- S.E. Millman, M.R. Corson, and G.R. Hoy, Phys Rev B25, 6595(1982).

18- S.E. Millman, B.W. Holmes, and G.O. Zimmerman, Solid State Commun., 43,903(1982).

19- M.R. Corson, S.E. Millman, G.R. Hoy, and H. Mazurek, Solid state Commu., 42,667(1982).

20- G.O. Zimmerman, B.W. Holmes and G. Dresselhaus, Extenden Abstracts of the 15th Biennial Conference on Carbon, University of Pennsylvania pp.42(1981).

21- S.E. Millman and G.O. Zimmerman, J. Phys.C:Solid State Phys., 16,L89 (1983).

22- Yu.S. Karimov, Sov. Phys. JETP 38,129(1974).

23- Yu.S. Karimov, Sov. Phys. JETP Lett. 19,159(1974).

24- M. Elahy, C. Nicolini, G. Dresselhaus, and G.O. Zimmerman, Solid State Commun. 41,289(1982).

25- Y. Kimishima, A. Furukawa, K. Koga, H. Nagona, and M. Suzuki, Extended Abs. on GIC, MRS Meeting(1984), Boston, Mass(USA).

26- H. Suematsu, K. Ohmatsu, and R. Yoshizaki, Solid State Commun 38,1103 3Q981).

27- S.E. Millman Synth. Met., 5,147(1983)

28- G. Kirczenow Phys Rev. B31, 5376(1985).

29- S. Hendricks, and E. Teller, J. Chem. Phys. 10,147(1942).

30- W. Metz and D. Hohlwein, Carbon 13, 87(1975),(Pergamon Press)

31- S.E. Millman, Phys. Lett. 92A,441(1982).

32- A.K. Ibrahim, and G.O. Zimmerman, Phys Rev. B, 34, 4224(1986).

33- C.V. Berney and C. Underhill, Synthetic Metals, 4,71(1981).

34- S. Flandrois, J.M. Masson, J.C. Rouillon, J. Gaultier, and C. Hauw, Synthetic Metals, 3,1(1981).

35- G.O. Zimmerman, A.K. Ibrahim, and F. Wu, Bulletin of the APS, 31,508(1986).

36- M. Suzuki and H. Ikeda, J. Phys.C:Solid State Phys., 14,L923(1981).

37- L. Lundgren, P. Svedlindh, and O. Beckman, J. of Mag. and Mag. Mat. 25,33(1981).

38- H.E. Stanley "Introduction to Phase Transitions and Critical Phenomena" Oxford University Press, New York-Oxford, (1971).

39- J.M. Kosterlitz and D.J. Thoules, J. Phys C: Solid State Phys 6, 1181(1973).

40- J.M. Kosterlitz, J. Phys. C: Solid State Phys 7,1046(1974).

41- D. de Klerk, Adiabatic Demagnetization, Handbuch der Physik XV S. Flügge Edtr., Springer-Verlag, Berlin(1956).

Table I

Stage index versus the relative peak size and the peak temperature of the susceptibility for $FeCl_3$ IGC.

Stage	Peak Size	Temperature
1	0.0846	1.793
2	0.2256	1.745
3	0.4381	1.746
4	1.4381	1.710
5	5.1877	1.735
6	1.8329	1.761
9	1.4706	1.768

FIGURE CAPTIONS

Fig. 1. Layered structure for stage 2 $FeCl_3$-GIC, the striped layers are the intercalant.

Fig. 2. The in-plane magnetic susceptibility vs temperature for different stages of $FeCl_3$-GIC near the transition temperature. The insert shows the logarithm of the peak height (χ_m) as a function of the stage index (n) to emphasize the exponential behavior for $1 \leq n \leq 5$.

Fig. 3. The in-plane magnetic susceptibility vs temperature for stage 6 $FeCl_3$-GIC. H denotes the applied dc magnetic fields in Gauss in the a-b direction.

Fig. 4. The in-plane magnetic susceptibility vs temperature for stage 3 $FeCl_3$-GIC. H denotes the applied dc magnetic fields in Gauss in the a-b direction.

Fig. 5. The in-plane magnetic susceptibility vs applied magnetic field for stage 6 $FeCl_3$-GIC near the transition temperature.

Fig. 6. The in-plane magnetic susceptibility vs applied magnetic field for stage 3 $FeCl_3$-GIC near the transition temperature.

Fig. 7. The low temperature c-axis magnetic susceptibility vs temperature near the transition temperature for stage 6 $FeCl_3$-GIC. H denotes the applied dc magnetic fields in Gauss.

Fig. 8. The c-axis susceptibility vs temperature for stage 3 and stage 6 $FeCl_3$-GIC extended to high temperatures.

Fig. 9. Natural logarithm of the shape-corrected in-plane susceptibility at zero dc magnetic field vs the reduced temperature for stage 6 $FeCl_3$-graphite intercalation compound.

Fig. 10. Natural logarithm of the in-plane susceptibility at zero dc magnetic field vs natural logarithm of the reduced temperature showing the universal power law behavior. The squares denote data for $T>T_c$ and the x denote data for $T<T_c$.

Fig. 11. Temperature dependence of the in-plane susceptibility maximum vs the applied

dc magnetic field for stage 6 $FeCl_3$-GIC. The squares are for H along the c-axis (H_c) and the x are for H along the a-b plane (H_a).

Fig. 12. Natural logarithm of the in-plane susceptibility maximum vs the applied dc magnetic filed for stage 6 $FeCl_3$-GIC. The squares are for H along the c-axis (H_c) and the x are for H along the a-b plane (H_a).

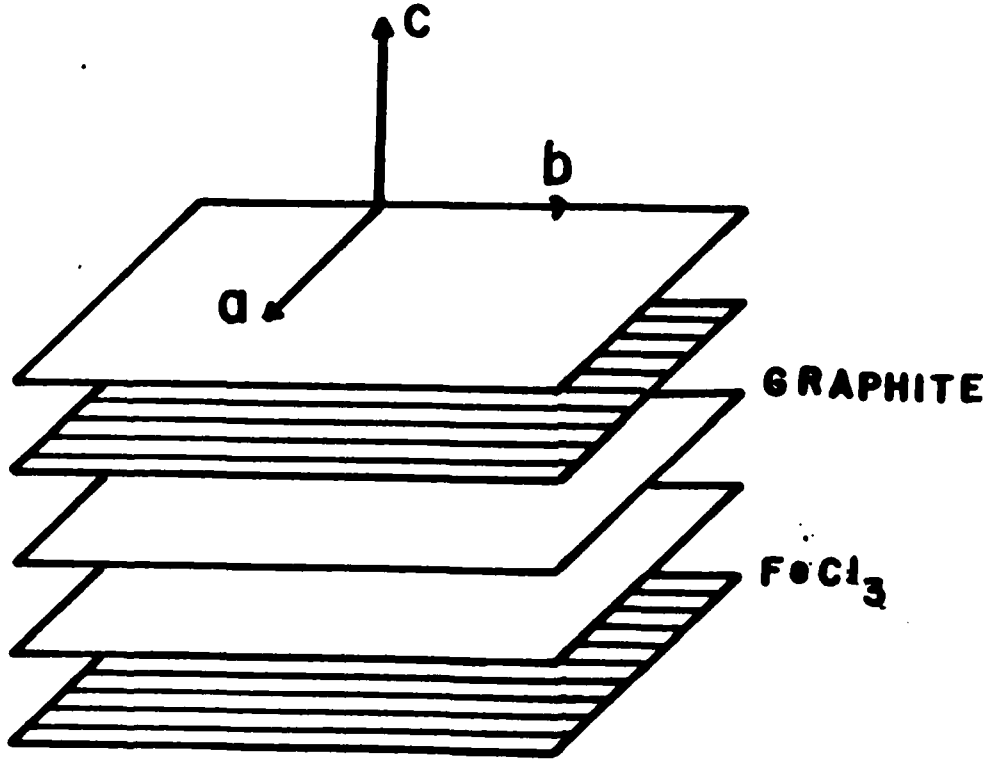

STAGE-2

Fig 1

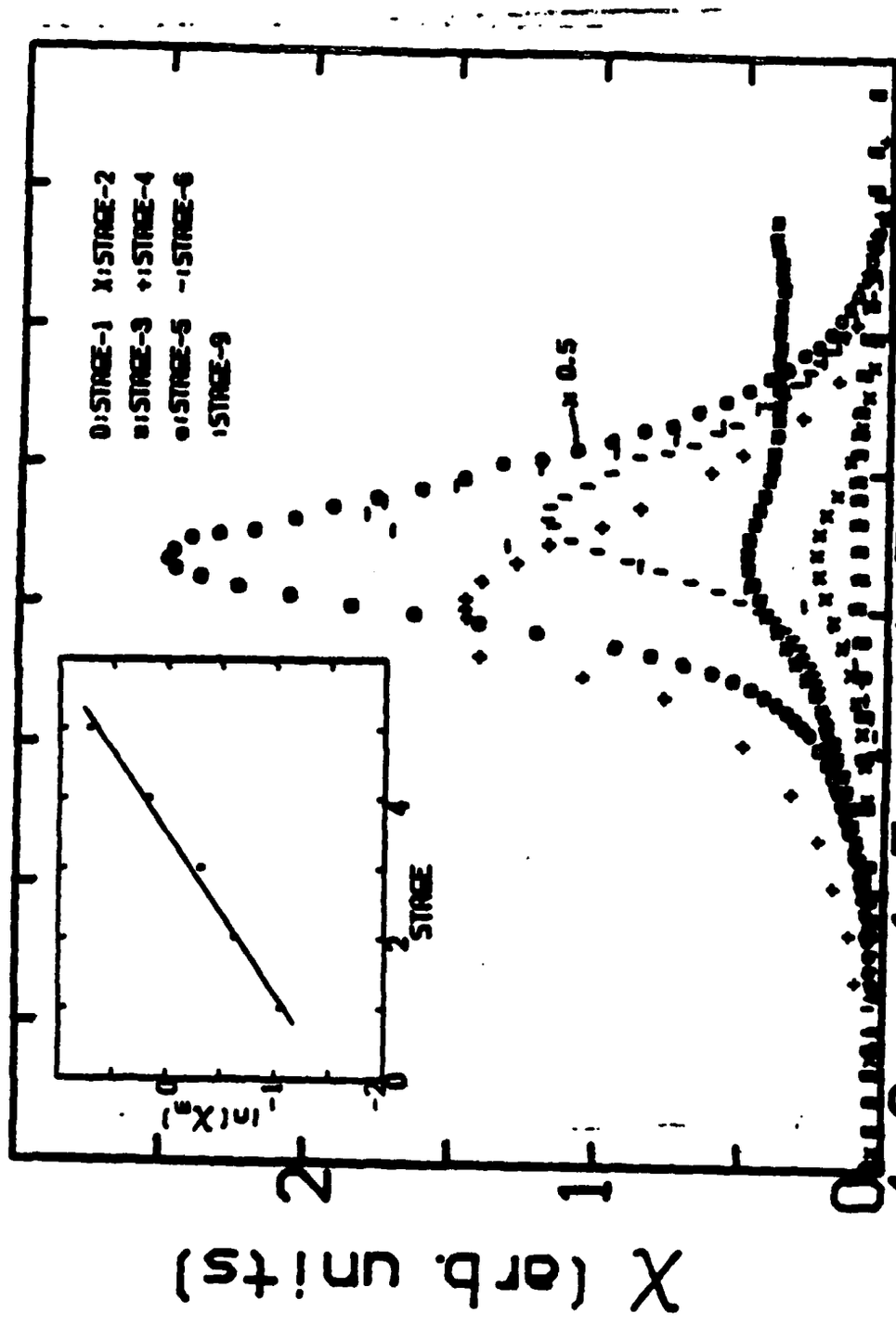
χ (arb. units)
T(K)
0:STAGE-1
X:STAGE-2
■:STAGE-3
+:STAGE-4
●:STAGE-5
-:STAGE-6
!STAGE-9
0.5
STAGE
ln(χ")

Fig 2

F 193

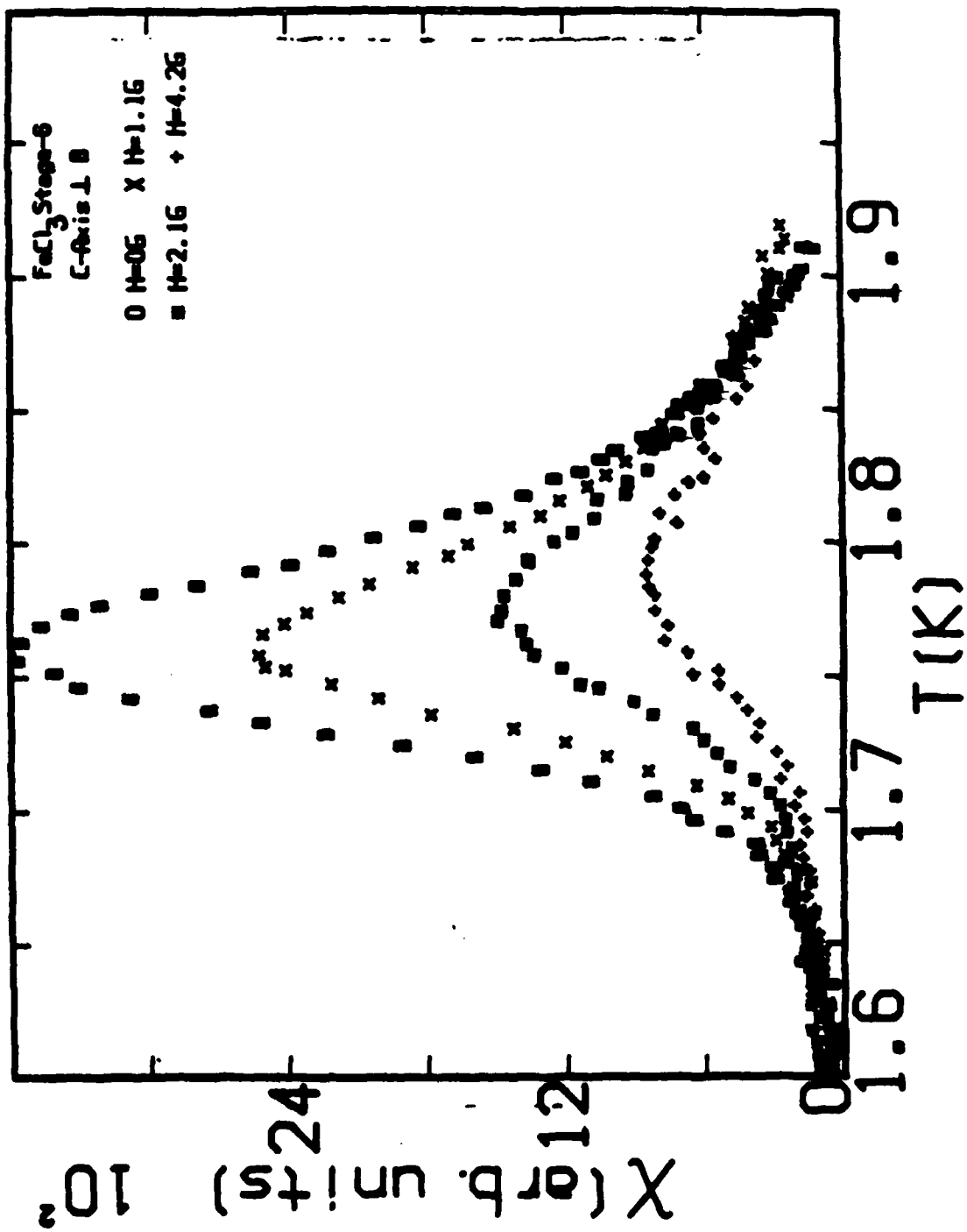
$FeCl_3$ Stage-8
C-Axis ⊥ B
O H=0G X H=1.1G
■ H=2.1G ◆ H=4.2G
χ (arb. units) 10^2
24
12
0
1.6
1.7
1.8
1.9
T(K)

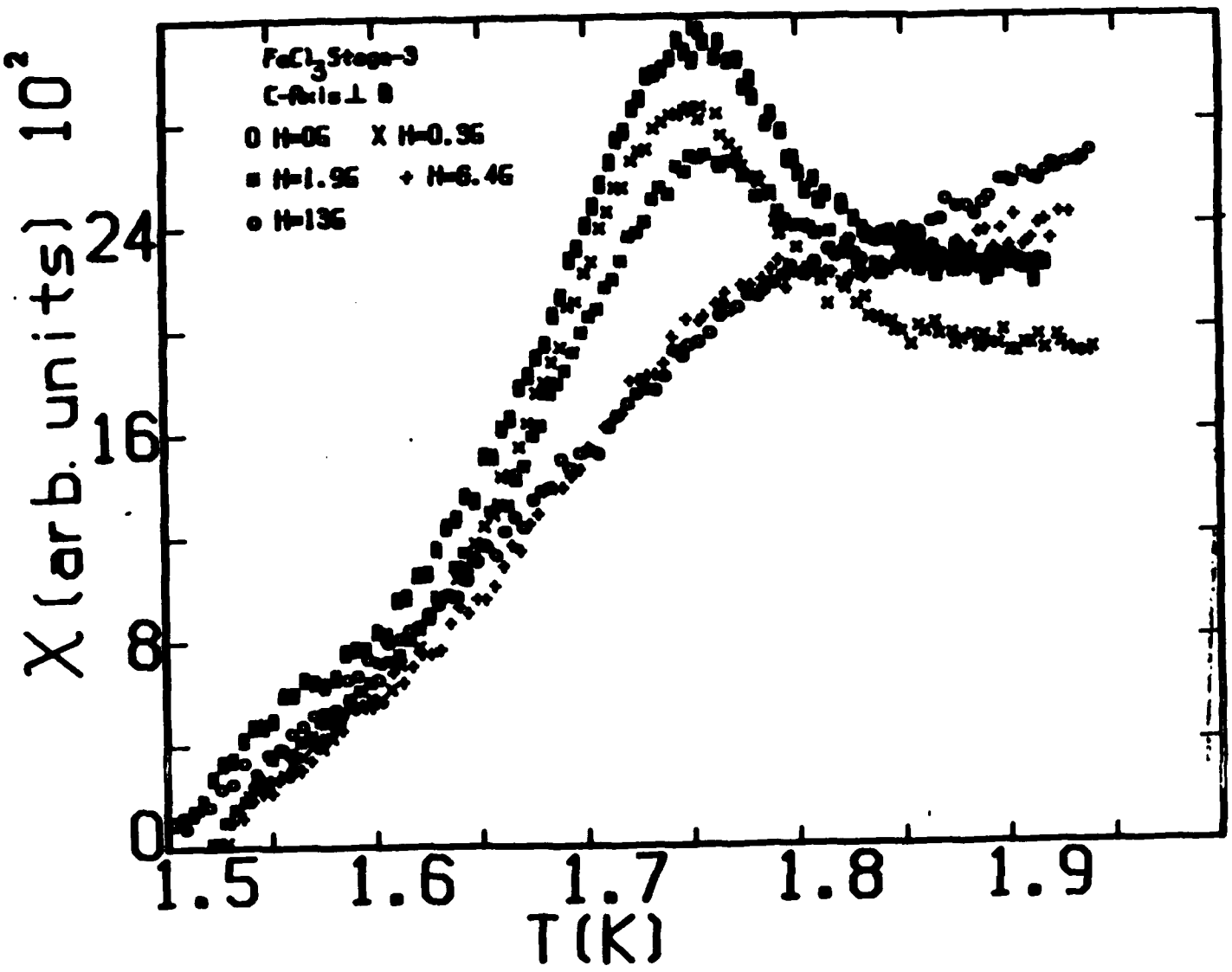
$FeCl_3$ Stage-3
C-Axis ⊥ B
O H=0G X H=0.5G
■ H=1.9G + H=6.4G
● H=13G
X (arb. units) 10^2
24
16
8
0
1.5
1.6
1.7
1.8
1.9
T(K)

Fig 4

F.G. 4

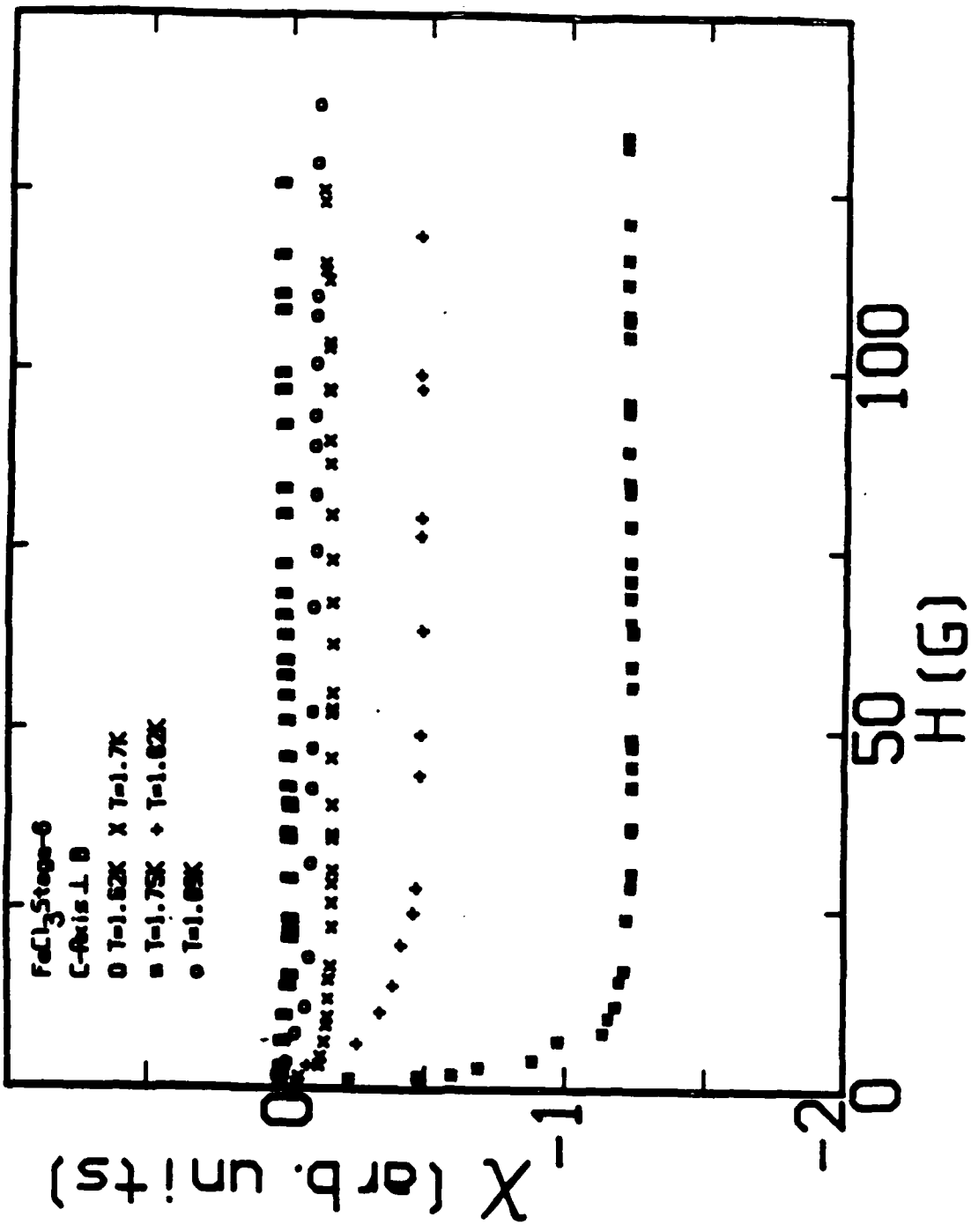
FeCl3 Stage-6
C-Axis ⊥ B
0 T=1.62K X T=1.7K
■ T=1.75K + T=1.82K
● T=1.85K
χ (arb. units)
0
-1
-2
0
50
100
H(G)

Fig 5

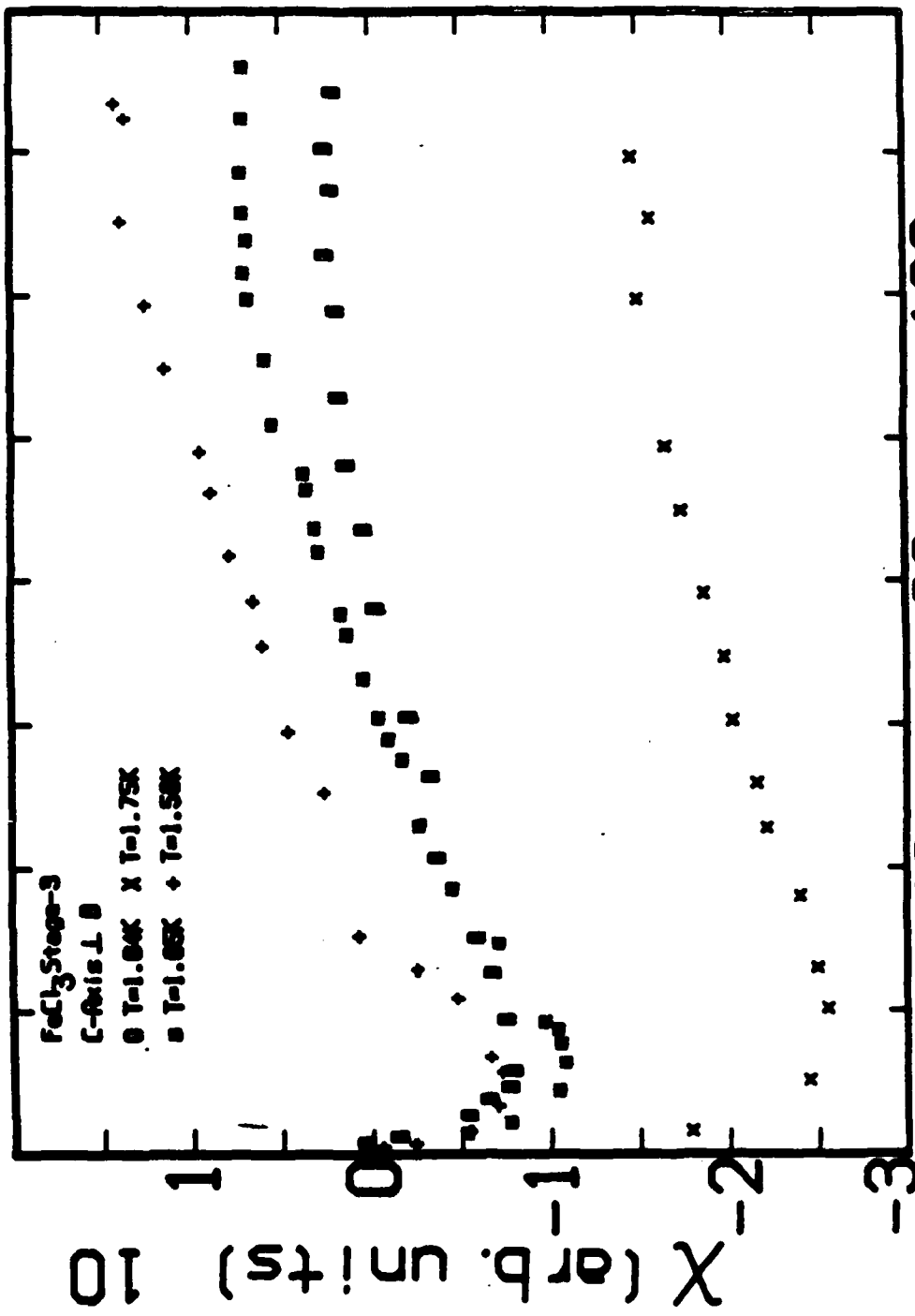
FeCl3Steop-3
C-Axis⊥ B
T=1.84K
T=1.75K
T=1.65K
T=1.50K
χ (arb. units) 10
H (G)
1
0
-1
-2
-3
0
40
80
120

Fig 6

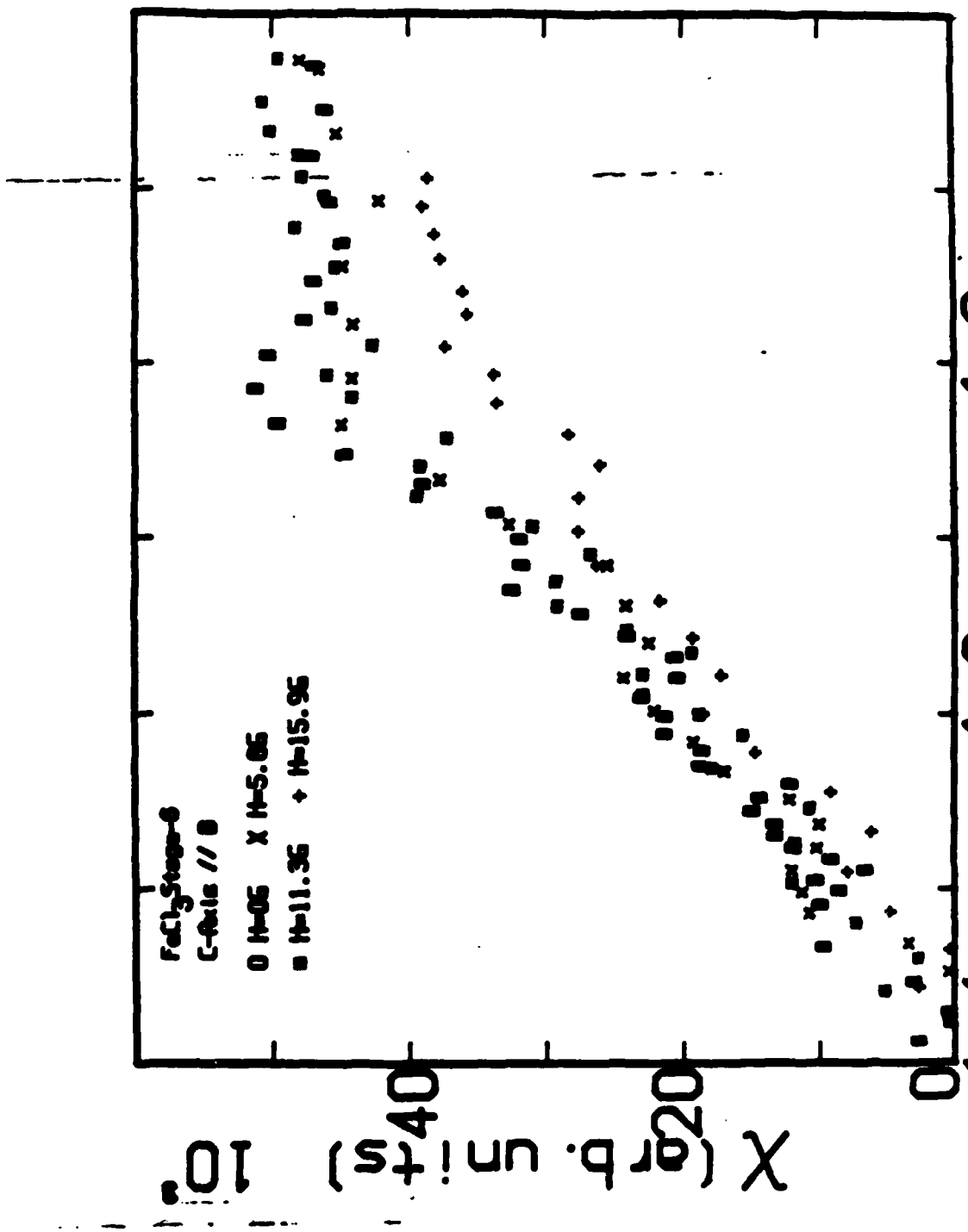
FeCl3Strong-S
C-Axis // B
O H=0G X H=5.0G
■ H=11.3G + H=15.9G
χ (arb. units) 10⁶
0
20
40
1.4
1.6
1.8
T(K)

Fig 7

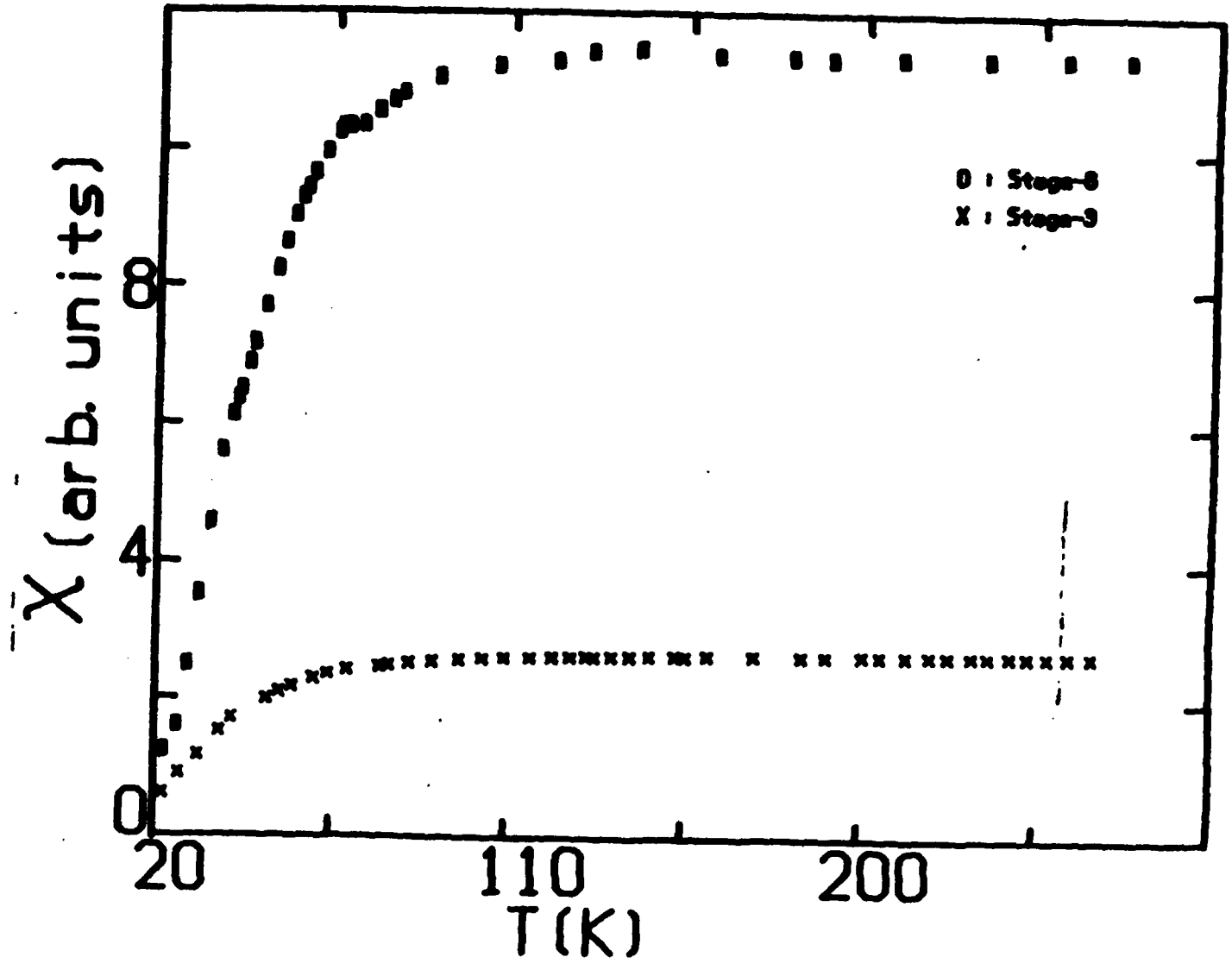

Fig 8

F.G. 8

Fig 9

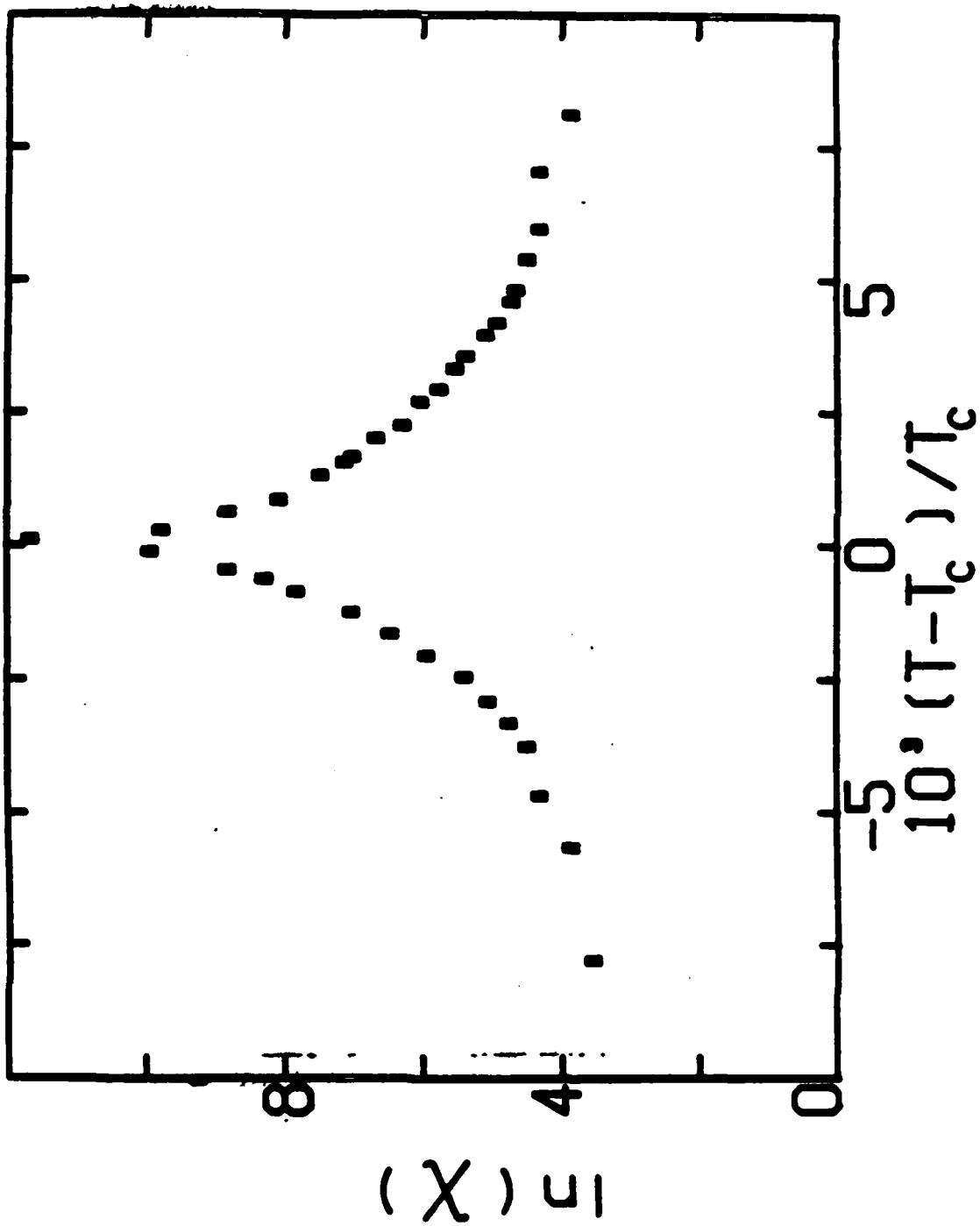

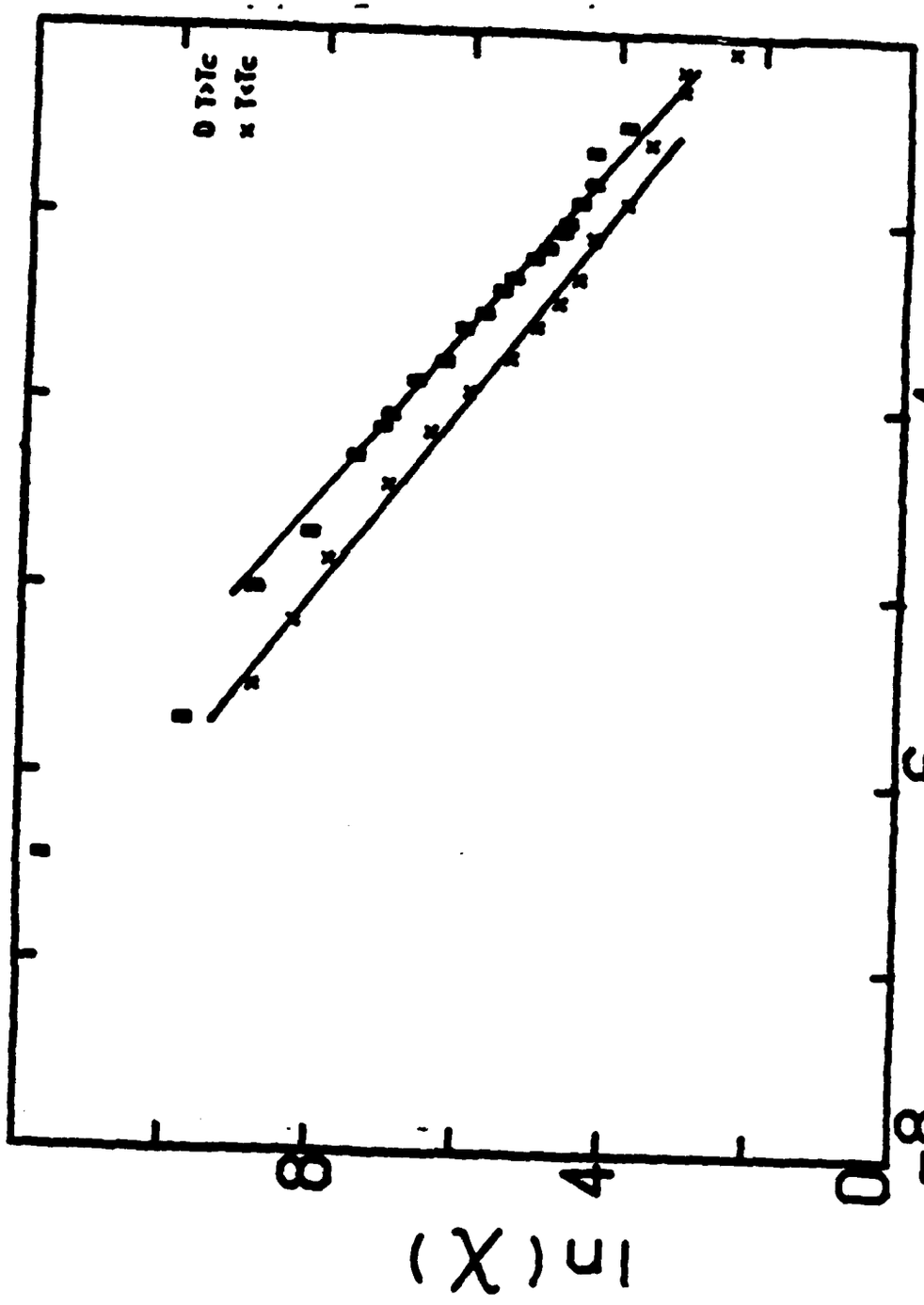

Fig 10

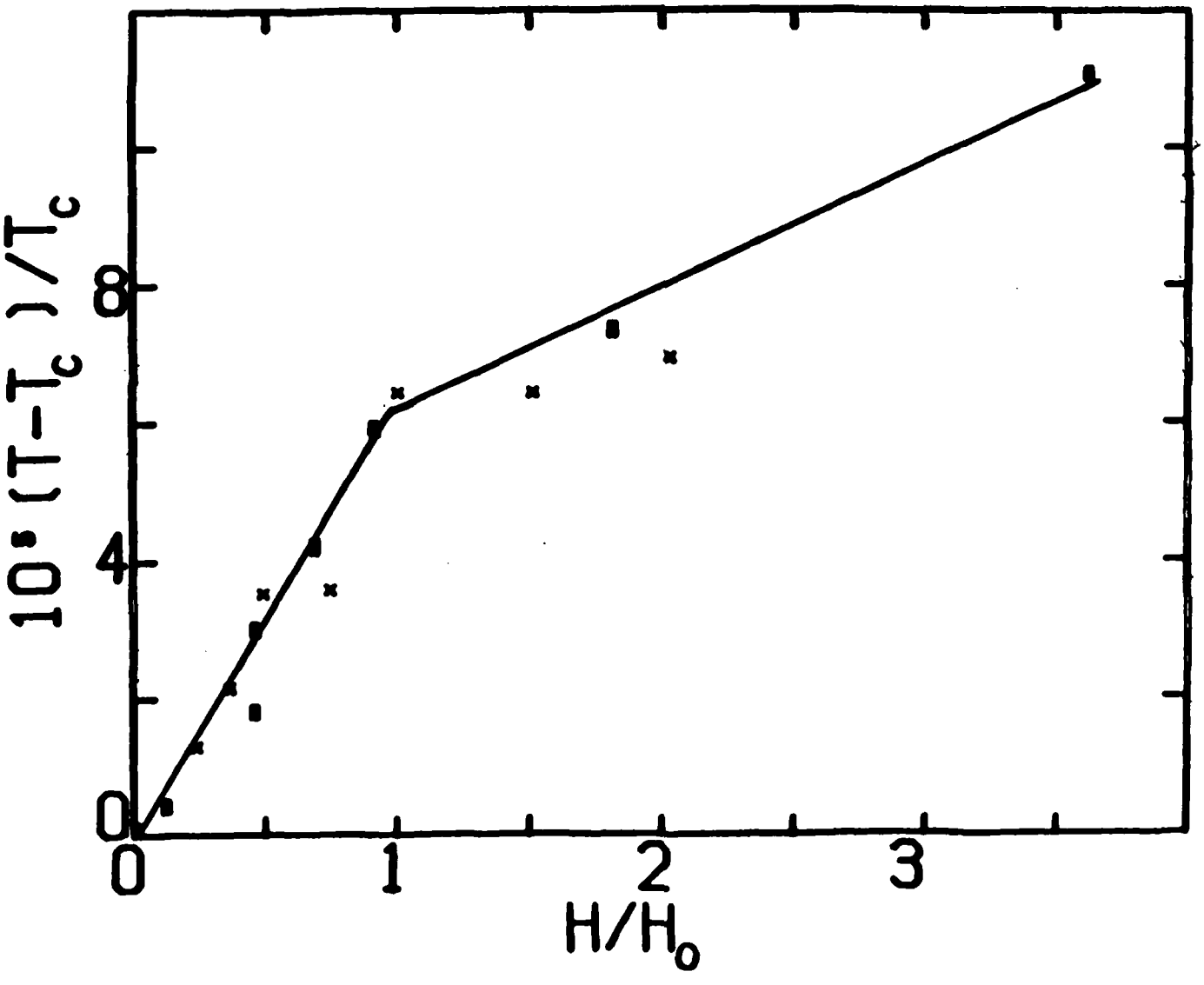

Fig. 11

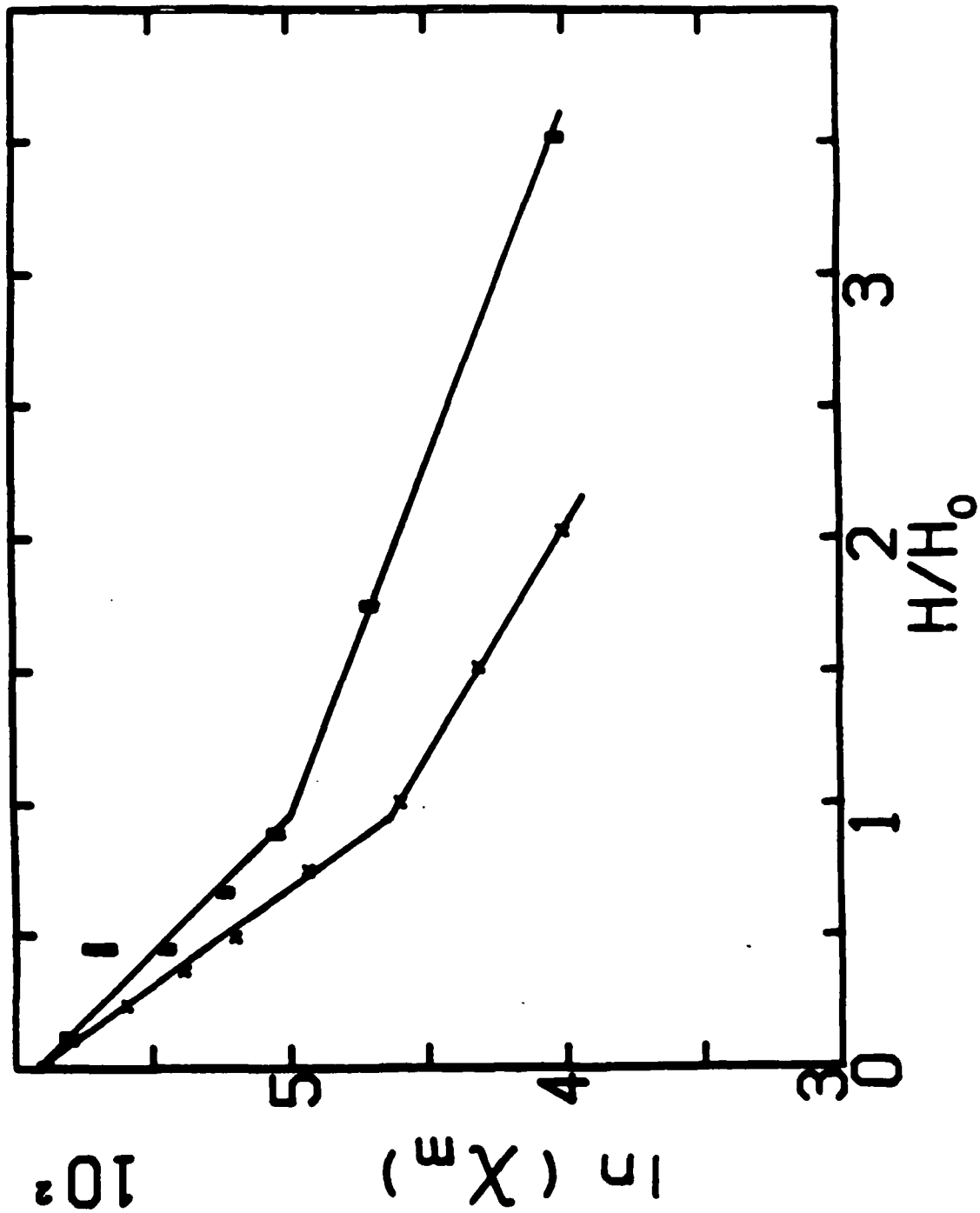

Fig 12

J. Phys. C: Solid State Phys., 16 (1983) L89–L93. Printed in Great Britain

APPENDIX III

LETTER TO THE EDITOR

Observation of spin glass state in $FeCl_3$: intercalated graphite

S E Millman† and G O Zimmerman
Physics Department, Boston University, Boston, Mass. 02215, USA

Received 9 August 1982

Abstract. $FeCl_3$ intercalated graphite compounds exhibit a sharp maximum in magnetic susceptibility at 1.7 K. By using Mössbauer spectroscopy as a characterisation tool, we show that this peak is dramatically enhanced as the number of iron vacancies in the intercalant lattice is increased. These results strongly suggest that the sharp susceptibility maximum is due to a spin glass transition where the iron vacancies inhibit long-range magnetic order, thus providing a new series of compounds to help elucidate the many unknown properties of the spin glass state.

The onset of a spin glass state is frequently signalled by a rather sharp peak in the susceptibility at low magnetic fields (Mydosh 1981, Maletta 1980). Although this state from a theoretical point of view is still a puzzle, one frequently invokes strong magnetic short-range order as a qualitative description of the sharp peak. Chemical short-range order would strongly affect such magnetic short-range order (Binder 1982). In this Letter we use a very recently developed characterisation technique for graphite—$FeCl_3$ compounds, Mössbauer spectroscopy, to analyse the microscopic structure of each sample. In particular, we find sites which are nearest neighbours to iron vacancies whose numbers vary from sample to sample. By comparing samples having x-ray diffractograms which are almost identical, we find that the amplitude of the sharp susceptibility peak shows a dramatic increase as the number of sites which are nearest neighbours to iron vacancies is only slightly increased, as if approaching a percolation threshold. In addition, we provide a new series of compounds, the magnetic graphite intercalation compounds on which the spin glass state can be studied, which has quite different physical properties from the usual metallic alloys.

Previous experiments by Elahy *et al* (1982) have shown that the existence of a sharp peak in susceptibility is a rather universal property among many magnetic compounds which may be intercalated into graphite. However, these experiments have been interpreted as being due to the existence of a two-dimensional XY model transition and have been compared to the theory of Kosterlitz and Thouless (Suzuki and Ikeda 1981). The sharp peak in susceptibility was proposed by Elahy *et al* (1982) as being the universal magnetic signature for magnetic intercalants of stage $\geqslant 2$. In this work we show that, in the limit of no iron vacancies, the susceptibility curves tend to an antiferromagnetic peak for stage 2 $FeCl_3$ intercalants. Even for samples exhibiting a large sharp peak in the

† Present address: IBM Research Laboratories, 5600 Cottle Rd, San Jose, CA 95193, USA.

0022-3719/83/040089 + 05 $02.25

C4—8

susceptibility curves the bulk of the iron atoms still enter into a long-range magnetically ordered state.

The samples studied were prepared by intercalating anhydrous $FeCl_3$ into highly ordered pyrolytic graphite using the two-zone vapour transport method. Employing this growth process, the graphite temperature is maintained at 350 °C while the temperature of the ferric chloride is varied to achieve different stages. An overpressure of about 250 Torr of chlorine gas was used to encourage staging. The intercalated compounds were characterised for identity and uniformity of staging using (00*l*) x-ray diffraction both before and after our susceptibility measurements. All samples were essentially single staged, showing only very weak secondary diffraction peaks due to other stages.

The molecular structure of graphite–$FeCl_3$ has been determined by x-ray and electron diffraction studies and by electron microscopy studies (Cowley and Ibers 1956, Evans and Thomas 1975). These studies have concluded that the molecular structure of graphite–$FeCl_3$ is essentially unchanged from that of its two constituents. As in pristine anhydrous $FeCl_3$, the iron ions form hexagonal planes where each iron atom is surrounded by an octahedron of chlorine ions.

The susceptibility measurements were made by a standard AC bridge method (Maxwell 1965) operating at about 40 Hz. The amplitude of the magnetic field at the sample was kept below 1 Oe. The susceptibility coils were kept at a constant temperature while the temperature of the samples was varied inside an isolated chamber. The temperatures above 4.2 K were measured by a calibrated carbon resistor and a calibrated metal resistance thermometer (Millman *et al* 1982). Below 4.2 K the sample was in direct contact with the helium bath and temperatures were determined from the vapour pressure of the helium bath.

Mössbauer spectra were taken in transmission geometry with the γ ray direction parallel to the graphite *c* axis. Temperatures were controlled to within 0.1 K and were measured by a calibrated diode.

In figure 1 we show the low-temperature portion of our susceptibility curves with the measuring field parallel to the basal plane for three stage 2 samples. Although the samples have almost identical x-ray diffractograms, the susceptibility curves show some quite dramatic differences. In particular, the sharp peak present at 1.7 K has a much different amplitude for the three samples. We will label the samples in order of increasing peak amplitude as samples 1 to 3. The susceptibility is given in arbitrary units but each curve has been normalised to the amount of iron in each sample. The relative amount of iron in each sample was calculated by comparing the areas under the Mössbauer curves of each of the samples at the same temperature. The only error arising in this calculation is that the background radiation is assumed to be sample-independent. However, since the same Mössbauer apparatus was used for this measurement we can assign at most a 5% error bar to possible slightly different sample alignments. We will show later by comparing the backgrounds of the susceptibility curves that this method of calculating the relative amount of iron is quite sensitive. Although one usually assumes that the stoichiometry $C_{6.6n}FeCl_3$ (where n is the stage) is valid, we have found that this method may be quite inaccurate, due either to formation of intercalant islands, a gradient in concentration through the bulk sample, or a loss of some of the intercalant over long periods of time (Millman 1982a).

The Mössbauer spectra of these samples at 10.0 K are shown in figure 2. Notice the small peaks which are superimposed on both sides of the main peak, as shown in the figure. Although we will discuss the interpretation of this site in more detail elsewhere (Corson *et al* 1982, Millman 1982b), briefly it has an isomer shift indicative of an Fe^{3+}

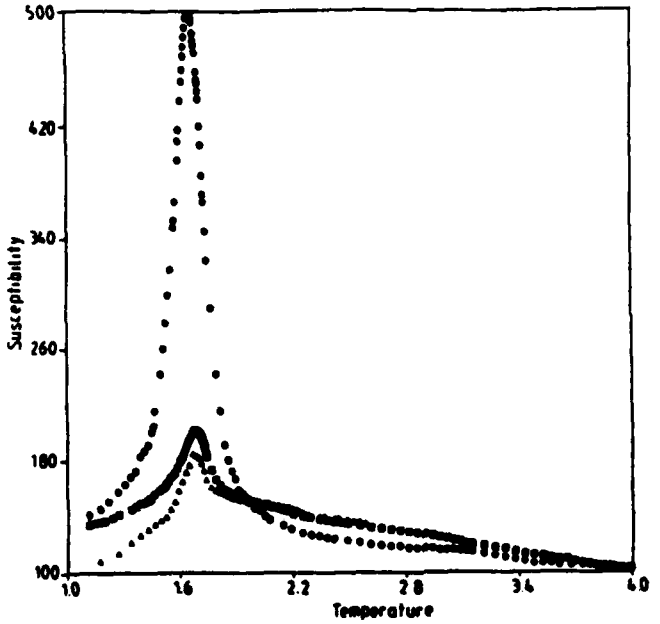

Figure 1. Susceptibility versus temperature for three different stage 2 graphite–$FeCl_3$ compounds. The susceptibility is plotted in arbitrary units but each sample has been normalised for the relative amount of iron it contains. △, sample 1; □, sample 2; ○, sample 3.

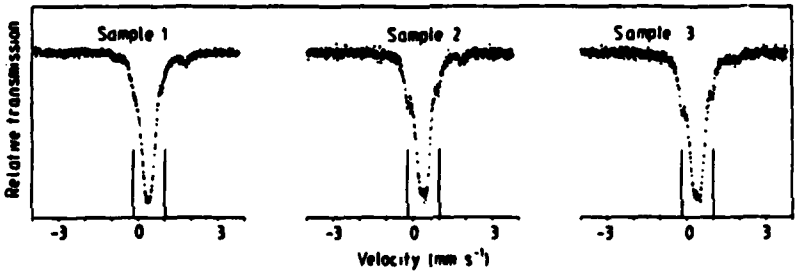

Figure 2. Corresponding Mössbauer spectra for the three samples whose susceptibility curves are shown in figure 1. The position of the two peaks which comprise the iron sites nearest neighbour to iron vacancies are indicated by the straight lines. Zero velocity is measured relative to the centre of gravity of an iron foil spectrum at room temperature.

ion but a quite large quadrupole splitting for an Fe^{3+} ion of 1.3 mm s^{-1}. The relative ratio of peak intensities is 5:3, which indicates that the major axis of the electric field gradient tensor is pointing in the basal plane. The large quadrupole splitting along with the direction of the major axis of the electric field gradient tensor indicates that these sites are nearest neighbours to iron vacancies in the intercalant planes. A model for iron vacancies in graphite $FeCl_3$ has already been proposed by Wertheim *et al* (1980). We will show later that the susceptibility curves are also consistent with the existence of an in-plane anisotropy axis. The main result of these Mössbauer spectra is that as the number of sites which are nearest neighbours to iron vacancies is increased the sharp peak in the susceptibility correspondingly increases. By comparing the relative areas of the Mössbauer spectra our least-squares fits to the spectrum show that 7 ± 1%, 9 ± 1% and 11 ± 1% of the total iron sites are nearest neighbours to iron vacancies.

The height of the sharp susceptibility peak does not seem to depend linearly on the number of sites nearest neighbour to iron vacancies. In fact, the relative magnitude of this peak increases for the three samples in the sequence 1, 1.5, 12.5 as the number of sites nearest neighbour to vacancies increases as 7, 9, 11. This nonlinear dependence on vacancies may indicate that a percolation threshold is being approached. We also find that the susceptibility curves show very anisotropic behaviour. If we measure the susceptibility perpendicular to the basal plane we find only a very tiny contribution of the sharp peak at 1.7 K, which can be completely explained as arising from a parallel susceptibility component due to the small crystalline misorientation known to exist in these compounds. Therefore, the susceptibility curves corroborate the Mössbauer measurements, which indicates a large in-plane anisotropy axis.

We remark that even for the sample exhibiting the largest peak in the susceptibility, the bulk of the spins still exhibit long-range magnetic order as we have reported elsewhere (Millman *et al* 1982). Since the sharp peak in susceptibility is shown to be quenched by DC fields as small as 20 Oe (Zimmerman *et al* 1981, Elahy *et al* 1982) it is quite easy to deconvolute the two contributions to the susceptibility. We show in figure 3 the curve of one of the samples, sample 2, for which the sharp peak has been quenched by a DC field of 80 Oe, along with that with no external DC field. We note that the backgrounds of the curves shown in figure 1 are almost identical in the paramagnetic regime (above 2.3 K) for samples 1 and 2 and only slightly smaller for sample 3. The slightly smaller background for sample 3 can be explained as arising from the increased number of spins for this sample which are contained in the spin glass peak. The consistency of the back-

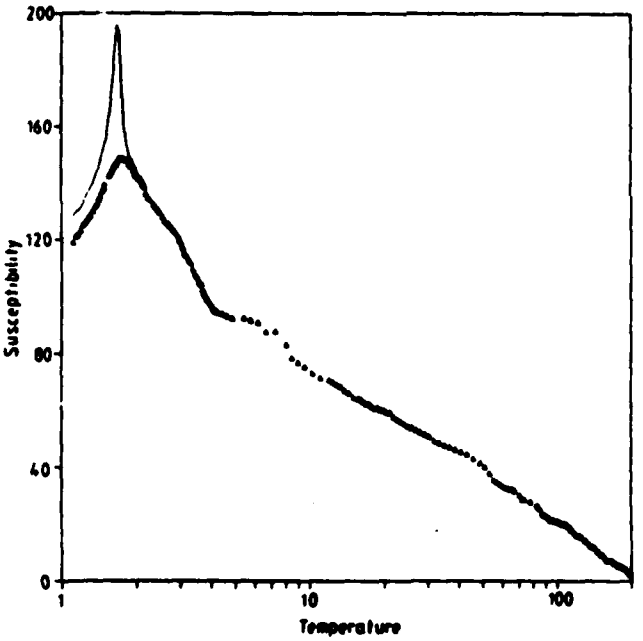

Figure 3. Susceptibility versus temperature over a wide range of temperature for sample 2 in figures 1 and 2. The line represents the susceptibility curve in zero external DC field while the triangles represent the susceptibility curve at 80 Oe, which has been applied to quench the spin glass peak. Notice how small the sharp spin glass peak is compared to the rest of the susceptibility curve even when drawn on a logarithmic scale. The susceptibility units are the same as those in figure 1.

grounds indicates that the normalisation of the susceptibility curves by Mössbauer spectroscopy is quite accurate.

These results indicate that the sharp peak observed in the susceptibility is not due to the two-dimensionality of the compound but rather to vacancies inhibiting the long-range order of some of the spins. Anhydrous $FeCl_3$ is known to contain competing interactions since its spin structure has been shown to be a spiral through neutron diffraction (Cable *et al* 1962). Therefore, increasing the number of vacancies is akin to putting non-magnetic impurities into a system containing competing interactions which for sufficient non-magnetic impurities will cause the system to go over to the spin glass state (Mydosh 1981, Maletta 1980). Although these results have only been shown for the $FeCl_3$ intercalant, the existence of similar sharp peaks in other magnetic intercalants suggests that intercalant vacancies also occur in these compounds. In fact, small intercalant islands of only about 100 Å in diameter have been observed in graphite–$NiCl_2$ (Flandrois *et al* 1981). It seems rather likely that if such small islands are occurring, then vacancies would also exist in these islands.

In conclusion, by using Mössbauer spectroscopy as a tool for calibrating the microscopic structure of $FeCl_3$ intercalated graphite compounds we have found a strong dependence in the magnetic susceptibility curves with the amount of sites which are nearest neighbours to iron vacancies. The sensitivity of Mössbauer spectroscopy is even more surprising when we consider that, assuming uncorrelated vacancies, the threefold honeycomb lattice implies that only 4% of the local number of intercalant atoms are vacant, even for sample 3. These results may also help in understanding the spin glass state better, since they introduce a new series of compounds for which it can be studied.

We are happy to acknowledge many helpful discussions with G Dresselhaus, M S Dresselhaus, R B Frankel, G Kirczenow, G Papaefthymiou and S Redner. We would also like to thank R B Frankel and G Papaefthymiou for making their Mössbauer spectrometer available to us. This work was supported by AFOSR subcontract F49620-81-C-0006 and by the Francis Bitter National Magnet Laboratory which is supported by the NSF.

References

Binder K 1982 *Solid State Commun.* **42** 377
Cable J M, Wilkinson M K, Woolan E O and Koehler W C 1962 *Phys. Rev.* **127** 714
Corson M R, Millman S E, Hoy G R and Mazurek H 1982 *Solid State Commun.* **42** 667
Cowley J M and Ibers J A 1956 *Acta Crystallogr.* **9** 421
Elahy M, Nicolini C, Dresselhaus G and Zimmerman G O 1982 *Solid State Commun.* **41** 289
Evans E L and Thomas J M 1975 *J. Solid State Chem.* **14** 99
Flandrois S, Masson J M, Rouillon J C, Gaultier J and Hauw C 1981 *Synthetic Metals* **3** 1
Maletta H 1980 *J. Physique, Paris* **41** C5 115
Maxwell E 1965 *Rev. Sci. Instrum.* **36** 553
Millman S E 1982a *Synt. Metals* in press
—— 1982b *Phys. Lett.* in press
Millman S E, Holmes B W and Zimmerman G O 1982 *Solid State Commun.* **43** 903
Mydosh J A 1981 *Recent Developments in Condensed Matter Physics* ed J T Devreese (New York: Plenum)
Suzuki M and Ikeda H 1981 *J. Phys. C: Solid State Phys.* **14** L923
Wertheim G K, van Attekum P M Th M, Guggenheim H J and Clements K E 1980 *Solid State Commun.* **33** 809
Zimmerman G O, Holmes B W and Dresselhaus G 1981 *Extended Abstracts of the 15th Biennial Conference on Carbon, University of Pennsylvania*, 42

PHYSICAL REVIEW B VOLUME 34, NUMBER 6 15 SEPTEMBER 1986

Relaxation effects in graphite intercalation compounds

A. K. Ibrahim and G. O. Zimmerman
Physics Department, Boston University, Boston, Massachusetts 02215
(Received 20 March 1986)

The ac susceptibility bridge technique is applied to the measurement of a long spin-lattice relaxation time associated with the magnetic anomaly which has been reported for $FeCl_3$ graphite intercalation compounds at 1.75 K. Investigations of this relaxation mechanism show that the specific heat of the spin system at low temperatures contributes to an anomaly in the relaxation time near the temperature of the magnetic anomaly. Our results indicate that the graphite layers between the magnetic intercalant layers act as nonmagnetic spacing layers allowing the *c*-axis spin-spin coupling to be varied.

INTRODUCTION

In graphite intercalation compounds (GIC's) the electrical resistivity is one of the properties most drastically changed by intercalation of both acceptor and donor materials,[1,2] it is also one which holds the greatest promise for technological applications.[3] If one wants to use the conventional four-probe technique to measure the resistivity of these materials, the high anisotropy of GIC's is expected to introduce difficulties in the measurements. As a result of these difficulties, experimentalists had thought of alternative means to measure the resistivity for these highly anisotropic compounds.

One of the widely-used approaches in the measurements of the electrical resistivity in GIC's is the low-frequency eddy-current technique.[4–6] The basic concept of this method is that when a sample is inserted into an ac field, the induced currents in the conductor reduce the magnetic flux which penetrates the conductor. If the signal is detected by a standard susceptibility bridge[7] the induced eddy current, which is proportional to the resistivity of the sample, is related to the out-of-phase or quadrature component of the n gnetic susceptibility.[8]

Because relaxatio ffects which induce an out-of-phase signal are also associated with low-temperature magnetic anomalies, which have been reported for a variety of GIC's,[9,10] one has to be careful in relating the out-of-phase component of the susceptibility to the resistivity of the system. Relaxation effects, therefore, which might contribute to the out-of-phase signal should not be ignored near a magnetic anomaly.

In our system, near the temperature of the magnetic anomaly, a spin-lattice relaxation mechanism is suggested as the contributor to the quadrature component of the magnetic susceptibility. When a spin system (magnetic ions) is disturbed from its thermal equilibrium by an external source, such as an applied magnetic field, the heat developed in this spin system has to be given to the lattice. We assume that the spins are in thermal equilibrium with each other and at a temperature slightly different from the lattice temperature. The transfer of heat between the spin system and the lattice is associated with a relaxation time (τ), which depends on the thermal conduction between the spins and the lattice and the specific heat of the spin system. Relaxation effects for GIC's in which low-temperature magnetic phase transitions were reported have not yet been explored. As shown in the following sections, investigation of such effects can provide information about the heat capacity of the system and also about the nature of the mentioned magnetic anomaly in these compounds.

In this work we have measured the long relaxation time in the $FeCl_3$-GIC system, using the susceptibility bridge technique. We have also used the conventional four-probe technique to investigate the electrical resistivity at the low-temperature anomaly which has been observed in the out-of-phase component of $FeCl_3$-intercalated graphite.[5] In fact, no anomaly in the resistivity along the *c* axis was observed at any temperature. These resistivity results, which will be shown in this work for comparison and whose details are presented elsewhere, are in qualitative agreement with the theory reported by Sugihara.[11] Therefore, it is clear that the anomaly of the out-of-phase component of the susceptibility of $FeCl_3$-intercalated graphite compounds is due to the relaxation effects in the system. Although we have concentrated on the measurements of the relaxation time of stage-6 $FeCl_3$ GIC, because of the similarity in the magnetic anomaly between the various stages, we can draw analogies from samples other than that stage. Thus we have chosen stages 5 and 9 for the comparison between the maximum in the out of phase susceptibility and the *c*-axis resistivity.

The crystal structure of $FeCl_3$ is a repeated sequence of three layers of hexagonally arranged atoms,[12] these layers are displaced relative to each other so that every iron atom is surrounded by an octahedron of chlorine atoms. Upon intercalation of $FeCl_3$ into the graphite, one electron is donated by the graphite host for every four iron atoms.[13] It is not yet clear what site these donated electrons occupy, room temperature Mössbauer data[14,15] and Raman spectroscopy[16] do not support the existence of $FeCl_2$ as a result of the acceptance by $FeCl_3$ of the donated electron.[17] However, there is a discrepancy in the low temperature Mössbauer data for $FeCl_3$. Millman and Kirczenow[18] have reported the existence of Fe^{2+} ions at temperatures as high as 100 K which is contradictory to the work of Ohhashi *et al.*[15] More theoretical and experimental work is necessary to understand the intercalation

mechanism and the associated charge transfer in this system.

Studies of the magnetic properties of low stage $FeCl_3$ GIC, as well as other systems, have shown a low-temperature phase transition and different mechanisms were proposed[9,10,19] to describe the origin of this transition. Limited transport measurements have been reported for low-stage $FeCl_3$ GIC. In-plane thermal conductivity data[20] show a dominant electronic contribution at low temperatures, while high-temperature data indicate a phonon contribution. The c-axis thermal conductivity, however, is driven by phonons at all temperatures. The authors[20] have also shown that the anisotropy of the thermal conductivity is much smaller than that of the electrical conductivity. It has been reported[21] that the in-plane resistivity data of stage-1 and -2 $FeCl_3$ GIC exhibit a low-temperature phase transition while stage 3 or 4 did not show any anomaly. It is the purpose of this work, which was initiated a few years ago at Boston University, to investigate in a full and comprehensive way the properties of the $FeCl_3$-GIC system.

EXPERIMENTAL

The $FeCl_3$-GIC samples were prepared using a standard two-zone furnace technique[3] where stage index was controlled by the temperature difference between the graphite host [highly-oriented pyrolytic graphite (HOPG)] and the $FeCl_3$ powder. The graphite samples were in the form of thin rectangular plates of dimensions $1.5\times0.5\times0.1$ cm^3. Well-staged samples were achieved by controlling the pressure of Cl_2 gas inside the intercalation tube, as well as the partial pressure of $FeCl_3$ through rigid temperature control. After intercalation, the samples were characterized for identity and uniformity of staging using x-ray (001) diffraction. The x-ray diffractograms were also used to determine the c-axis repeat distance I_c after cycling the samples from room to liquid helium temperature and showed that the cycling did not affect this staging distance.

A standard ac bridge technique[7] was employed to probe the signal which is in-phase with the exciting field (related to the relaxation of the system or the out-of-phase susceptibility χ'') and the signal which is out-of-phase with the exciting field (related to the in-phase magnetic susceptibility of the system χ'). These components were picked up by a two-phase lock-in analyzer which can detect signals down to 1 μV. The data were taken at several frequencies ranging between 40—1000 Hz.

A computer-controlled system, via analog-to-digital (A/D) and digital-to-analog (D/A) converters, was used to operate the apparatus at all desirable conditions. The temperatures of the samples above 2 K were measured by a calibrated silicon diode thermometer, while temperatures below 2 K were determined by means of the He vapor pressure. The susceptibility coils, were always kept in a cryogenic bath, thus changing the temperature of the sample did not change the temperature of the coils. At high temperatures (room to nitrogen temperature), the coils were immersed in liquid nitrogen.

An ac current in the primary circuit of magnitude about 4 mA was used to keep the amplitude of the exciting ac field below 0.1 G, thus nonlinear susceptibility effects were excluded. To investigate the relaxation as a function of the magnetic field, an external dc field in the range of (0—50 G) was applied to the samples. The magnetic dc and ac fields configurations are shown in Fig. 1. It shows schematically several layers of GIC's with the probing ac and the external dc magnetic fields parallel to the a-b plane, thus the induced eddy currents would be normal to that plane along the c axis. Mechanical vibrations can cause serious problems in this kind of experiment, thus careful attention has been paid to ensure that the sample was firmly attached to the sample holder and in a rigid configuration with the susceptibility coils.

The four-probe method was used to probe the out-of-plane resistivity, and an on-off current technique enabled us to subtract out any ambient or spurious voltage from that created by the measuring current. A special computer program was made to transfer the data from a Symbolics, Inc. MACSYM-350 (ANALOG DEVICES) computer, which monitors the apparatus and collects the data, to a Digital Equipment Corporation VAX11 minicomputer for routine analysis.

RESULTS AND ANALYSIS

The most striking result in this work is the temperature dependence of the out-of-phase component of the magnetic susceptibility which exhibits an anomaly in the form of a sharp peak at temperatures near 1.75 ± 0.05 K in zero dc magnetic field. This anomalous behavior is correlated with the same anomaly which we have seen in the in-phase component of the magnetic susceptibility.[9] Figure 2 shows the correlation between the in-phase and the out-of-phase component as a function of temperatures for stage-6 $FeCl_3$ GIC at $f=39.7$ Hz and in zero dc field. As shown in the figure, both the in-phase part (χ') and the out-of-phase part (χ'') exhibit anomalies in the form of sharp peaks with the maximum in χ'' shifted to lower temperatures.

The samples were oriented inside the coils in such a way as to probe the in-plane susceptibility and the out-of-plane resistivity as explained in the preceding section. To

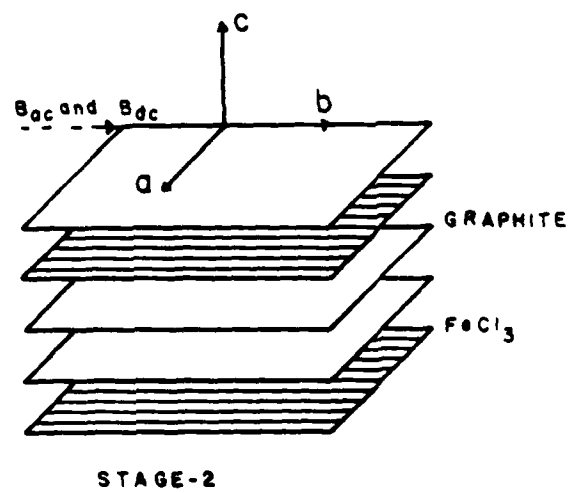

FIG. 1. Layered structure for stage-2 $FeCl_3$ GIC. B_{ac} and B_{dc} are the applied ac and dc magnetic fields along the b axis

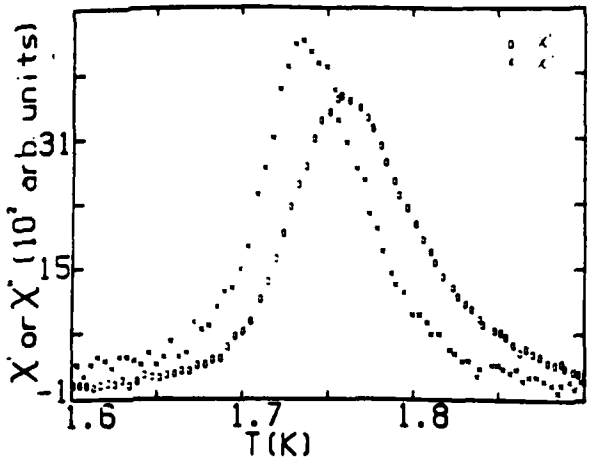

FIG. 2. The in-phase and out-of-phase components of the magnetic susceptibility versus temperatures near the transition point for stage-6 $FeCl_3$ GIC.

determine whether the correlation between χ' and χ'' is due to a resistivity anomaly or due to the long relaxation time in the system, the four-probe resistance measurement technique was engaged simultaneously with the susceptibility measurements. Figure 3 shows the out-of-phase components χ'' as a function of temperature for stages 5 and 9, and Fig. 4 shows the out-of-plane resistivity for the same samples and in the same temperature range. As shown in the figures, there is no anomaly in the electrical resistivity measured by the four-probe method and the resistivity basically behaves as predicted by Sugihara.[11] Therefore, we can conclude that the low-temperature maximum in χ'' cannot be ascribed to an anomaly in the resistivity, but is related to the relaxation of the spin system.

Based on the above results and the theoretical descriptions of Casimir and Du Pré,[22] we have made a detailed investigation of the relaxation mechanism for stage-6 $FeCl_3$ GIC. The real and imaginary parts of the complex susceptibility are related to the relaxation time of the system and the frequency by the following equations:[23]

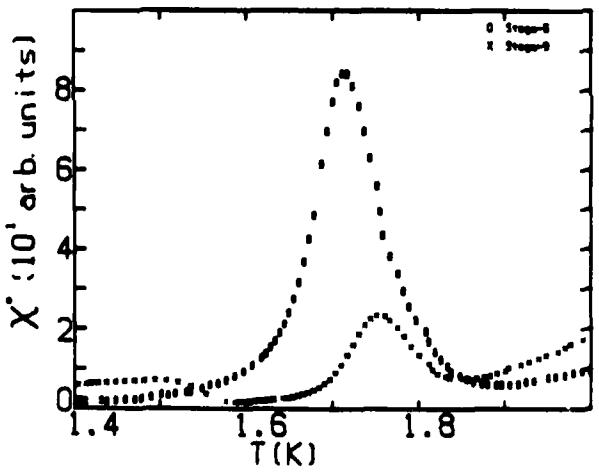

FIG. 3. The out-of-phase susceptibility component versus temperature for stage-5 and -9 $FeCl_3$ GIC's near the transition temperature.

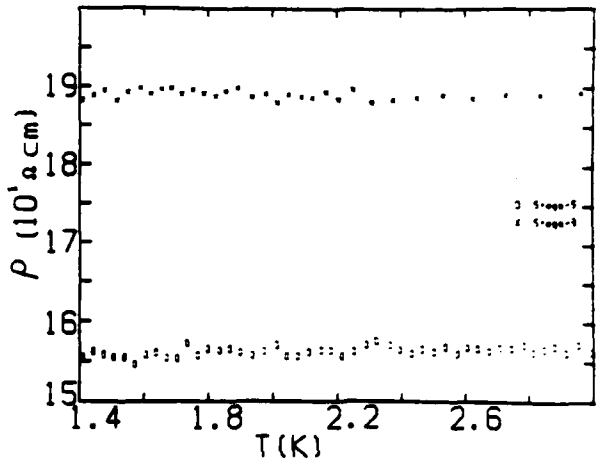

FIG. 4. The c-axis resistivity versus temperature in the vicinity of the magnetic anomaly for stage-5 and, -9 $FeCl_3$ GIC's.

$$\chi' = \frac{G}{(1+\omega^2\tau^2)} + \chi_0 - G \,, \tag{1}$$

$$\chi'' = \frac{G\omega\tau}{(1+\omega^2\tau^2)}, \; G = \chi_0(1 - C_m/C_h) \,, \tag{2}$$

where C_m and C_h are the heat capacities at constant magnetization and at constant field respectively, and χ_0 is the static susceptibility. τ is the relaxation time of the spin system, and ω is the angular frequency of the exciting field.

The out-of-phase magnetic susceptibility component data were taken as function of frequency and at temperatures between 1.1 and 2.4 K. Since that component varied significantly with frequency only in the temperature range between 1.65 and 1.85 K, constant temperature cuts were made in this temperature range and the measured values of the quadrature component of the magnetic susceptibility at constant temperature fit to the function given in Eq. (2). We used a nonlinear least-squares computer fitting program allowing G and τ to be varied to achieve the best

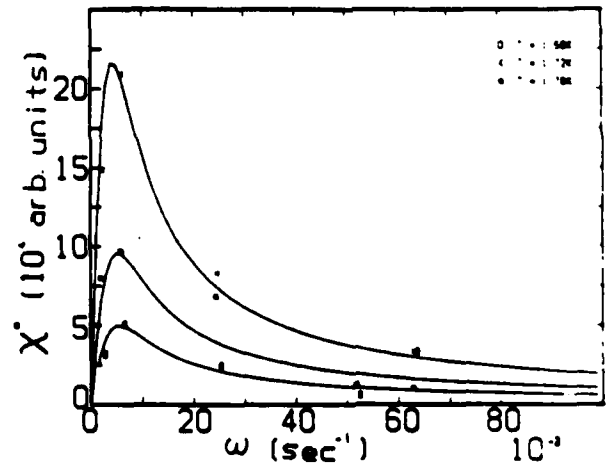

FIG. 5. The out-of-phase component of the magnetic susceptibility versus the angular frequency for stage-6 $FeCl_3$ GIC. The continuous lines are the theoretical functions and the symbols are the experimental data.

fit. Figure 5 shows the fits of the measured data at temperatures 1.68, 1.72, and 1.78 K. As shown in the figure, the data indicate a good fit to the Casimir—Du Pré relation in the low-frequency region and a somewhat worse fit at frequencies near 1 kHz. This is due to the fact that in the high-frequency region, it is difficult to decouple the two components of the measured susceptibility from each other because capacitive and skin effects impose an upper limit on the sensitivity of the bridge. The high-frequency points, however, were given a lower weight.

The fitting parameters τ and G were found to be temperature dependent and, in fact, both of them exhibit maxima near the temperature of the susceptibility anomaly. In Fig. 6 the values of these parameters are represented as a function of the temperature and, as shown in the figure, the peak of the relaxation time is shifted towards lower temperature from that in G. It is interesting to note that the out-of-phase component of the susceptibility, as shown in Fig. 2, shifts towards lower temperatures as the relaxation time does, while the in-phase component as well as the fitting parameter G are shifted towards higher temperatures.

The parameter G can be also written as

$$G = \chi_0(1-\chi_s/\chi_t)\,, \tag{3}$$

where χ_t and χ_s are the susceptibility at constant temperature and entropy, respectively. In the low-frequency region and at low temperature, one can assume that χ_s is small and expect G to have a maximum which coincides with that of the in-plane susceptibility which is proportional to χ_0. This explains the correlation between the graphs in Fig. 2 and Fig. 6 which showed a shift towards higher temperatures for χ' and G relative to χ'' and τ, respectively. Measurements at low-frequency provide an isothermal spin system so that the spin-spin relaxation can be ignored. The relaxation time, on the other hand, depends on the temperature through the specific heat at constant field of the spin system and the heat conduction between the spin system and the lattice system. Thus, in order to extract useful information, careful examination has to be carried out in this case.

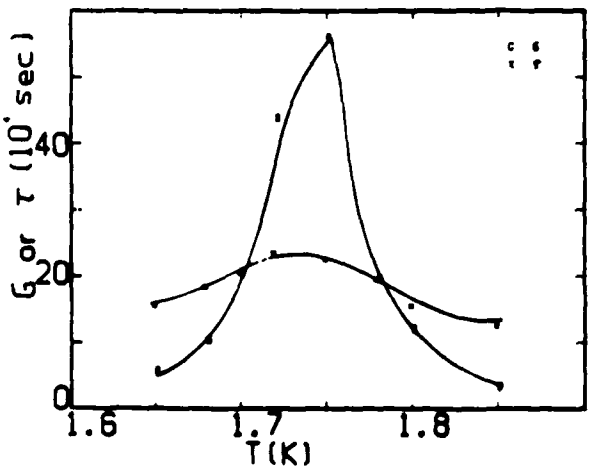

FIG. 6. The fitting parameters G and τ versus temperatures for stage-6 $FeCl_3$ GIC. The continuous lines are used to guide the eye.

We have also measured the spin-lattice relaxation time in stage-3 $FeCl_3$ GIC and found that the relaxation times in stage 3 were shorter by a factor of 4 compared to those of stage 6. According to the Casimir—Du Pré picture, relaxation occurs when heat is transferred from the spin-system, in our case $FeCl_3$ whose temperature changes in a sinusoidal fashion, to a lattice which is at a constant temperature and serves as a heat reservoir:

$$\tau = C/K\,, \tag{4}$$

where C is the spin specific heat and K is the thermal conductivity. If heat transfer were due to the electrons in the bounding layers, the relaxation time τ would be too short for us to measure by this method. It was also shown that the spacing between adjacent graphite layers is nearly independent of staging.[24,25]

Because of this, and the fact that near a magnetic transition the specific heat is related to the magnetic susceptibility χ by[26]

$$C = \frac{d(\chi T)}{dT}\,, \tag{5}$$

we can attribute the difference between the stage-3 and -6 relaxation times to the differences in their respective specific heats at the anomaly. Table I gives the relative magnitudes of the susceptibility, normalized per iron atom, of various stages of $FeCl_3$ GIC at the susceptibility maximum. As shown in Table I, stage 3 has a maximum whose size is approximately a factor of 4 smaller than that of stage 6.

Another possible mechanism for the difference in the relaxation times between the various stages could be the intercalate bounding layers of graphite. One imagines that the Fe^{3+} spins relax to the $FeCl_3$ lattice which then relaxes to the graphite layers mainly through the chlorine graphite interaction due to phonons. An enhancement in the low-frequency phonon spectrum of intercalated graphite over that of HOPG was actually calculated[27] and observed.[28] Since high stages have a smaller density of low-frequency phonons than low stages, according to equation (4) the conductivity K in the low stages would be enhanced and thus again lead to a shorter relaxation time. However, the changes in the relaxation times can be adequately accounted for by the relative size of the specific heats without considering the changes in the thermal conductivity. Thus we conclude that the change in thermal conductivity between different stages of $FeCl_3$ is small compared to the specific heat effect.

Therefore the maximum in the relaxation time is attributed to the specific heat of the spin system which is con-

TABLE I. Stage index versus the relative peak size of the in-phase magnetic susceptibility for $FeCl_3$ GIC.

Stage	Peak size
1	0.0846
2	0.2256
3	0.4381
4	1.4381
5	5.1877
6	1.8329
9	1.4706

sistent with theoretical calculations based on a model of two-dimensional interacting dipoles.[29] This model shows an increase in the specific heat of the system near the transition point which is similar to that exhibited by many other systems near their critical points and is attributed to critical fluctuations. Mössbauer studies[30] of anhydrous $FeCl_3$ describe the broadness of the resonance lines near the critical temperature as a result of the increase in fluctuations of the internal field direction which are caused by the spin relaxation in the system.

If the quantity $\omega\tau$ is eliminated between Eqs. (1) and (2), then another representation of χ' and χ'' can be given by the following equation:

$$(\chi'-\chi_0+\tfrac{1}{2}G)^2+(\chi'')^2=\tfrac{1}{4}G^2\,. \tag{6}$$

As long as the relaxation is controlled by one relaxation time, Eq. (6) predicts that when χ' is plotted versus χ'' the points should lie on a circle. Figure 7 shows the experimental data of χ' versus χ'' at different frequencies at the peak temperatures and 1.72 K, which is about 30 mK below the peak temperature.

The existence of the spin relaxation at the critical point for both anhydrous $FeCl_3$ and $FeCl_3$ GIC supports the correlation between the magnetic properties of these two systems. Thus, qualitatively, we suggest that the three-dimensional anomaly which is observed at about 8 K in anhydrous $FeCl_3$ is the source of the low-temperature anomaly in $FeCl_3$ GIC. The staging process decreases the interactions between the intercalant layers in such a way as to have a two-dimensional interacting spin system. Our data indicate that the graphite layers between the magnetic intercalant layers act as nonmagnetic spacing layers allowing the c-axis spin-spin coupling to be varied.

The application of a small dc magnetic field of the order of 5 G smears out the anomaly in the susceptibility[31] and thus no relaxation was observed at this field. The out-of-phase component (χ'') as a function of temperature and in different external dc magnetic fields is represented

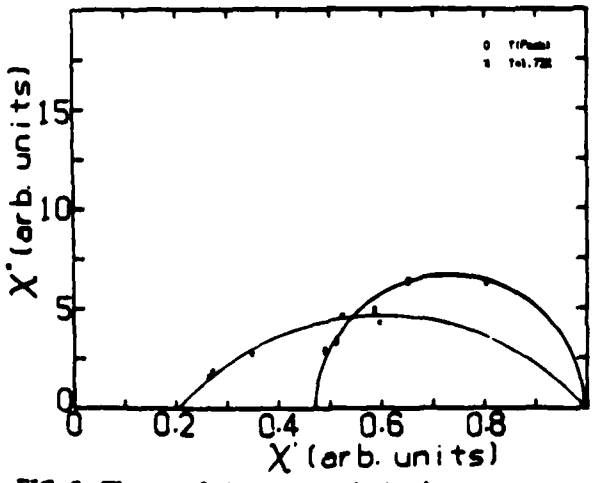

FIG. 7. The out-of-phase versus the in-phase components of the magnetic susceptibility at different frequencies and at the peak temperature and at $T=1.72$ K. The continuous lines are on a circle.

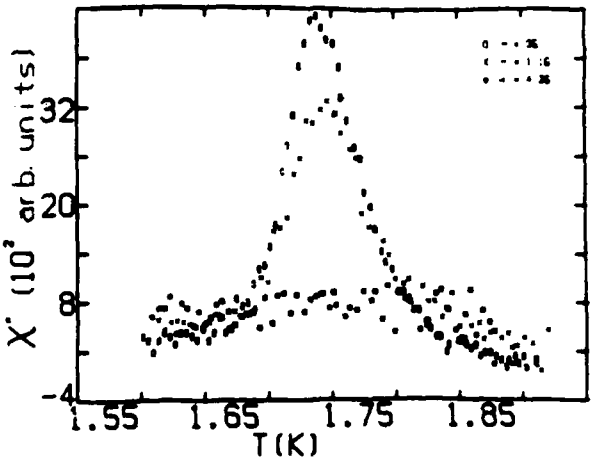

FIG. 8. The out-of-phase component of the magnetic susceptibility versus temperatures for stage-6 $FeCl_3$ GIC. The B's are the applied dc magnetic fields in Gauss.

in Fig. 8; as shown in the figure at a field of 4.2 G the anomaly has disappeared.

This anomaly, if it is a three-dimensional transition between two magnetic phases, is expected to exist in fields as high as 1 kG; however, the disappearance in such a small field emphasizes the two-dimensional nature of this phase transition. In addition, the stage dependence of this anomaly shows more pronounced peaks for higher stage samples in both components of the susceptibility.

CONCLUSION

We have shown that for systems which possess a magnetic anomaly the out-of-phase component of the susceptibility is dominated by spin-lattice relaxations, thus it would not be reliable to relate the electrical resistivity of these systems to the out-of-phase component. Fitting our data to a temperature-dependent relaxation shows that the relaxation time itself exhibits an anomaly near the transition temperature of the magnetic anomaly. On a qualitative basis, and in agreement with a two-dimensional mean-field calculation,[28] we have found that the relaxation anomaly is related to a similar one in the specific heat at constant field.

In agreement with reported thermal conductivity measurements[20] and phonon density calculations[27] at low temperatures, the out-of-plane phonon vibrations are determined to be the carriers of the heat from the spin system to the graphite lattice. The contribution of the conduction electrons is not significant in the temperature range over which our measurements were carried out. Finally, we have shown that the intercalant $FeCl_3$ controls the magnetic properties of the $FeCl_3$-GIC system and becomes more two dimensional as the stage is increased.

ACKNOWLEDGMENTS

The authors wish to acknowledge support by the U.S. Air Force Office of Scientific Research Grant No AFOSR-82-0286.

[1]A. R. Ubbelohde, Proc. R. Soc. London, Ser. A 327, 289 (1972).
[2]F. L. Vogel, G. M. T. Foley, C. Zeller, E. R. Falardeau, and J. Gan, Mater. Sci. Eng. 31, 261 (1977).
[3]M. S. Dresselhaus and G. Dresselhaus, Adv. Phys. 30, 139 (1981).
[4]F. L. Vogel, R. Wachnik, and L. A. Pendrys, Solid State Sci. 38, 288 (1981).
[5]A. K. Ibrahim, G. O. Zimmerman, and K. Galuszewski, Extended Abstracts on Graphite Intercalation Compounds, Materials Research Society Meeting, Boston, 1984 (unpublished).
[6]Y. Iye, O. Takahashi, S. Tanuma, and Y. Koike, Fifteenth Biennial Conference on Carbon, Philadelphia, 1981 (unpublished).
[7]M. D. Daybell, Rev. Sci. Instrum. 38, 1412 (1967).
[8]D. Shoenberg, *Superconductivity* (Cambridge University Press, Cambridge, 1952).
[9]M. Elahy, C. Nicolini, G. Dresselhaus, and G. O. Zimmerman, Solid State Commun. 41, 289 (1982).
[10]M. Suzuki, I. Oguro, and Y. Jinzaki, Extended Abstracts on Graphite Intercalation Compounds, Materials Research Society Meeting, Boston, 1984 (unpublished).
[11]K. Sugihara, Phys. Rev. B 29, 5972 (1984).
[12]S. Blairs and R. A. J. Shelton, J. Inorg. Nucl. Chem. 28, 1855 (1966).
[13]G. K. Wertheim, P. M. von Attekum, H. J. Guggenheim, and K. E. Clements, Solid State Commun. 33, 809 (1980).
[14]B. V. Liengme, M. W. Bartlett, and J. R. Sams, Phys. Lett. 25, 127 (1967).
[15]K. Ohhashi and I. Tsujikawa, J. Phys. Soc. Jpn. 36, 422 (1974).
[16]N. Caswell and S. A. Solin, Solid State Commun. 27, 961 (1978).
[17]M. L. Dzurus and G. R. Hennig, J. Am. Chem. Soc. 79, 1051 (1957).
[18]S. E. Millman and G. Kirczenow, Phys. Rev. B 28, 5019 (1983).
[19]S. E. Millman, B. W. Holmes, and G. O. Zimmerman, Solid State Commun. 43, 903 (1982).
[20]J. P. Issi, J. Heremans, and M. S. Dresselhaus, Phys. Rev. B 27, 1333 (1983).
[21]L. A. Pendrys, T. C. Wu, C. Zeller, H. Fuzellier, and F. L. Vogel, Extended Abstracts, Fourteenth Biennial Conference on Carbon, 1979 (American Carbon Society, Philadelphia, 1979), Vol. 14, p. 306.
[22]H. B. G. Casimir and F. K. Du Pré, Physica 5, 507 (1938).
[23]B. W. Holmes, Ph.D. thesis, Boston University, 1980 (unpublished).
[24]M. S. Dresselhaus and G. Dresselhaus, Adv. Phys. 30, 139 (1981).
[25]A. Herold, in *Physics and Chemistry of Materials with Layered Structures*, edited by F. Levy (Dordrechet, Reidel, 1979), p. 323.
[26]M. E. Fisher, Philos. Mag. 7, 1731 (1962).
[27]R. Al-Jishi and G. Dresselhaus, Phys. Rev. B 26, 4523 (1982).
[28]G. Dresselhaus, R. Al-Jishi, J. D. Axe, C. F. Majkrzak, L. Passel, and S. K. Satija, Solid State Commun. 40, 229 (1981).
[29]G. O. Zimmerman and A. K. Ibrahim (unpublished).
[30]J. P. Stampfel, W. T. Oosterhuis, B. Window, and F. des. Barros, Phys. Rev. B 8, 4371 (1973).
[31]G. O. Zimmerman, C. Nicolini, and K. Galuszewski, Extended Abstracts on Graphite Intercalation Compounds, Materials Research Society Meeting, Boston, 1984 (unpublished).

APPENDIX V

Submitted for publication to The Physical Review

C-Axis Conductivity in Graphite Intercalation Compunds*

R. Powers, A.K. Ibrahim, G.O. Zimmerman, and M. Tahar

Physics Department, Boston University

Boston, MA 02215

The four probe technique is used to measure the c-axis resistivity of various stages of $FeCl_3$ acceptor graphite intercalated compounds. Comprehensive investigation of the resistivity behavior between room and liquid helium temperatures for stages 2-5, and 9 is presented. The experimental results are compared with one of the existing theoretical models. There is good agreement between the experimental data and the predictions of one of the theoretical models. The results of this work reveal that the conduction along the c-axis in acceptor compounds is a hopping mechanism assisted by phonons and impurities. In lower stage compounds, the conduction is dominated by impurity-assited hopping, and the resistivity shows metallic temperature behavior at high temperatures and tends to saturate at low temperatures. For higher stage compounds, phonon-assisted hopping dominates the conduction. The resistivity approaches constant values at high temperatures and exhibits an activated behavior which is proportional to T^{-2} at low temperatures. Stage 5 seems to be an intermediate stage where the conduction has the contribution of both phonon and impurity hopping mechanisms.

* supported by the Air Force Office of Scientific Research Grant AFOSR 82-0286.

INTRODUCTION

In graphite intercalation compounds (GIC's), the electical conductivity is one of the most promissing physical quantities for which real applications might take place [1]. The in-plane and c-axis conductivities are among the properties most drastically changed by intercalation of acceptor and donor GIC's [2,3]. This unexpected change of the conductivity attracts numerous theoreticians and experimentalists to investigate these GIC's. Inspite of that, there is a lack of a coprehensive theory and experimental results which can describe the electrical conduction in these materials. The high anistropy of the conductivity, which can be a factor of 10^6 for some compounds [4], and the staging property introduce difficulties to the current theories which attempt to formulate a complete and realistic picture about the conduction in these compounds.

The conduction in GIC's has been described by Sugihara et al [5] and Sugihara [6] in terms of a scattering mechanism caused by in-plane and out-of-plane vibrations. The interaction between phonons and these out-of-plane vibrations is the contributor to the c-axis conduction. The authors of reference [6] suggest that this conduction is a hopping mechanism assisted by phonons and impurities. The in-plane conduction is not yet based on any satisfaction theory, however recent papers [7,8] concluded that a strong charge screening mechanism takes place in the c-direction and most of the free carriers are confined to the carbon planes adjacent to the intercalated layers. It is the purpose of this work to investigate the c-axis conduction in the $FeCl_3$- graphite intercalated system and provide experimental results which can be compared with existing theoretical models.

The $FeCl_3$-GIC system is one of the earliest systems to have been investigated by numerous researchers. However the understanding the low temperature magnetic phase transition, the unexpected behavior of the transport and electronic properties, and the

staging mechanism in this system, as well as other GIC systems, still are open questions. Metz et al [9] have made a structural investigation using x-ray diffraction data and concluded that the stacking of layers is disordered and under special circumstances, depending on the preparation condition, nearly periodic compounds can be produced. IR and Raman spectroscopy of $FeCl_3$-graphite [10] indicate in-plane compression within the graphite layers and most of the effective charge is in the graphite bounding layers, with the rest of the charge distributed among the graphite interior layers. Thermal conductivity measurements [11] showed that the electronic thermal conductivity of the graphite bounding layers increases upon intercalation, whereas the lattice thermal conductivity decreases. Magnetic susceptibility measurements [12,13] on $FeCl_3$ indicate the existence of a low temperature magnetic phase transition.

In this work, the c-axis resistivity measurements of the $FeCl_3$-graphite system using the convetional four-probe technique were stimulated by the investigation of the low temperature anomaly of the magnetic susceptibility [13]. Contactless bridge measurements had been made on various stages and a peak in the susceptibility was observed at around 1.75K. This peak was also noted in the out-of-phase component of the susceptibilty which indicated a possible contribution from the resistivity of the sample [14]. For the chosen sample orientation in the measurements, this contribution would have been primarily from the c-axis resistivity. Thus it was decided to investigate the resistivity by means of independent measurements concurrently with the contactless bridge method.

Although numerous theoretical and experimental investigations of the in-plane conductivity have been reported, less attention was paid to the c-axis conductivity of GIC's [15]. Theoretically, very limitted work has been reported, Markiewicz [16] has proposed a simple band model for calculating the c-axis conductivity in a series of GIC's. In this model, it was assumed that for acceptor compounds the bandwidth is small enough so one can treat these compounds as two-dimensional systems. Although there is a small

contribution due to band conduction, it is generally overpowered by other mechanisms. The hopping mechanism suggested by Sugihara [6] excludes the contribution of the band conduction along the c-axis in acceptor compounds. Experimentally, Ohta et al [17] have measured the temperature dependence of the c-axis resistivity for stages 1 and 2 of ICl-graphite compounds. Their data exhibit order-disorder transition at room temperature and anistropy of the order of 10^3 for stage-1 and 10^4 for stage-2. This anistropy was attributted to the hopping mechanism proposed by Sugihara [6]. The investigation of the c-axis resistivity of $SbCl_5$ by Uher and Morelli [18] indicates that low stage compounds exhibit metallic-like conduction, which was described by a model based on defect-mediated short-circuiting channels along the c-axis. In in higher stages, however, a metal-insulator transition was observed at low temperature and the conduction is essentially caused by a thermally activated hopping mechanism. Measurements of the c-axis resistivity for stage 2 $FeCl_3$-GIC's by Issi et al [19] indicate that resistivity, after subtracted the residual part, has T^2 dependence at low temperature and a T dependence at high temperature. A compendium of various measurements of the c-axis conductivity for several GIC's, both acceptor and donor, was presented recently by McRae et al [20]. It shows that there are some common characteristic signatures in the c-axis conductivity in both acceptor and donor GIC's. Nevertheless, those characteristics are not fully understood and, to reach a comprehensive picture about this conduction, more theoretical and experimental works on several different systems should be done.

EXPERIMENTAL

The $FeCl_3$-GIC samples were prepared using a standard two-zone furnace technique [1] where stage index was controlled by the temperature difference between the graphite host highly ordered pyrolytic graphite (HOPG) and the $FeCl_3$ powder. The samples were in the form of thin rectangular plates of dimensions 1.5x0.5x0.1 cm^3. Well-staged samples were achieved by controlling the pressure of Cl_2 gas inside the intercalation tube, as well as the partial pressure of $FeCl_3$ through rigid temperature controll. After intercalation, the samples were characterized for identity and uniformity of staging using x-ray (00l) diffraction. Only single stage, well staged samples were used in the magnetic measurements. The x-ray diffractograms were also used to determine the c-axis repeat distance I_c after cycling the samples from room to liquid helium temperature, and showed that the cycling did not affect this staging distance.

Most of the samples measured were characterized by means of the Mössbauer effect, details are reported in references [13,21]. In higher stage samples, where stage-disorder is expected [22], the Hendricks-Teller [23], and Mets and Hohlwein [9] analysis technique were used to calculate the intensity, width and location of the x-ray reflections. We find that our experimental x-ray data on the stage 9 samples reported in this article are in good agreement with that calculated for the pure and well-staged stage 9. Although a small admixture of stage 10 can not be excluded, this stage serves as an example of a high stage sample.

Samples, for resistivity measurements, of approximate dimensions 3 mm by 5x5 mm^2 were peeled out from the intercalated samples using scotch tape. These dimensions were chosen primarily for convenience when mounting the samples in our sample holder, whereas optimal signal would have been obtained by minimising the in-plane area while maintaining comfortable lead separation on the faces and maximising the c-axis thick-

ness. Because of the high in-plane conductivity relative to that of the c-axis, the non-uniform current injection would not be a problem. The leads were attached to the sample in the conventional four-prope configuration. Contacts were made on the sample using GC conductive silver print (GC ELECTRONICS). The samples were inserted in the axial slot of a phenolic rod which was then wrapped with mylar tape to insure that the sample did not move in the slot and that subsequent stress to the leads was minimized. The leads were attached to the main leads leading from the cryostat by wrapping and then glueing with silver print.

The sample holder was mounted in a vacuum case which was surrounded by a helium dewar with an outer nitrogen dewar jacket. The vacuum case contained an exchange gas of air or helium, depending on the temperature region being investigated. Temperatures between room and liquid nitrogen temperature were reached by means of liquid nitrogen in the outer dewar. Liquid helium was then transfered with a minimal amount of exchange gas to cool down to helium temperature in a controlled fashion. Pumping on the exchange gas enabled us to controll the temperatures for both liquid nitrogen and liquid helium ranges. The temperature was measured using a calibrated silicon diode thermometer mounted close to the sample, and wired in a four point contact configuration.

Measurement of the resistance of the sample was controlled by a MACSYM 350 (ANALOG DEVICES,INC) based computer system. A computer program was used to collect, simultaneously, the susceptibility and the c-axis voltages. The sample voltage was first read with zero current through the sample by a channel on an analog input card in the MACSYM. Then the sample current was set to 5 ma by a channel on an analog output card in the MACSYM. This value of current was chosen as a tradeoff between low power dissipation in the dewar and low noise in the signal. The voltage at 5 ma was taken and then the current was switched off. The sample voltage was then read

again. The average of the zero current voltages, representing the thermal voltage in the junctions of the leads, was subtracted from the voltage at 5 ma. Finally the sample resistance was calculated from this corrected voltage. The data then were trasfered to a Digital Equipment Corporation VAX11 minicomputer for routine analysis.

Results and Analysis

The data plotted in Fig(1) are the absolute resistivity versus temperature for stages 2,3,4,5,9 of $FeCl_3$ GIC, and HOPG. Several features can be observed in the data: 1) For stage index less than 5 the temperature behavior of the resistivity is metallic-like, and the resistivity saturates at low temperatures. The metallic behavior is most pronounced for stages 2 and 3 and less so for stage 4. 2) Note that for stage 5 the resistivity exhibits metallic-like behavior at high temperatures and crosses to activated behavior at low temperatures. 3) Observe that the highest stage sample, stage 9, exhibits activated behavior throughout the entire range of temperatures shown. These behaviors are more easily seen on a plot of resistivity normalized to room temperature versus temperature, shown in Fig(2). In this figure, stage number increases in the positive y direction (except for HOPG). This presentation supports more clearly the identification of stage 5 as the stage at which a definite transition in behavior occurs [13,24]. Stage 2 and 4 samples behave qualitively alike whereas stage 9 behaves fundamentally differently and is similar to HOPG in character as one would expect for higher stages. As the number of pristine graphite layers between the intercalate layers becomes large enough to screen out the out-of-plane interactions, the c-axis conduction is expected to be controlled by the graphite layers.

The absolute resistivity versus the inverse of the stage index is presented in Fig(3) at 293 K, 77 K, 4.2 K. At 293 K and 77 K the peak in resistivity is at stage 5. This is, qualitatively, in agreement with the results of the magnetic properties measurements for the $FeCl_3$-graphite system [13]. In those measurements, it was shown that the system behaves as a two-dimensional system and stage 5 exhibits maximum characterstics of the two-dimensional nature relative to the other stages. If the charge carriers are confined between the planes, one would expect the conduction along the c-axis to be minimum and thus the resisitivity in this direction should rise.

The resistivity temperature coefficient versus the inverse of the stage index for the temperatures 4 ,77, and 293 K are presented in Fig(4). These coefficients are the slopes of the resistivity versus temperature curves at the particular temperature normalized to the room temperature resistivity values. As it turns out, the labeling of the y-axis gives the change in resistivity per degree kelvin as a percentage of the resistivity at room temperature. All the values are seen to be small in absolute magnitude- less than one half of a percent per degree. It is the sign of the coefficient which is important. This gives the type of temperature dependence- positive coefficients indicate "metallic" temperature behavior and negative coefficients indicate "activated" behavior. Again the fundamental difference in behavior between stages with stage index less than five and greater than 5 is readily apparent. Also note that for all stages the resistivity coefficient at room temperature is very nearly equal to zero.

Athough we tried to compare our data with various theories, we found the best qualitative agreement with the model proposed by Sugihara [6]. In this model it was concluded that the c-axis conduction in acceptor GIC's is a hopping conduction assisted by phonons and impurities. The total conductivity in a particular stage sample is the sum of the conductivity due to phonon-assisted hopping and that due to impurity-assisted hopping. The temperature dependences of the two hopping mechanisms differ. Phonon-assisted hopping conductivity is expected, theoretically, to vary as T^2 for low temperatures and to be constant at high temperatures. Impurity-assisted hopping, however, is constant at low temperatures and decreases linearly with T at higher temperatures. Phonon-assisted hopping dominates the conductivity in high stages, whereas impurity-assisted hopping, as a result of the larger number of defects introduced by intercalation, should dominate in low stages. These qualitative results have been shown to agree with data taken for $SbCl_5$ acceptor GIC's [18] and our data for $FeCl_3$ GIC's, as shown below. The model of Sugihara [6] can be summarized by the following equations:

a) Phonon-hopping Conduction

$$\sigma_{cp} \propto \begin{cases} T^2 & \text{at low temperatures;} \\ T & \text{-independent at high temperature.} \end{cases} \quad (1)$$

b) Impurity-hopping Conduction

$$\sigma_{ci} \propto \begin{cases} T^{-1} & \text{at high temperatures;} \\ T & \text{-independent at low temperature.} \end{cases} \quad (2)$$

$$\sigma_c = \sigma_{cp} + \sigma_{ci}. \quad (3)$$

Here σ_{cp}, σ_{ci}, and σ_c are the c-axis phonon-, impurity-, and total-assisted hopping conductivity, respectively.

We have used the above theory to analyze the data of two stages, stage 2 as an example of a low stage and stage 9 as an example of a high stage of $FeCl_3$ GIC's. For stage 9, we find an interesting quantitative agreement of our data with theory. The data presented in Fig(5) is the c-axis conductivity of stage 9 versus temperature from 4 K to 70 K. The data points are shown by the squares. A fit has been made to a T^2 dependence. It can be seen that the fit is excellent from 10 K to about 60 K. This is the maximum temperature for agreement with theory found in an exhaustive series of fits for a large range of low temperatures. Similarly for the data of stage 2, a fit has been made to a T dependence. The result of the fit is shown in Fig(6). The data points are shown by the squares. As shown in the figure the data agree well with a linear T dependence in a temperature range between 300 K and 100 K. Therefore the data of the two stages, which are chosen as examples of low and high stages, are in excellent agreement with the prediction of the Sugihara's theory. The results of the these fits are as follows: In stage

9 the data were compared to a fit to the equation $\sigma_{cp} = A + BT^2$, where the fitting parameters A and B have the values; $A = 0.530$ Ω-cm, $B = 65.3 \times 10^{-6}$ Ω-cmK^{-2}. In stage 2, however, the impurity contributions are expected to dominate the c-axis conductivity, and thus the data were compared to a fit to the equation $\sigma_{ci} = C + DT$. The fitting parameters C, and D have the values $C = 0.346$ Ω-cm, and $D = 2.92 \times 10^{-3}$ Ω-cmK^{-1}.

Now all the data shown in Fig(2) can be analyzed on the basis of the Sugihara's model. The data of stages 2 and 4, classified as low stages, shown in the figure exhibit metallic-like behavior in the high temperature region and nearly temperature indpendence at low temperatures. Stage 2 is expected to have a relatively large number of impurities in comparison to that of stage 4. This would explain the difference in the temperature dependence of the resistivity for the two stages. Stages 2 and 3 have a similar behavior. Therefore, the temperature dependence of the c-axis resistivity for the lower stages behaves consistently with the Sugihara's theory. In the high temperature region the data for stage 2 of this work and those of Issi et al [11] are in quantitative agreement. At low temperatures, however, subtracting the residual parts from the total resistivity leads to a complicated temperature dependence. The overall behavior of the c-axis resistivity in this system is controlled by the competition between two mechanisms, namely the phonon- and impuriy-assisted hopping conductions. The data of Fig(2) indicate that both of these mechanisms contribute to the c-axis resistivity of stage 5. Therefore the resistivity of stage 5 is expected to exhibit both the activated and metallic behaviors. Clearly the data of stage 5 in figure 2 are consistent with this prediction. The large c-axis resistivity of stage 5 is due to the delocalization of the electrons in the a-b plane as a result of its two-dimensional nature. The c-axis resistivity of higher stages, shown for stage 9 in Fig(2), shows semiconductor-like behavior of dominant phonon-assisted hopping conduction which is characterized by the T^2 dependence. This is also consistent with the prediction of the theory for the higher stage samples. The c-axis re-

sistivity of higher stage samples, as expected, exihibits similar behavior to that of the pristine graphite. The data of Uher and Morelli [18] are also consistent with the prediction of the Sugihara's theory, however, none of their stages exhibits intermediate transition, similar to that of stage 5 of this work, between phonon and impurity contributions.

One of the remarkeable features about the $FeCl_3$-GIC's is the existance of stage 5 as a boundary stage between low and high stages. Moreover, the magnetic susceptibility data[13] indicate that the two-dimensional nature of this system has exponetial dependence on the stage index and it was shown that it is maximum at stage 5. In fact, the conductivity anistropy (σ_c/σ_{ab}) versus the stage index, shown in Fig. (7), has a similar exponential behavior and between stage 2 and stage 5 the anistropy is maximum at stage 5. Once the system comes completely into a two dimensional state, the out-of-plane phonon contributions to the conductivity decrease and thus the anistropy is increased. This results again amphasizes the two-dimensinality of this system. In figure (7), the natural logarithm of the anistropy (σ_c/σ_{ab}) is plotted versus the stage index. As shown on the figure, the data for stage 2 through 5 follows an exponential law. On the same figure the natural logarithm of the susceptiblity peak, at the reported phase transition[12,13], is plotted versus the stage index. As shown in the figure, the data from two independent measurements follow the same general exponential behavior.

In order to see if there are hysteretic effect, thermal cycling of the resistivity was also performed for all stages. No hysteresis was observed in any of the stages except an insignificant one for stage 9. The data plotted in Fig(8) are the scan up and scan down of the c-axis resistivity versus temperature for stage 9. We do not expect that the hysteresis shown in the data below 100 degrees to be related to the sample structure and attribute it to the nature of the experiment. In this temperature range the resistivity drastically varies with temperature. In the experiment it was difficult to control the cooling rate to collect the data at the same points as during the warming rate. There-

fore the $FeCl_3$-GIC's, unlike the $SbCl_5$-GIC's, has no significant hesteresis which would be related to microscopic transition mechanisms such as the pinning of discommensurations caused by defect sites in HOPG [18]. The high temperature order-disorder transition [25] which occurs near room temperature in stages 1 and 2 ICl-graphite intercalated compounds [17] does not exist in the $FeCl_3$-graphite compounds. The absence of the histeresis and such high temperature structural phase transitions and the long period room temperature stability suggest that the $FeCl_3$ sytem is a suitable candidate among the series of GIC's for further structural studies.

CONCLUSION

The result of experimental measurements indicates that the temperature dependence of c-axis resistivity has a universal behavior, consistent with the existing theories, for acceptor graphite intercalated compounds. Detailed investigations in terms of the model reported by Sugihara have shown that the lower stages of $FeCl_3$- graphite intercalated compounds exhibit metallic-like conduction along the c-axis, whereas higher stages show an activated behavior. The conduction along the c-axis in this system is a result of the competition between two mechanisms, the phonon-assisted hopping and the impurity-assisted hopping. The first contributes dominatly in higher stages at low temperatures, while the second contributes in lower stages at high tempratures. As a manifestation of the competition between the two hopping mechanisms, stage 5 behaves as intermediate stage and exhibits nearly constant temperature dependence between room and liquid helium temperatures. The results of this work and those of the magnetic measurements, reported elsewhere [13], independently support the existence of a two-dimensional state in this system with stage 5 exhibiting the greatest two-dimensional characteristics.

Acknowledgment

We would like to acknowledge with thanks Dr. A.W. Moore for donating the

HOPG, Dr. G. Dresselhaus, Dr. M.S. Dresselhaus, and Dr. K. Sugihara for many helpful discussion and preperation of initial samples.

REFERENCES

1- M.S. Dresselhaus and G. Dresselhaus, Adv. Phys. 30,139(1981).

2- A.R. Ubbelohde, Proc. Roy. Soc. (London) A327, 289(1972).

3- F.L. Vogel, G.M.T. Foley, C. Zeller, E.R. Falardeau, and J. Gan, Mater. Sci. Eng. 31,261(1977).

4- G.M.T. Foley, C. Zeller, E.R. Falardeau, and F.L. Vogel, Solid State Commu. 24,371(1977).

5- K. Sugihara and H. Sata, J. Phys Soc.(Japan), 18, 332(1963)

6- K. Sugihara, Phys Rev. B29, 5972(1984).

7- S. Pietronero, S. Strusler, H.R. Zeller, and M.J. Rice, Phys. Rev. Lett. 41, 763(1978).

8- F. Batallan, J. Bok, I. Rosenman, and J. Melin, Phys Rev Lett, 41, 330(1978).

9- W. Metz and D. Hohlwein, Carbon 13, 87(1975),(Pergamon Press)

10- C. Underhill, S.Y. Leung, G. Dresselhaus, and M.S. Dresselhaus, Solid State Commu., 29, 769(1979).

11- J.P. Issi, J. Herman, and M.S. Dresselhaus, Phys Rev B27, 1333(1983).

12- M. Elahy, C. Nicolini, G. Dresselhaus, and G.O. Zimmerman, Solid State Commun. 41,289(1982).

13- A.K. Ibrahim, G.O. Zimmerman, Phys Rev (in press).

14- A.K. Ibrahim, G.O. Zimmerman, Phys Rev 34,4224(1986).

15- R.G. Chambers, and J.G. Park, J. of App. Phys. (Britian), 12, 507(1961).

16- R.S. Markiewicz, Solid State Commu. 57,237(1986).

17- Y. Ohta, K. Kawamura, and T. Tsuzuku, Conf. Internationale sur la Carbons, Bordeaux, Texts Courts. p.298 (1984) and International Conf. on Carbon(1985).

18- C. Uher and D.T. Morelli, Phys Rev 27,2477(1983).

19- J.P. Issi, B. Poulaert, J. Herman, and M.S. Dresselhaus, Solid State Commu., 44, 449(1982).

20- E. McRae, J.F. Mareche, and A. Herold, Extended Abs. on GIC, MRS Meeting

(1986), Boston, Mass(USA), unpublished.

21- M.R. Corson, S.E. Millman, G.R. Hoy, and H. Masurek, Solid state Commu., 42,667(1982).

22- G. Kirczenow Phys Rev. B31, 5376(1985).

23- S. Hendricks, and E. Teller, J. Chem. Phys. 10,147(1942).

24- A.K. Ibrahim, R. Powers, G. Zimmerman, and M. Taher, IMMM Conf., Baltimore (USA),1986, and J. of App. Phys. to be published.

25- K. Tashiro, M. Saito, and T. Tsuzuku; presented in the international Symposium on GIC, tsukuba, Japan (1985).

FIGURE CAPTIONS

Fig. 1. The c-axis resistivity vs temperature for stages 2 (□), 3 (○),4 (△), 5 (+), 9 (×) $FeCl_3$-GIC's, and HOPG (◇).

Fig. 2. The c-axis resistivity normalized to the room temperature values vs temperature for stages 2 (□), 3 (○),4 (△), 5 (+), 9 (×) $FeCl_3$-GIC's, and HOPG (◇).

Fig. 3. Room temperature c-axis resistivity vs the inverse of the stage index for stages 2 (□), 3 (○),4 (△), 5 (+), 9 (×) $FeCl_3$-GIC's, and HOPG (◇).

Fig. 4. Resistivity coefficient of temperature at room (□), liquid nitrogen (○), and liquid helium (△) temperatures vs the inverse of the stage index for stages 2,4,5,9 $FeCl_3$-GIC's, and HOPG.

Fig. 5. The fits of the c-axis conductivity vs temperature for stage 9 $FeCl_3$-GIC's. The (□) are the data points.

Fig. 6. The fits of the c-axis conductivity vs temperature for stage 2 $FeCl_3$-GIC's. The (□) are the data points.

Fig. 7. Natural logarithm of the anistropy (σ_c/σ_{ab}) (□)and the peak height of the magnetic susceptibility (△) vs stage index for $FeCl_3$-GIC's.

Fig. 8. Scan up (□) and scan down (○) of resistivity vs temperature for stage 9 $FeCl_3$-GIC.

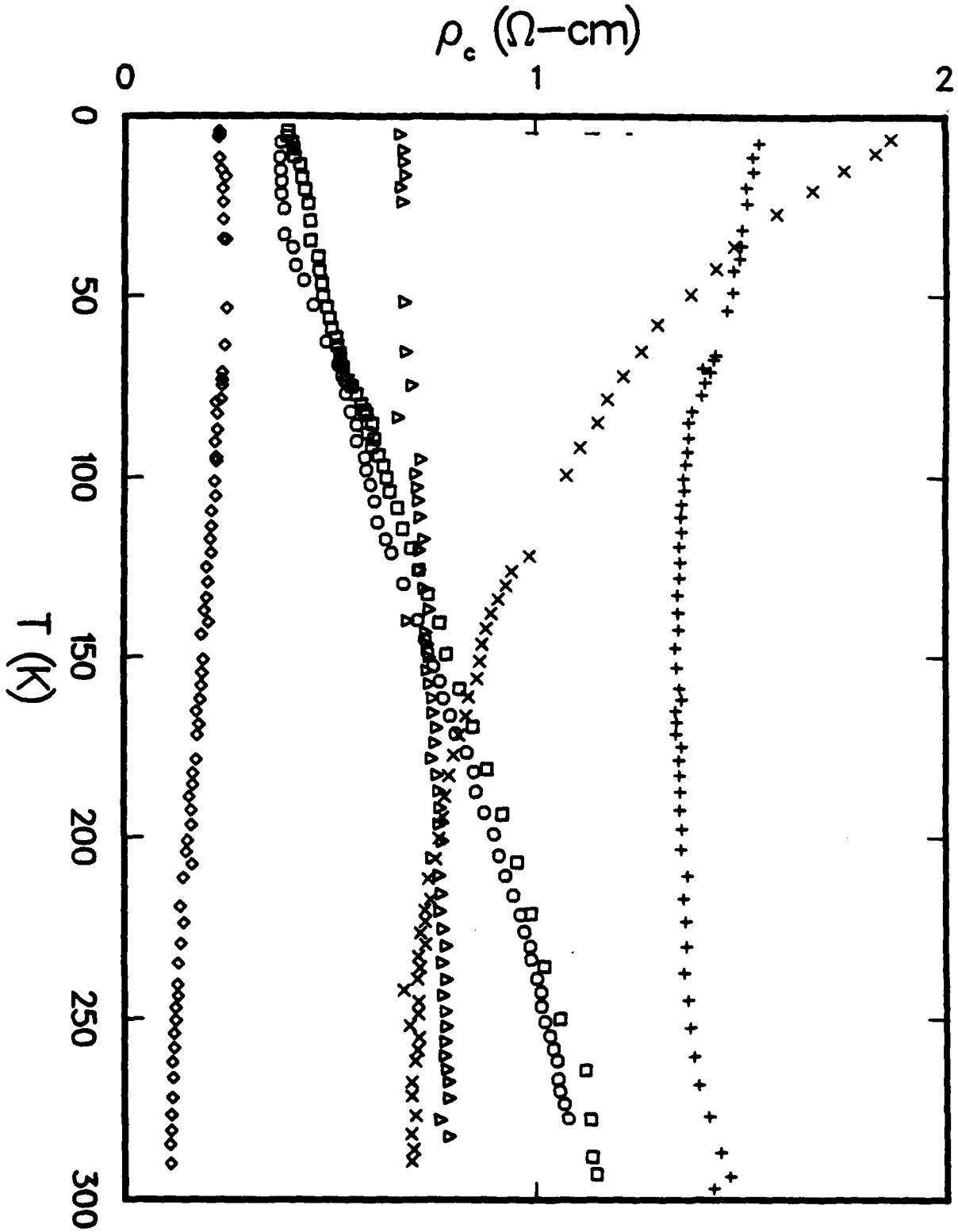
ρ_c (Ω–cm)
0
1
2
T (K)
0
50
100
150
200
250
300

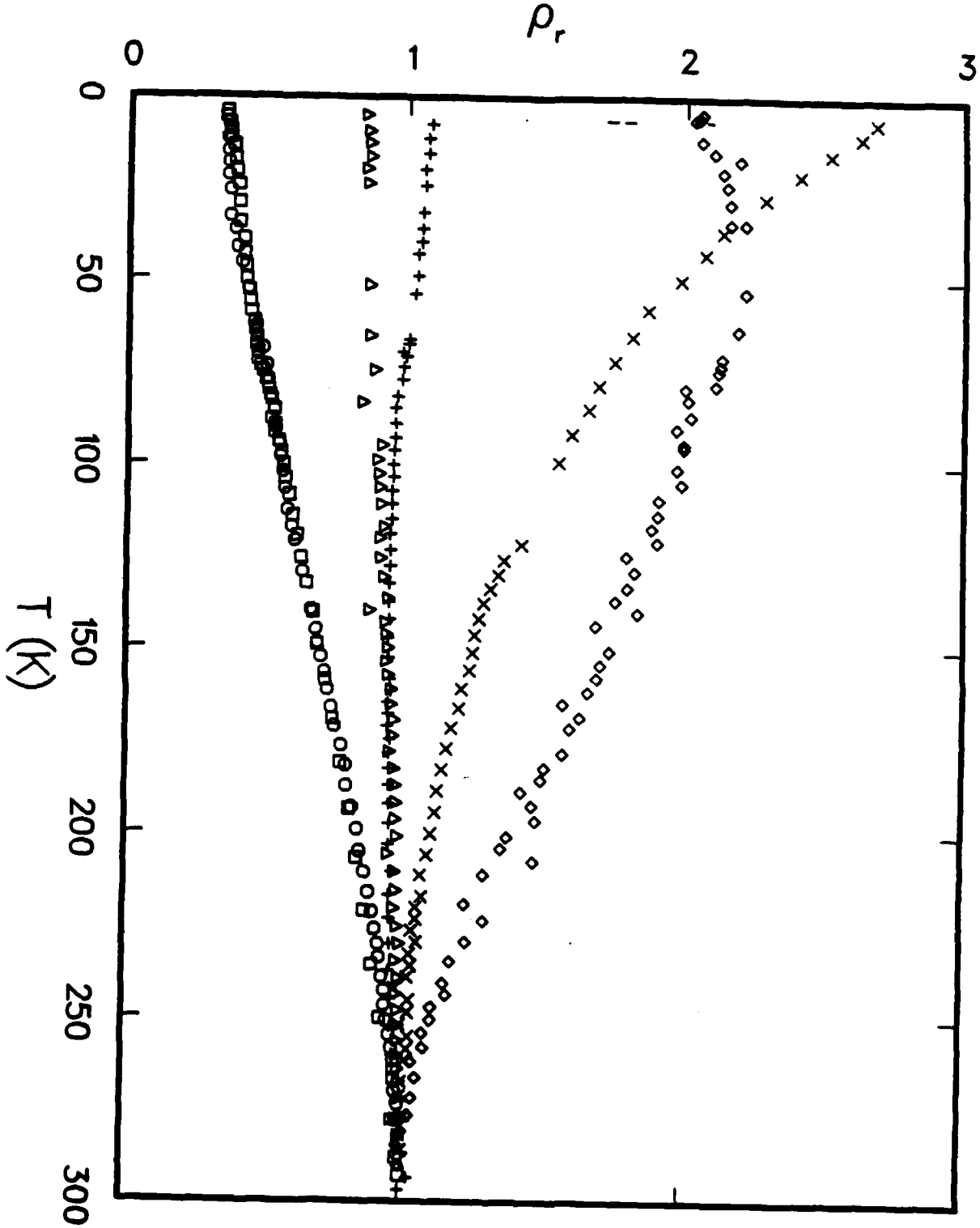
ρ_r
0
1
2
3
0
50
100
150
200
250
300
T (K)

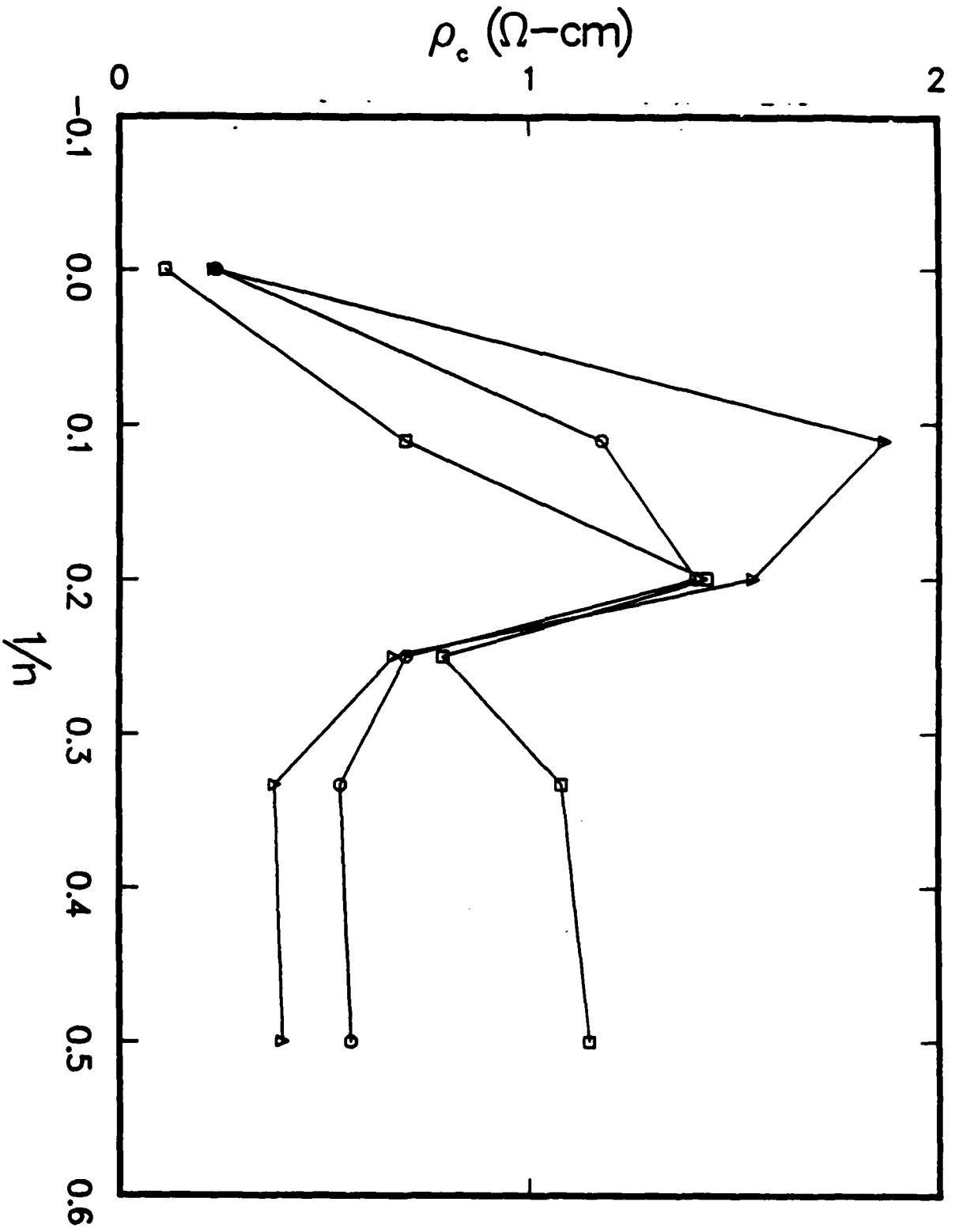
ρ_c (Ω–cm)
0
1
2
1/n
−0.1
0.0
0.1
0.2
0.3
0.4
0.5
0.6

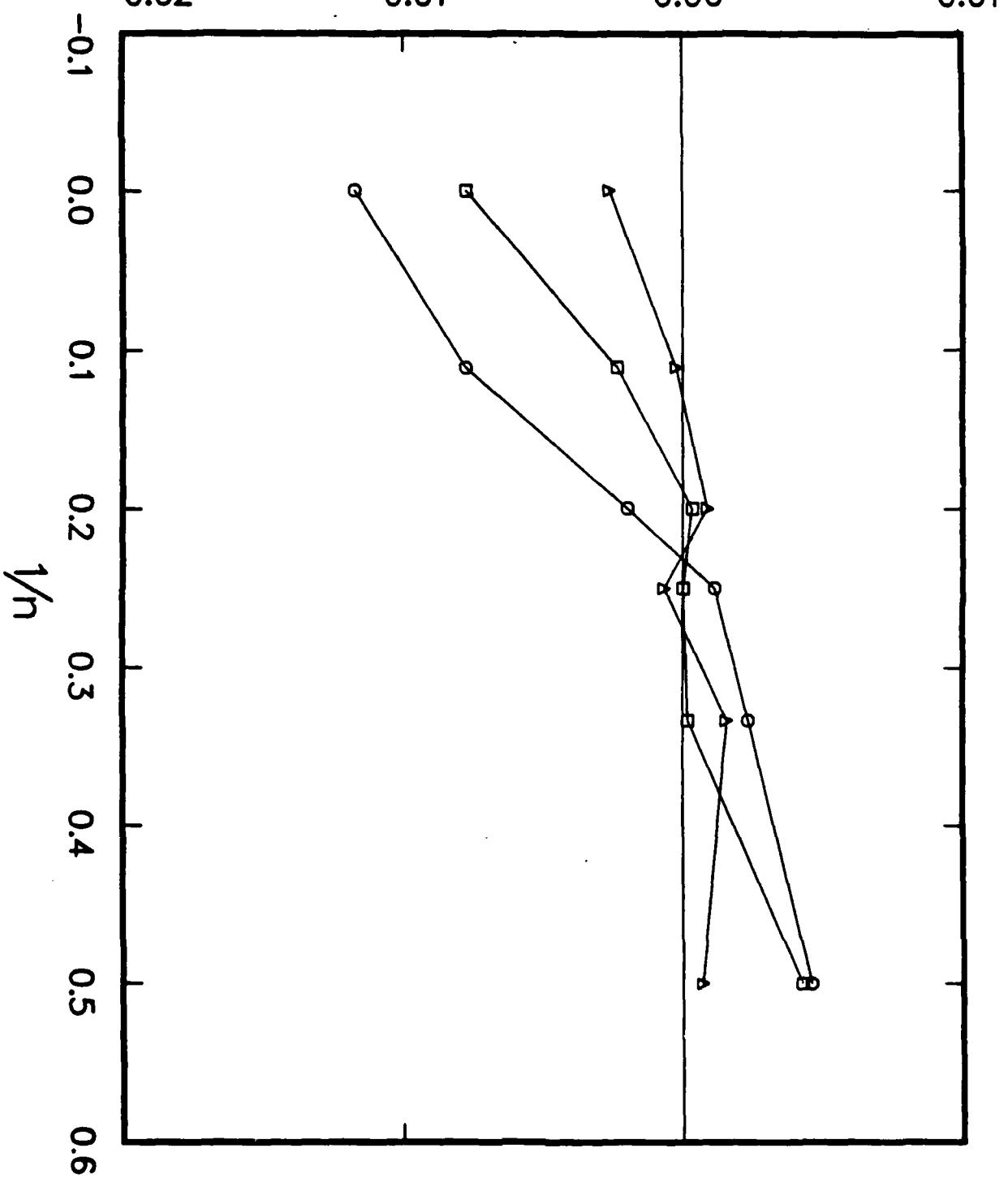
$d\rho_r/dT\ (K^{-1})$
−0.02
−0.01
0.00
0.01
1/n
−0.1
0.0
0.1
0.2
0.3
0.4
0.5
0.6

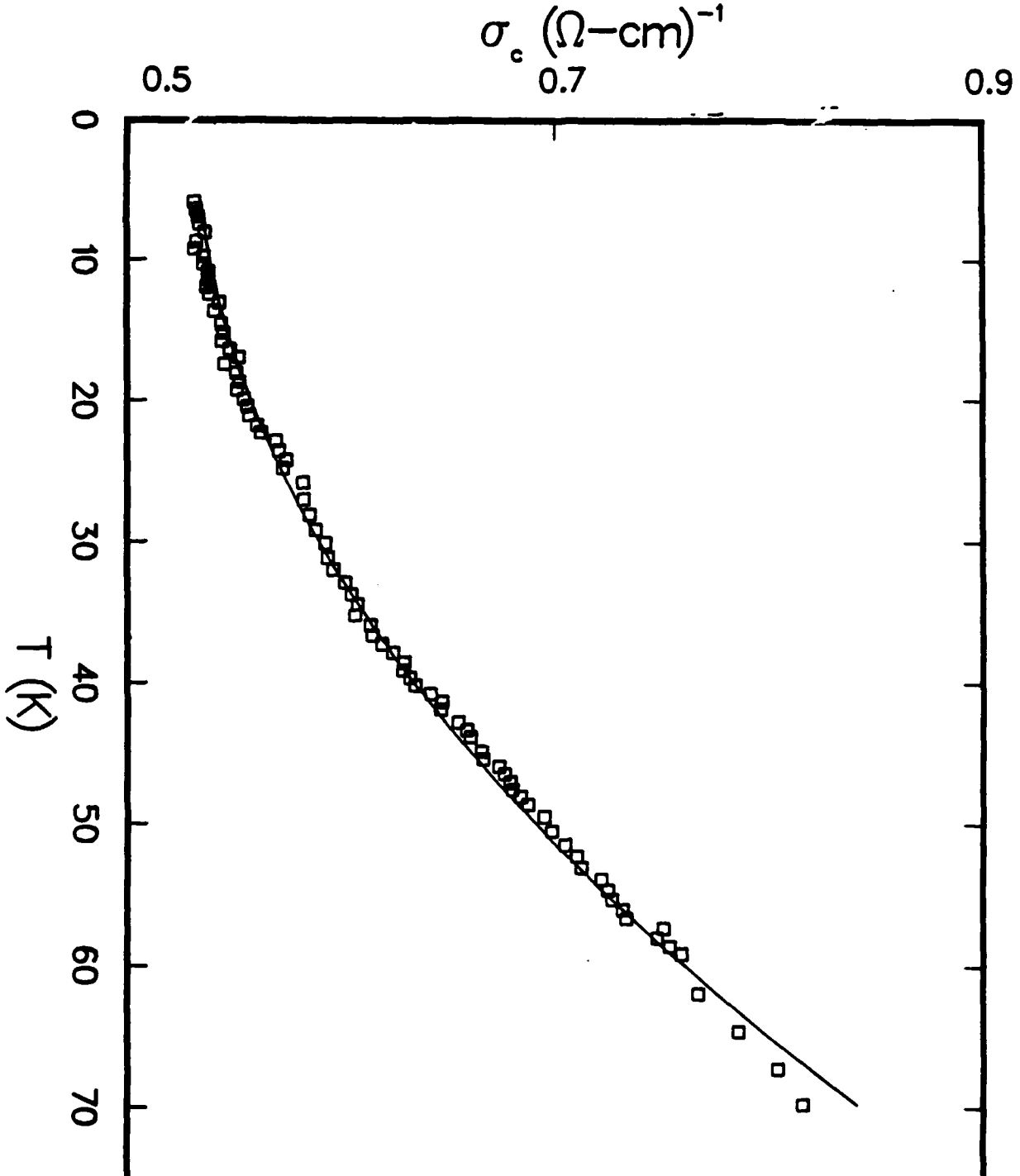
σ_c $(\Omega-cm)^{-1}$
0.5
0.7
0.9
T (K)
0
10
20
30
40
50
60
70
80

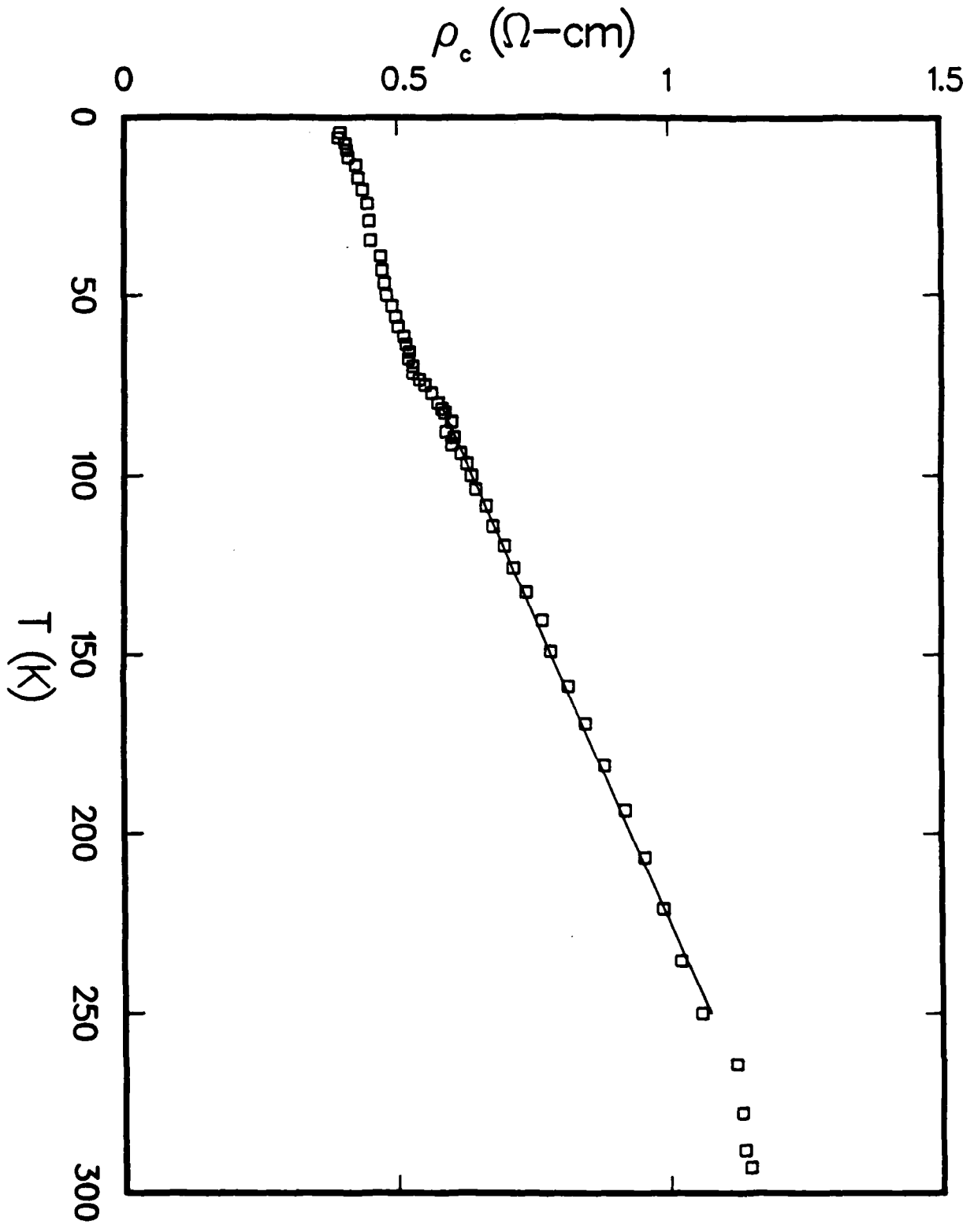
ρ_c (Ω-cm)
0
0.5
1
1.5
T (K)
0
50
100
150
200
250
300

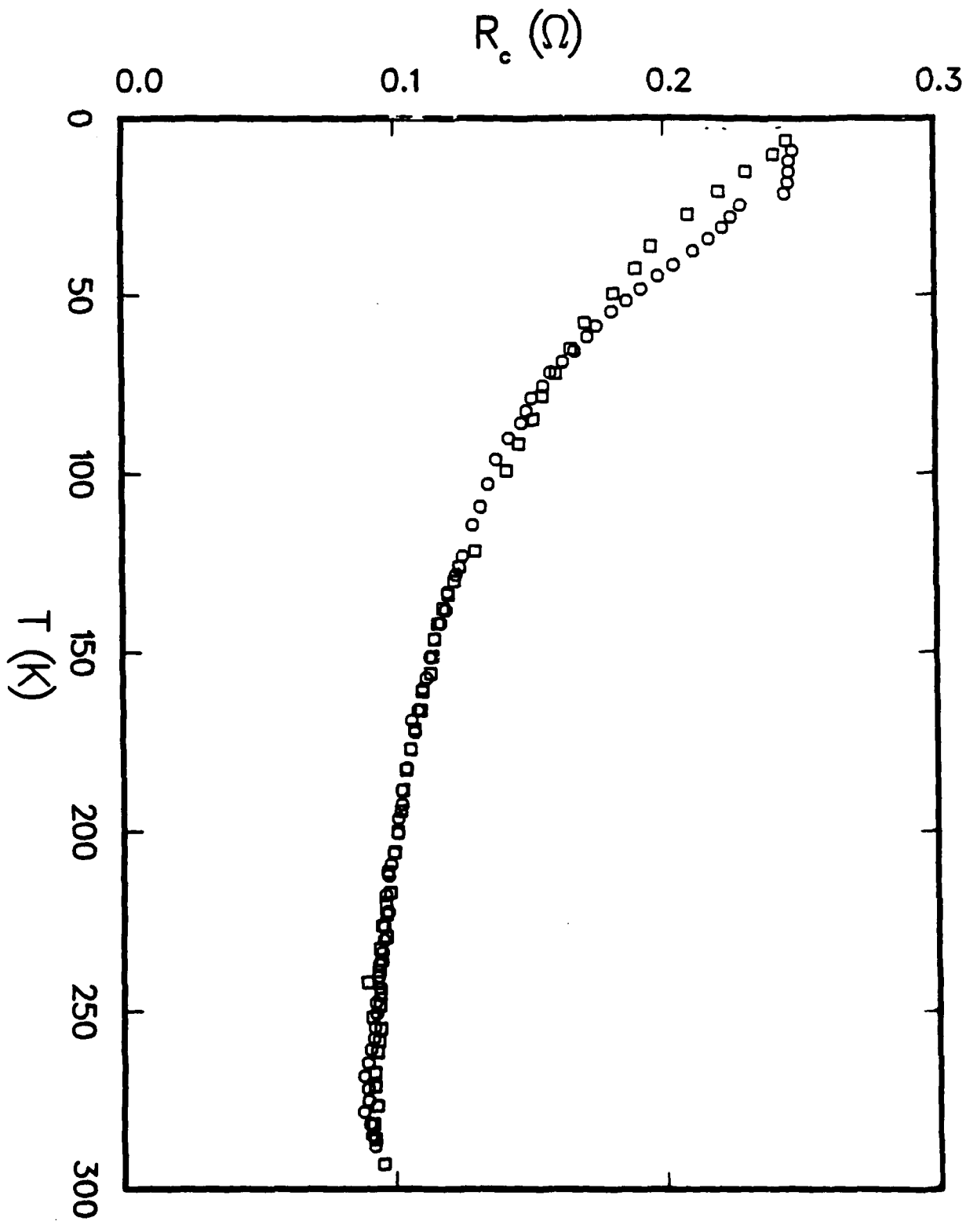
R_c (Ω)
0.0
0.1
0.2
0.3
T (K)
0
50
100
150
200
250
300

AD-A181 481 INVESTIGATION OF THE ELECTRIC AND MAGNETIC PROPERTIES OF INTERCALATED GRAPHITES(U) BOSTON UNIV MA DEPT OF PHYSICS G O ZIMMERMAN 1987 AFOSR-TR-87-0410 2/2

UNCLASSIFIED AFOSR-82-0286 F/G 11/4 NL

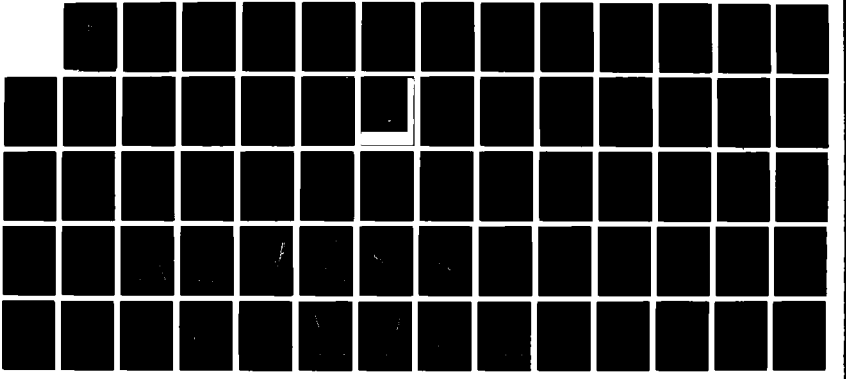

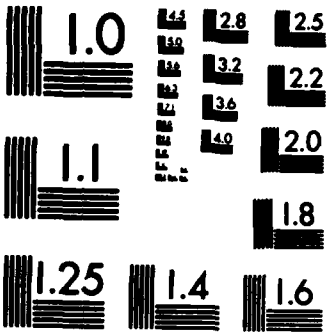

MICROCOPY RESOLUTION TEST CHART
NATIONAL BUREAU OF STANDARDS-1963-A

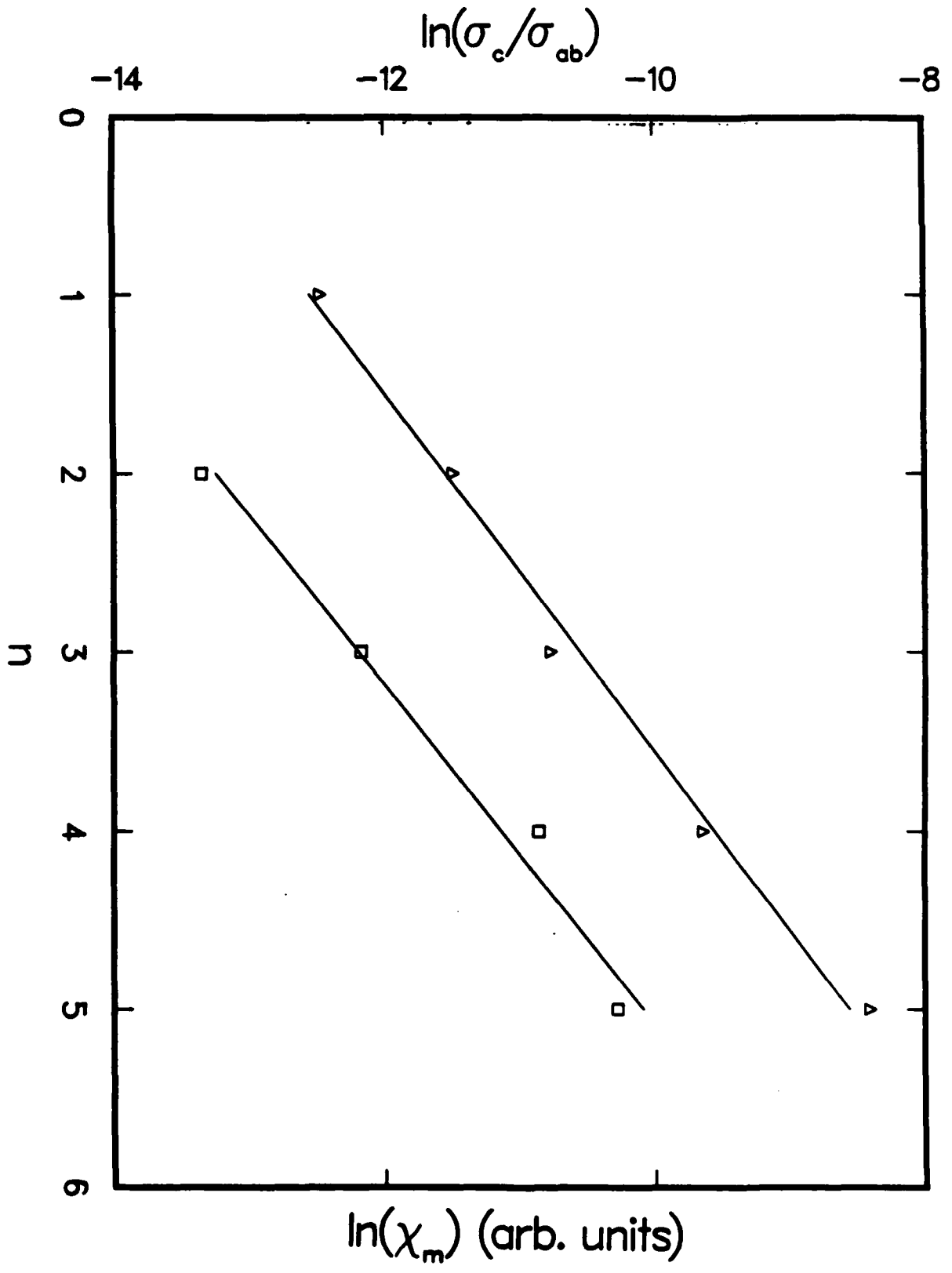
ln(σc/σab)
−14
−12
−10
−8
0
1
2
3
4
5
6
n
ln(χm) (arb. units)

TO BE PUBLISHED - JOURNAL OF APPLIED PHYSICS APRIL 1981

APPENDIX VI

HALL EFFECT AND MAGNETORESISTANCE IN LOW DIMENSIONAL MAGNETIC SYSTEMS*

A.K. Ibrahim, R. Powers, G.O. Zimmerman, and M. Tahar

Physics Department, Boston University

Boston, MA 02215

ABSTRACT

We have measured the Hall effect and magnetoresistance of stages 5 and 9 $FeCl_3$-graphite intercalated compounds in a magnetic field up to 20T and at several temperatures. Our preliminary results indicate that the Hall Coefficient(R_H) of stage-5 is positive at all field values and has insignificant variation between room and liquid helium temperature. In stage-9, howevere, R_H has a complicated field and temperature dependence. The magnetoresistance of the two stages at all temperature and field values is positive and stage-5 exhibits strong Shubinkov-deHaas oscillations at helium temperature. Fourier transforms of these oscillations are performed and the results indicate that stage-5 has a dominant fundamental frequency which is attributed to the hole carriers, whereas stage-9 exhibits a modulation of several frequencies which are related to different carrier pockets.

INTRODUCTION

Because of the drastic change in the physical properties upon the transition from a three-dimensional state to a two-dimensional one, low dimensional systems have recently been the subject of numerous research efforts. The extremely high anisotropy in most of the physical properties of highly oriented pyrolytic graphite (HOPG) makes this system an interesting candidate for low dimensional studies. Moreover this anistropy can be increased by the intercalation of acceptor or donor compounds into the graphite (IGS's)[1]. Because, electronically, only the graphite layers next to the intercalant change significantly upon intercalation[1-2], the intercalation of magnetic species into the graphite can

thus provide a layered magnetic compound with variable spacing between the magnetic layers. Therefore IGC's are useful systems for two-dimensional magnetic and structural studies[3-4].

In the last few years, IGC's have been extensively investigated by numerous research laboratories. However less attention was paid to galvanomagnetic (GM) effect studies in these compounds, and only a limited amount of theoretical and experimental work has been reported[5-6]. As an extension to the comperhensive investigation of the $FeCl_3$-graphite intercalated system, which was begun few years ago at our laboratory, we have measured the Hall effect and the magnetoresistance of stages 5 and 9 of this system(stage index refers to the number of graphite layers between two consecutive intercalant layers). In higher stages, where there are enough inner layers to screen out the interactions between the magnetic intercalant layers, one can expect the behavior to approximate a two-dimensional magnetic system. The measurements were carried out in a field up to 20T and at several temperatures.

both the long period air stability[7] and the ease of the technique of preparation [2] of $FeCl_3$-graphite compounds attract researchers to investigate this system. The measurements of the magnetic properties of this system were performed by several authors[8-10], the results of the magnetic susceptibility measurements indicate the existance of a low temperature phase transition in the form of a sharp peak in the susceptibilty. Other investigations such as x-ray structural[11], thermal conductivity[12], Ramman spectroscopic and infrared[13], and relaxation effect[14] measurements have been reported. However there are no comprehensive studies of GM effects reported for the $FeCl_3$-graphite system. Quantum oscillations(QO), which provide information about the Fermi surfaces and density of carriers, were obeserved in some IGC's[15-16]. In addition to the Hall effect and magnetoresistance We also investigate the quantum oscillations in stages 5 and 9 of $FeCl_3$ IGC's.

EXPERIMENTAL

The $FeCl_3$-GIC samples were prepared using a standard two-zone furnace technique where stage index was controlled by the temperature difference between the graphite host (HOPG) and the $FeCl_3$ powder. The samples were in the form of thin rectangular plates of dimensions 1.5x0.5x0.1 cm^3. Well-staged samples were achieved by controlling the pressure of Cl_2 gas inside the intercalation tube, as well as the partial pressure of $FeCl_3$ through rigid temperature control. After intercalation, the samples were characterized for identity and uniformity of staging using x-ray (00l) diffraction. The x-ray diffractograms were also used to determine the c-axis repeat distance I_c after cycling the samples from room to liquid helium temperature, and showed that the cycling did not affect this staging distance.

Most of the samples measured were characterized by means of the Mössbauer effect, which can reveal the ratio of iron atoms next to iron vacancies to that of the total number of iron atoms in the intercalant layer as well as that of Fe^{2+} to that of Fe^{3+} [17]. The initial measurements were performed on the same samples used in the Mössbauer investigations. The same samples and others were characterized periodically over a span of several years, having been stored at room temperature in a dry nitrogen enviroment, and showed no deterioration over a period of up to three years [7]. The Hendricks-Teller analysis technique[18] was also used to check the stage-disorder of stage 9 sample. Indeed, our x-ray data were in good agreement with the data calculated from the theoretical analysis of a pure and well-staged stage 9 sample. Galvanomagnetic measurements were performed in high magnetic field at the Francis Bitter National Magnet Laboratory(MIT). Layers of about 1.5x.5x.001cm^2 were peeled from the samples and then mounted on flat substrates. The five probe-dc technique was used to measure the Hall voltage and the transverse magnetoresistance.

Results and Analysis

A- The Hall Effect

The Hall resistivity versus the applied magnetic field at room, liquid nitrogen, and liquid helium temperatures is shown in Fig.(1) and Fig.(2) for stage 5 and stage 9, respectively. As shown in Fig.(1) the Hall voltage is positive and nearly linear with the field at all temperature and field values, indicating the dominance of hole carriers in stage 5. Stage 9, however, exhibits a different character at room temperature since the Hall voltage fluctuates between positive and negative values. The Hall coefficient, thus, has a complicated field dependence at room temperature indicating the near equality of the electron and hole densities. The Hall coefficient of HOPG[19-20] at low temperatures exhibits similar behavior to that of stage 9 at room temperature. As shown in Fig.(2), at liquid nitrogen and liquid helium temperatures, the Hall voltage is positive at all the field values, however, it is not as linear in the field as that of stage 5. Therefore, the Hall coefficient of stage 5 has the least complicated field dependence relative to those of stages 2 and 9, and HOPG(see ref.20 for data on HOPG and stage-2).

At this stage of our work, we have not performed detailed investigation of the temperature dependence of the Hall coefficient or the magnetoresistance. However, qualitative information can be extracted from our preliminary results. The Hall resistivity data shown in figures 1 and 2 for stages 5 and 9 and those of HOPG and stage-2[20] indicate that the Hall coefficient of stage 5 is less senstive to the variation with temperature relative to the other stages and HOPG as well. The Hall coefficient R_H, for a single-carrier and two-carrier models, is related to the carrier mobilities μ_h, μ_e, and the carrier densities n_h, n_e by the following equations

$$R_H = \frac{-1}{n_e e c} \quad or \quad \frac{1}{n_h e c}, \tag{1}$$

$$R_H = \frac{1}{n_e e}\left[\frac{n_h/n_e - (\mu_e/\mu_h)^2}{(n_h/n_e + \mu_e/\mu_h)^2}\right]. \tag{2}$$

According to Eq.(1), the Hall coefficient R_H would be constant between liquid nitrogen and liquid helium temperatures only if the carrier concentration is constant in this temperature range. However Eq.(2), the two-carrier model, indicates that the constancy of R_H is controlled by the temperature dependence of the four quantities n_h, n_e, μ_h, and μ_e or at least the carrier concentration and the mobility ratio.It would be unrealistic to assume the constancy of these four quantities.

Therefore, based on the field and temperature dependence of the Hall Coefficient, the conduction in stage-5 is dominated by one kind of charge carrier. Our measurements of the c-axis conductivity in this system[21] indicate that stage-5 has the minmum c-axis conductivity among the other stages of $FeCl_3$-graphite compounds. Moreover, the temperature coefficient of the resistance is nearly zero in stage-5 while the other stages exhibit postive and negative resistivity-temperature dependence. These results suggest that, in stage 5, the carriers are confined into layered planes and the electronic transport has the behavior of a two-dimensional system. The above quantitative descriptions are also supported by the results of the QO, as shown in part B of this work, and the observed low temperature magnetic phase transition in this system[10]. It has been shown that[22], this phase transition has the nature of a two-dimensional magnetic system and stage-5 among all other stages of $FeCl_3$-graphite compounds exhibits the maximum transition[23].

The behavior of the Hall data of stage-9 is different from that of stage-5, it has a complicated field and temperature dependence similar to that of HOPG. At room temperature the Hall voltage changes sign from negative to positive values at a field of about 4T. Thus the single-carrier model of Eq.(1) is not applicable at this temperature and one has to use the two-carrier model of Eq.(2) to, qualitatively, analyze these data. Because of the difference in the effective masses of the electrons and holes, one can ex-

pect the high field to drift holes more than electrons. Thus at room temperature holes contribute dominantly to the Hall voltage in the high field region . In terms of Eq.(2), this result can be described as a change of the inequality $\frac{n_h}{n_e} < (\frac{\mu_e}{\mu_h})^2 < 1$ in low field to $\frac{n_h}{n_e} > (\frac{\mu_e}{\mu_h})^2$ in high field. Thus it is possible that one could have positive Hall Coefficient even when $\frac{n_h}{n_e} < 1$. At low temperatures the Hall voltage is dominantly contributed by holes and then exhibits very weak QO at helium temperature. Thus QO oscillations exist in the Hall voltage of stage-9, stage-2[20], and HOPG[20], however less significant oscillations are observed in stage-5.

B-Magnetoresistance

The tranverse magnetoresistivity $\frac{\Delta\rho}{\rho_o}$ as a function of the applied field at room, nitrogen, and helium temperatures is presented for stage 5 and stage 9 of $FeCl_3$-graphite compounds in Fig.(3) and Fig.(4), respectively. The value of $\Delta\rho$ increases with the field at all temperatures, there is no sign of saturation up to a field of 20T in stage-9, but in stage-5 there is a weak indication of saturation at very high fields. At room and nitrogen temperatures the two stages exhibits similar field and temperature dependence, however at helium temperature, although the over all behavior is still the same, the size of the change in $\Delta\rho$ is different. The magnetoresistance of both stages oscillates at helium temperature, but the magnitudes of the oscillations in stage 5 are relatively larger and faster than those of stage-9. The magnetoresistance of HOPG, and stages 2,5, and 9 exhibit similar field and temperature dependance.

The similarities between the magnetoresistance data of HOPG and the three stages of $FeCl_3$ suggest that the transport mechanism in this system can be described in terms of a two-dimensional model. The scattering of the charge carriers is, thus, an in-plane mechanism controlled by the graphite lattice and the density of free carriers. The increase of the number of free carriers due to the charge transfer between the graphite and the intercalant is accounted for by the sharp decrease in the magnitude of $\Delta\rho$ of the

three stages relative to that of HOPG. Magnetoresistance data are, generally, analyzed on the basis of a simple two-carrier model in which an average Hall mobility could be obtained from the formula

$$\mu^* = (\frac{\Delta\rho}{\rho_o H^2})^{\frac{1}{2}}. \tag{3}$$

For conductors that obey a one-carrier model, the carrier density(n) determined by $ne\mu^*\rho_o = 1$ should be equal to that determined by Eq.(1). However, these simple one-carrier and two-carrier models fail to give adaquate results for many IGC's. Details of these calculations will be given in a later paper.

The QO of the magnetoresistance of stages 5 and 9 are plotted as a function of the applied field in Fig.(5)(note that the data of stage-5 are multiplied by a factor of 70). As shown in the figure, the size of the oscillations relative to the base line in stage 5 is significantly larger than that of stage-9. The oscillations in the electric resistivity arise from the oscillations in the relaxation time for the scattering carriers. Because these oscillations are a manifestation of the periodic variation in the density of states at the Fermi energy, the large amplitude of the oscillations in stage-5 can be attributed to a longer in-plane relaxation time. The results of the in-plane conductivity measurements also indicate that stage-5 has a relatively large value compared with that of stage-9. In Fig.(6) the oscillations in stage-5 are plotted as a function of the inverse field. As shown in the figure, the fundamental frequency is modulated by other very weak harmonics. As it was pointed out in the previous section, this result is consistent with the Hall data which indicate that in stage-5 the transport mechanisms are dominantly controlled by one kind of charge carrier.

Fourier transforms of these oscillations are displayed in Fig.(7) for stage 5 and stage 9. The dominant frequency of stage-5 which is attributed to the hole oscillations occurs at about 538T. In stage-9, as shown in the figure, oscillations of different frequencies are

observed at 0.55T, 4.4T, and 8.8T. Some high frequencies of insignificant amplitudes are also observed in stage-9. It is clear that some of these frequencies in stage-9 are due to the HOPG layers in the system. The large frequency of stage-5 indicates a similar large size in the extremal Fermi surface cross-sectional area which is a measure of the carrier density at the Fermi energy.

CONCLUSION

The results of galvanomagnetic measurements for stages 5 and 9 of $FeCl_3$- graphite compounds indicate that the conduction in stage-5 is dominanted by hole carriers, whereas stage-9 exhibits a complicated field and temperature dependence similar to that of HOPG. Both the Hall data and the magnetoresistance data suggest that transport mechanisms in $FeCl_3$ have the behavior of two-dimensional magnetic systems. Quantum oscillations in the magnetoresistance are obeserved in both stages, however the size of the oscillations in stage-5 is very large relative to that in stage-9. Fourier tranforms of these data show a dominant single frequency in stage-5 and the modulation of several frequencies in stage-9.

REFFRENCES

* Supported in part by the Air Force Office of Scientific Research Grant AFOSR 82-0286. Also with the Francis Bitter National Magnet Laboratory, supported by the National Science Foundation.

1- A. Hérold, in Physics and Chemistry of Materials with Layered Structures, edited by F. Levy (Dordrechet, Reidel,1979),p.323.

2- M.S. Dresselhaus and G. Dresselhaus, Adv. Phys. 30,139(1981).

3- Yu.S. Karimov, Sov. Phys. JETP 41,772(1976).

4- A. Erbil, R.J. Birgeneau and M.S. Dresselhaus, Phys. Rev. Lett. 49,1427 (1982).

5- O.G. Onn, G.M.T. Foley, and J.E. Fischer Phys. Rev. B19,6474(1979).

6- H.Suematsu, S. Tanuma, and K. Higuchi Physica 99B,420(1980).

7- Millman thesis, Boston University(1982), Unpublished.

8- Yu.S. Karimov, and A.V. Zvarykina, Sov. Phys.-Solid State 13,2388(1972).

9- D. Hohlwein, P.W. Readman, A. Chamberod, and J.M.D. Coey, Phys. Status Solidi B64, 305(1974).

10- S.E. Millman, B.W. Holmes, and G.O. Zimmerman, Solid State Commun., 43,903(1982).

11- D. Hohlwein and W. Metz, Z. Krist. 139,279(1974).

12- J-P. Issi, J. Heremans, and M.S. Dresselhaus, Phys. Rev. B27, 1333 (1983).

13- C. Underhill, S.Y. Leung, G. Dresselhaus, and M.S. Dresselhaus, Solid State Commu. 29,769(1979).

14- A.K. Ibrahim, and G.O. Zimmerman, Phys Rev. B34(1986).

15- G. Dresselhaus and S.Y. Leung, Solid State Commu. 35,819(1980).

16- A.S. Bender and D.A. Young J. Phys. C5,2163(1972).

17- M.R. Corson, S.E. Millman, G.R. Hoy, and H. Mazurek, Solid State Commu. 42,667(1982).

18- S. Hendricks and E. Teller, J. Chem. Phys 10,147(1942).

19- W.H. Lowrey and I.L. Spain, Solid State Commu. 22,615(1977).

20- A.K. Ibrahim, R. Power, and G.O. Zimmerman, Extended Abs. on IGC, MRS Meetin (1986) Boston, MA(USA)(unpublished).

21- A.K. Ibrahim, R. Powers, M. Tahar, and G.O. Zimmerman, Bulletin of the APS 31,644(1986).

22- M. Elahy and G. Dresselhaus, in Intercalated Graphite, Symp. Proc. of MRS, 19,207(1983).

23- A.K. Ibrahim, and G.O. Zimmerman, to be published.

Figure Captions

Figure 1 The Hall resistivity versus the applied field of stage-5 at helium(1), nitrogen(2), and room(3) temperatures.

Figure 2 The Hall resistivity versus the applied field of stage-9 at helium(1), nitrogen(2),

and room(3) temperatures.

Figure 3 The magnetoresistance versus the applied field of stage-5 at helium(1),nitrogen(2), and room(3) temperatures.

Figure 4 The magnetoresistance versus the applied field of stage-9 at helium(1),nitrogen(2), and room(3) temperatures.

Figure 5 The oscillations in the magnetoresistance versus the field at helium temperature of stage-5(1) and stage-9(2)(Stage 5 data are multiplied by 70).

Figure 6 the oscilattions in the magnetoresistance versus the inverse ofield of stage-5(nonoscillatory part is subtracted).

Figure 7 Fourier transform of data obtained from stage-5 and stage-9 at helium temperature. The top x-axis refers to stage-9 data, where the bottom one refers to stage-5 data.

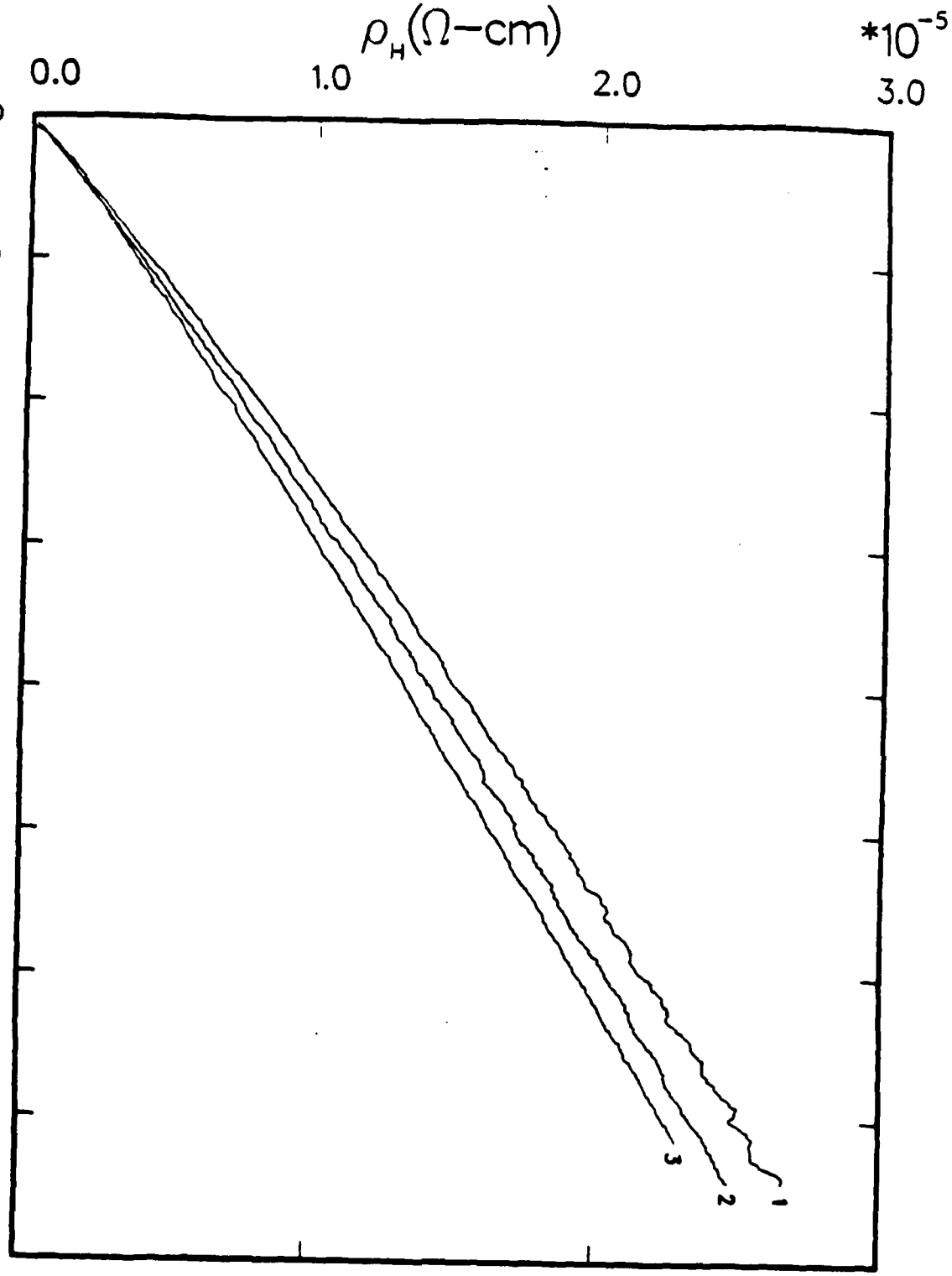

Fig (1)

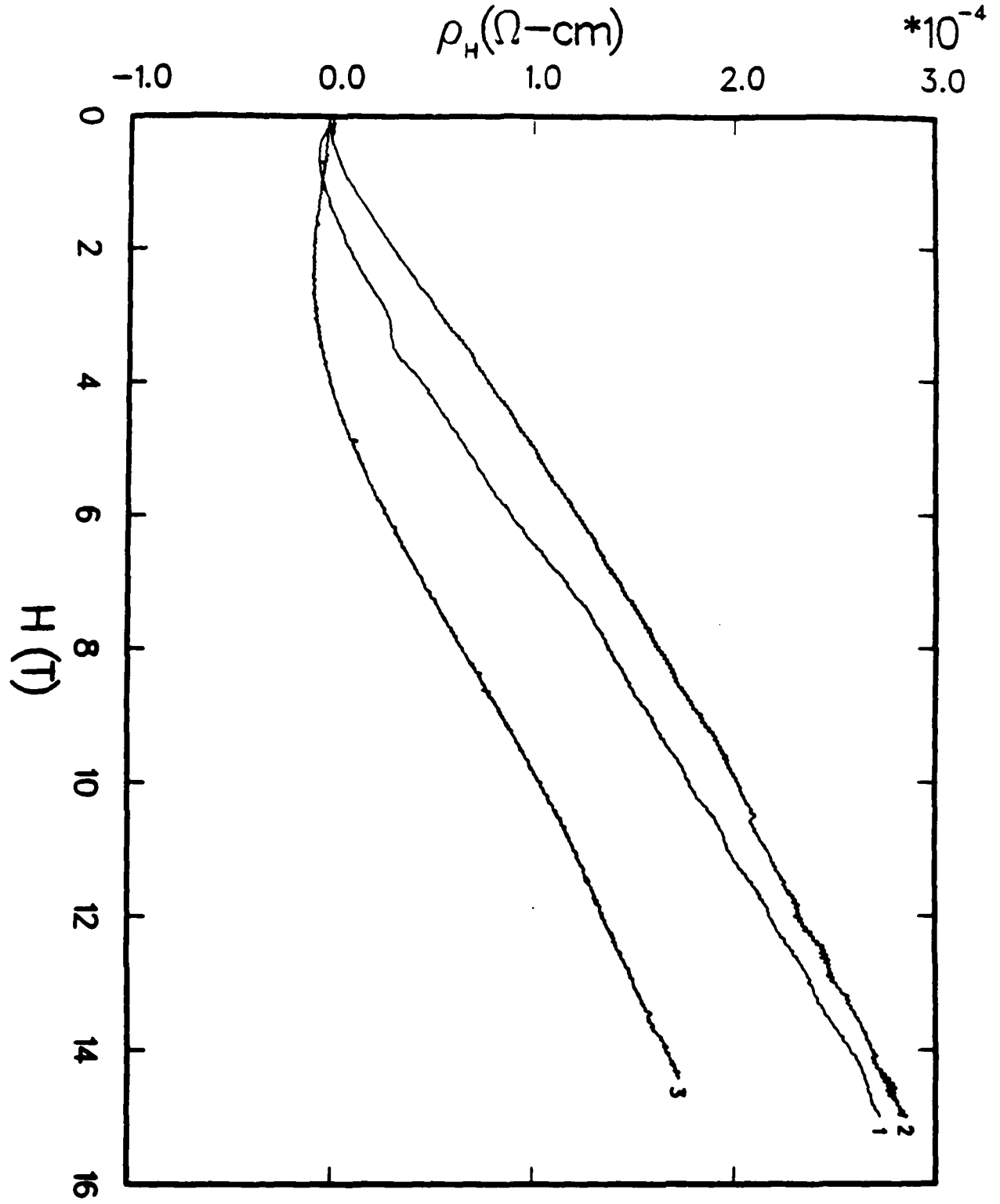

Fig 9(a)

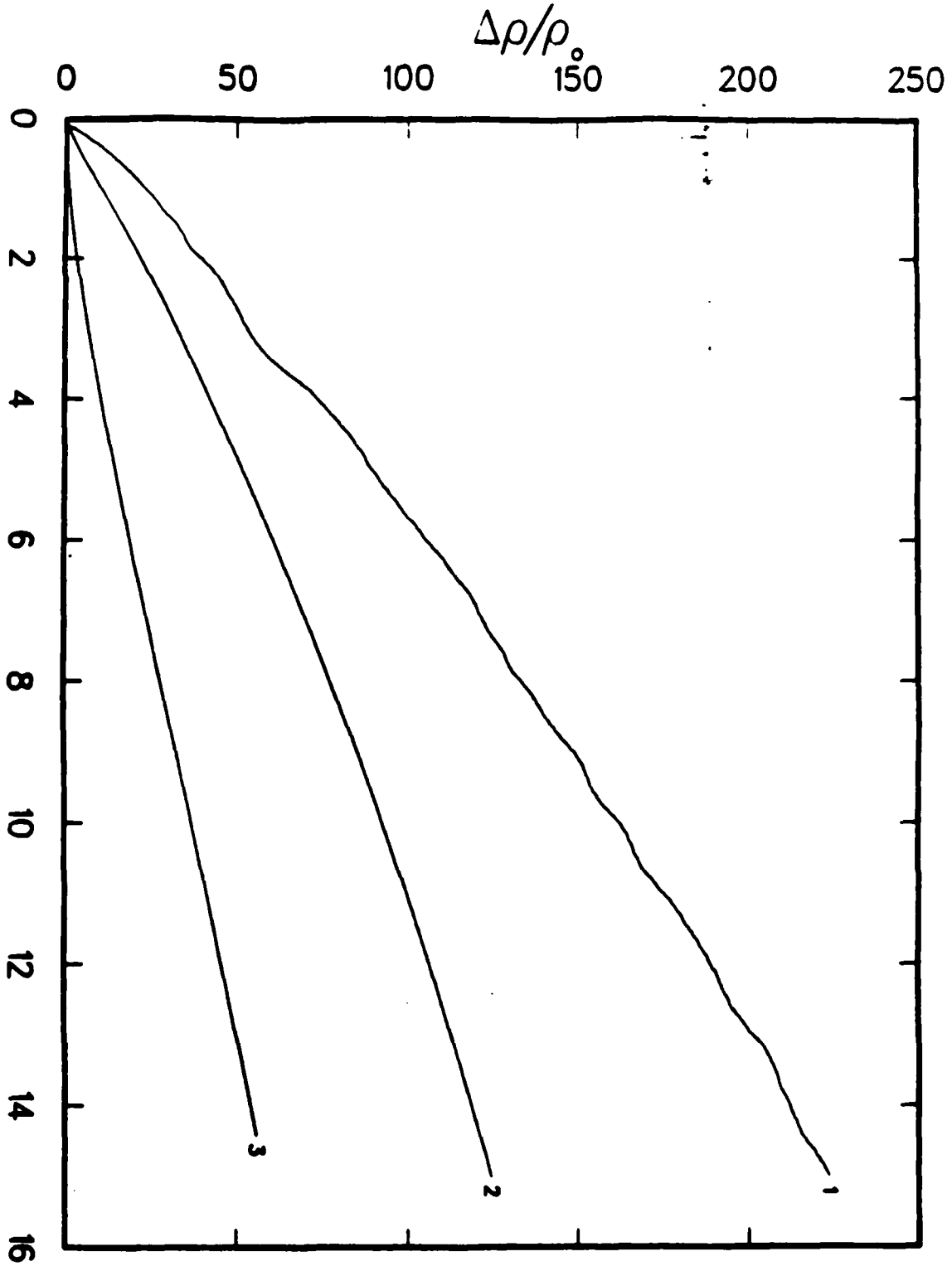

Fig 9 (3)

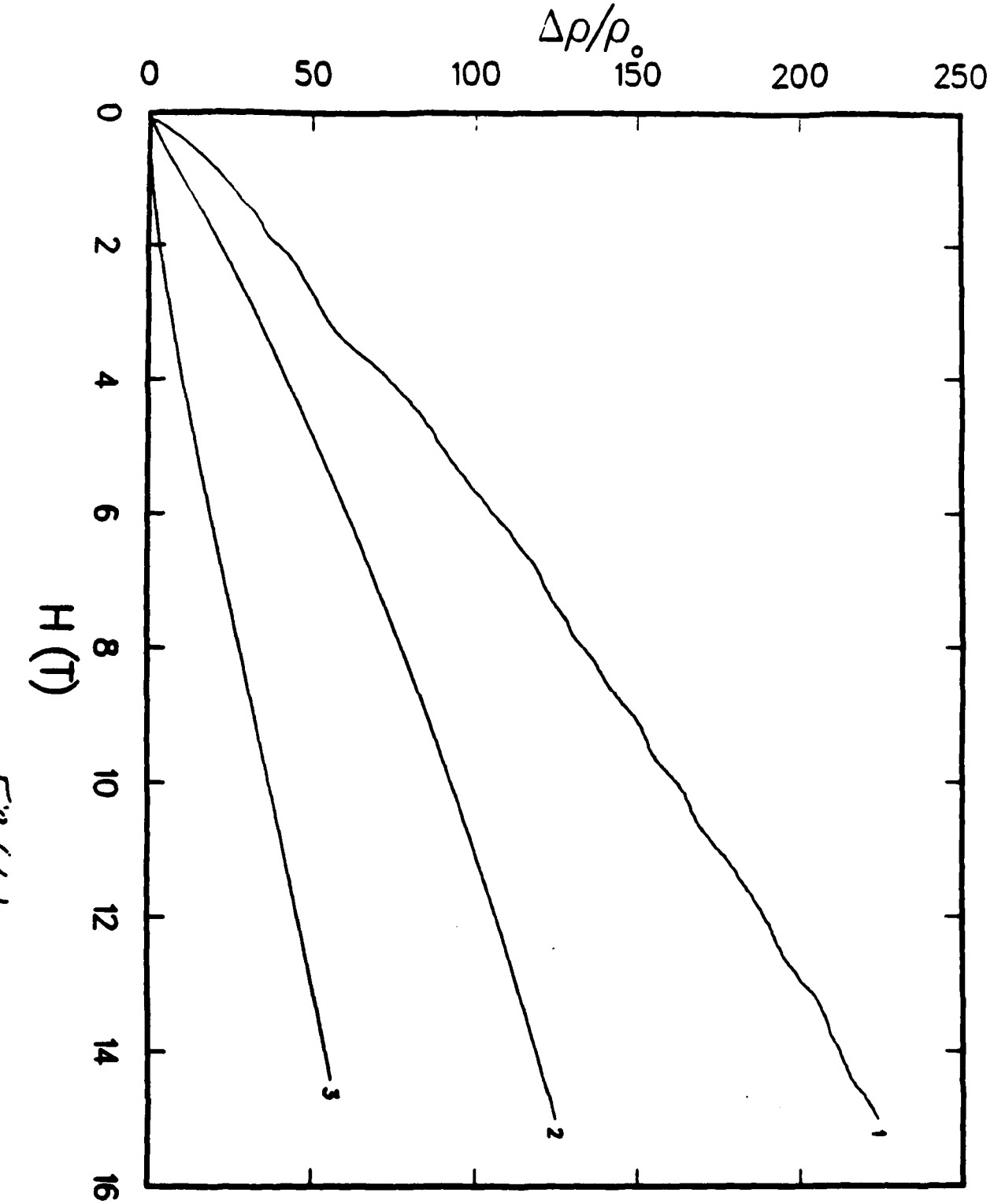
$\Delta\rho/\rho_o$
0
50
100
150
200
250
H (T)
0
2
4
6
8
10
12
14
16
1
2
3

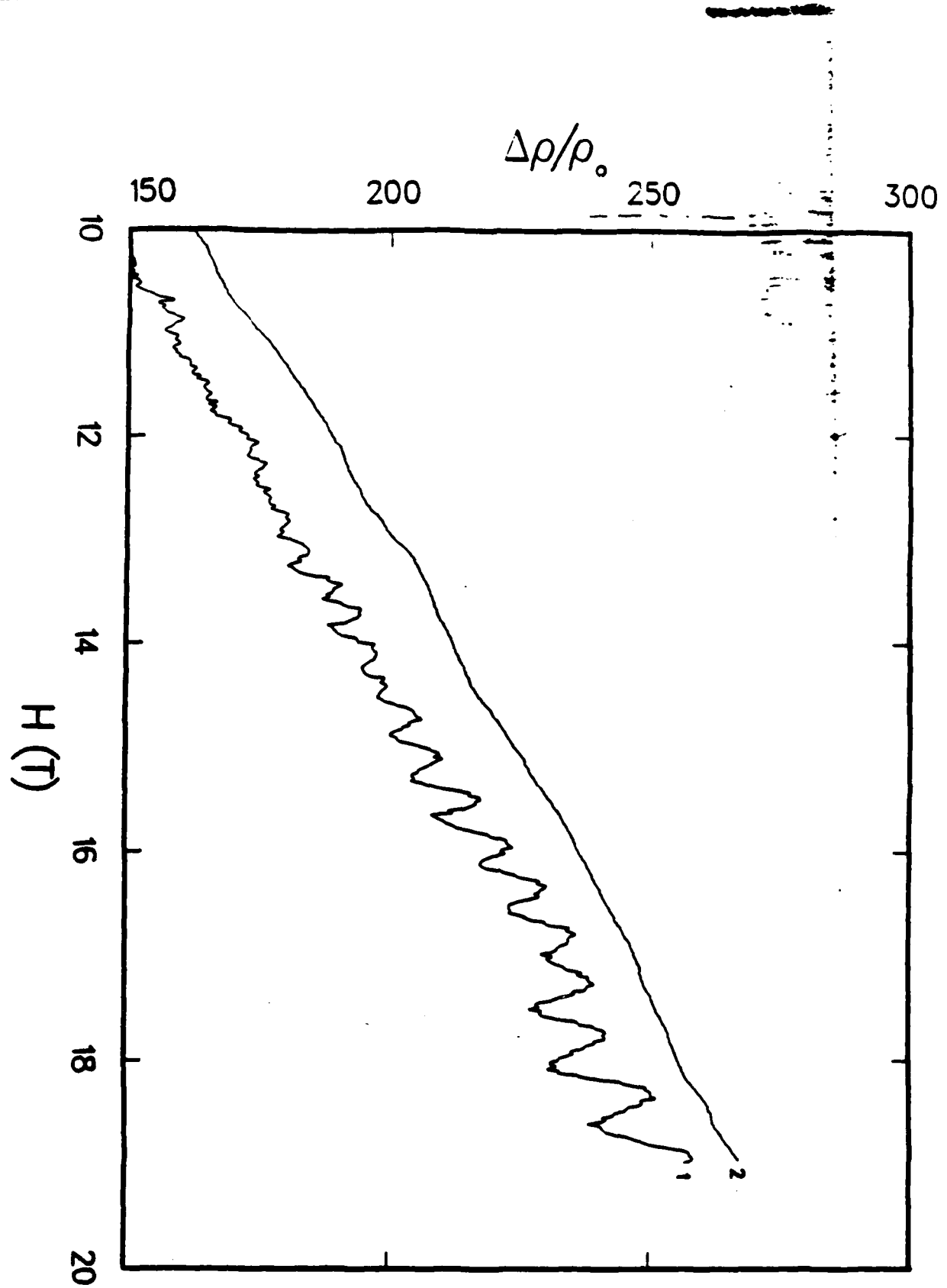

Fig (5)

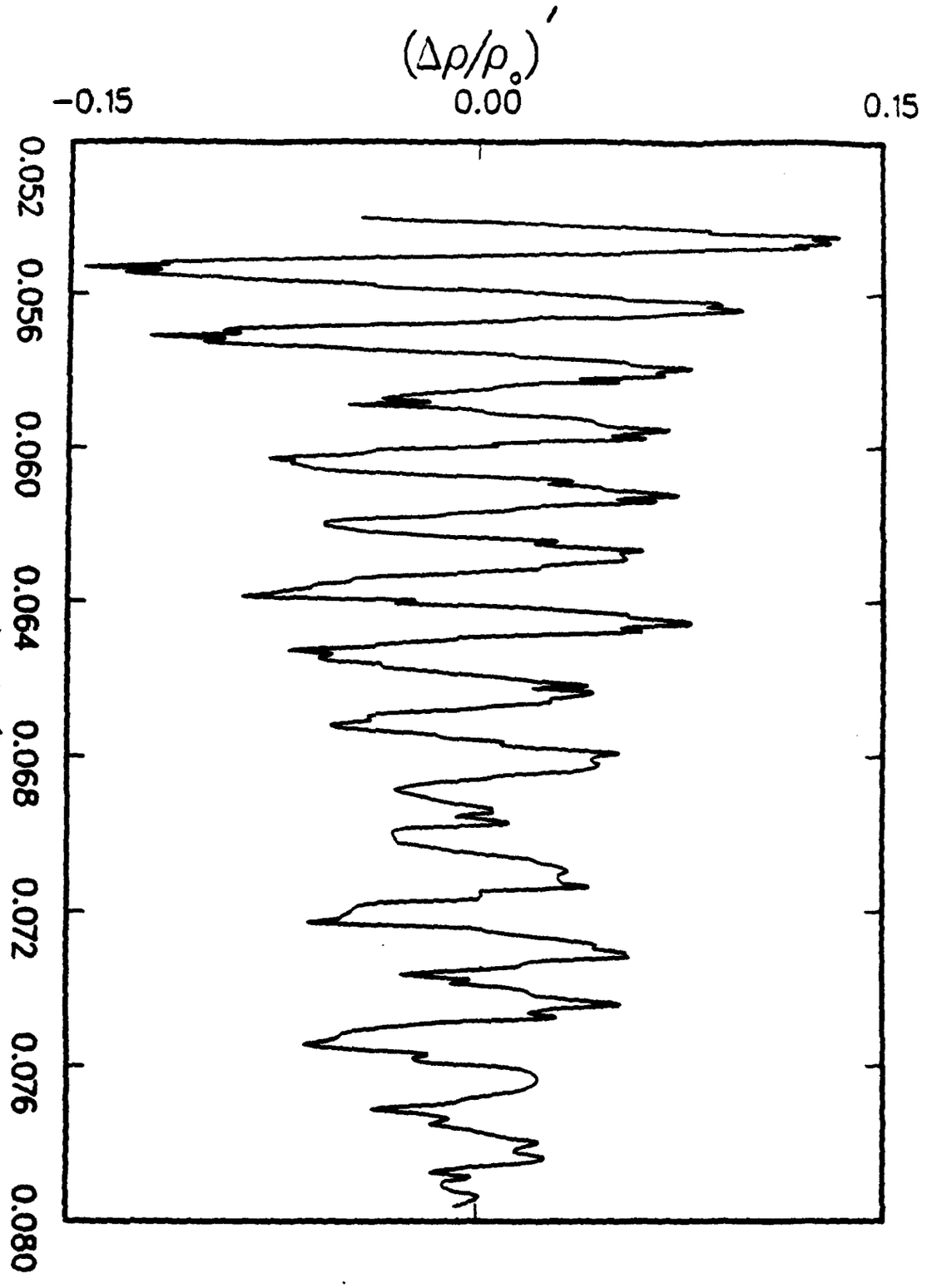
$(\Delta\rho/\rho_o)'$
−0.15
0.00
0.15
0.052
0.056
0.060
0.064
0.068
0.072
0.076
0.080
1/H (T^{-1})

Fig (6)

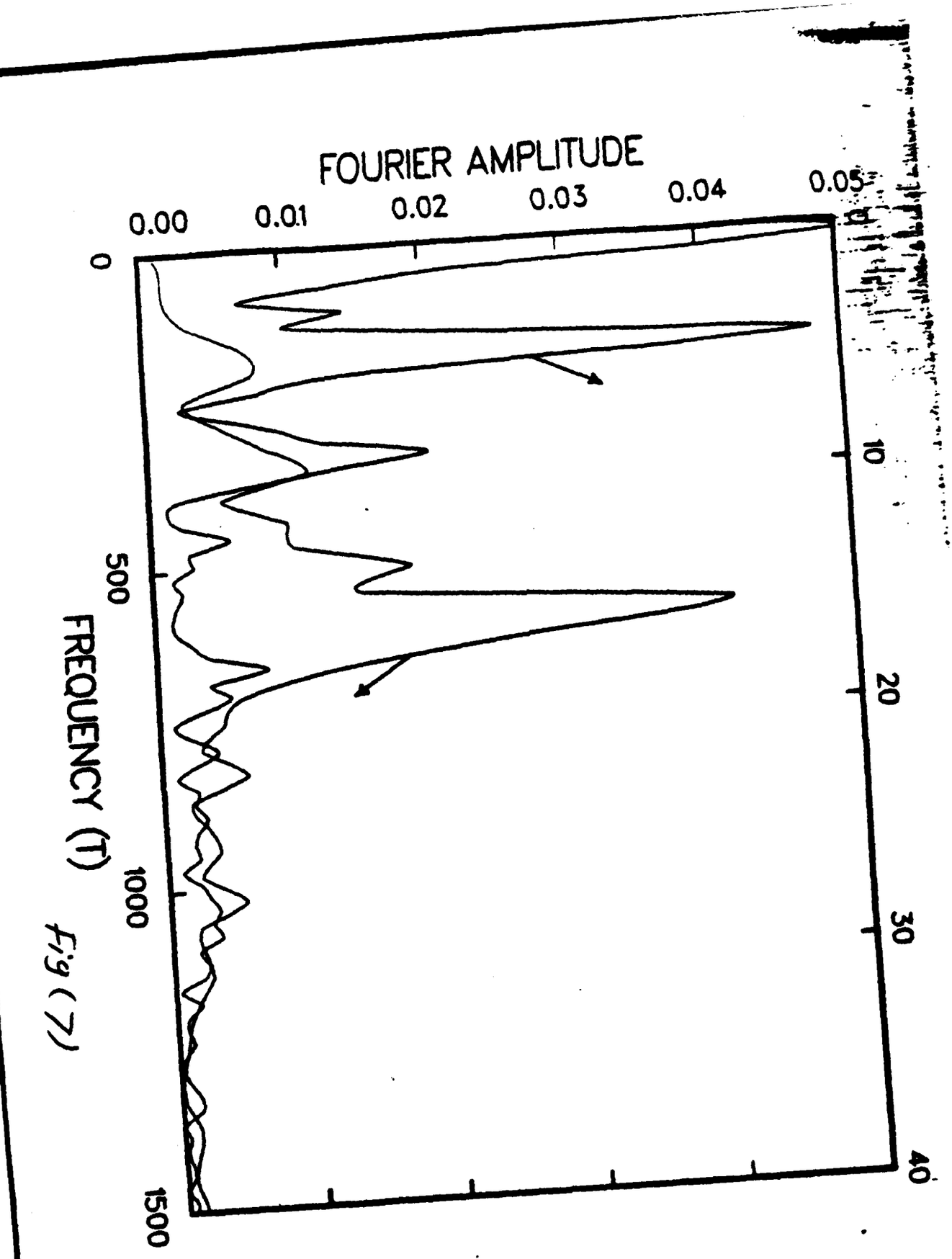
FOURIER AMPLITUDE
0.00
0.01
0.02
0.03
0.04
0.05
0
500
1000
1500
FREQUENCY (T)
10
20
30
40

Fig (7)

EXTENDED ABSTRACTS

GRAPHITE INTERCALATION COMPOUNDS

Edited by
M. S. Dresselhaus, Massachusetts Institute of Technology
G. Dresselhaus, Massachusetts Institute of Technology
S. A. Solin, Michigan State University

Proceedings of Symposium K
1986 Fall Meeting of the Materials Research Society

December 3-5, 1986
Boston Marriott Hotel at Copley Place
Boston, Massachusetts

Principal Symposium Support
NASA Lewis Research Center
Office of Naval Research

MRS
Materials Research Society
Pittsburgh

GALVANOMAGNETIC EFFECTS IN GRAPHITE AND GRAPHITE INTERCALATED COMPOUNDS

A.K. Ibrahim, R. Powers, and G.O. Zimmerman*+
Physics Department, Boston University

INTRODUCTION

Electronic properties of highly oriented pyrolytic graphite (HOPG) can be drastically changed by the intercalation of acceptor or donor compounds. The charge density transferred from or into the graphite layers plays an important role in controlling the electronic properties of the graphite intercalated compounds (GIC's). Although the transport properties of these compounds have been extensively studied, the roles of the charge transfer between the intercalants and the graphite are only partly understood. Galvanomagnetic (GM) measurements and the related quantum oscillations (QO) are among those reliable techniques which provide information about the electronic structure of these compounds. In this work, we have measured the GM effects in the stage-2 $FeCl_3$-graphite compound and in HOPG. The measurements were carried out in fields up to 20T at several temperatures. In high magnetic field at helium temperature, QO were observed in the magnetoresistance ($\Delta\rho$) and in the Hall effect for stage-2 whereas HOPG exhibits oscillations only in $\Delta\rho$. These magnetoresistance oscillations of HOPG are in qualitative agreement with previously reported data [1,2].

EXPERIMENTAL

$FeCl_3$-GIC samples were prepared using a standard two-zone furnance technique [3] where stage index was controlled by the temperature difference between the graphite host (HOPG) and the $FeCl_3$ powder. The samples were in the form of thin rectangular plates of dimensions 1.5x0.5x0.01 cm^3. The five probes-DC technique was used to measure the Hall effect and the magnetoresistance. The current was kept lower than 5 MA to avoid thermal effects. The measurements were carried out at the National Magnet Laboratory (MIT). Measurements have been made for two specimens cut from each sample (HOPG and stage-2) and several scans were taken to ensure the reproducibility of our data.

RESULTS AND ANALYSIS

A-THE HALL EFFECT DATA:

The Hall resistivity of HOPG verses the applied magnetic field at room, liquid nitrogen, and liquid helium temperatures is shown in fig.(1). At room temperature the Hall Voltage is negative at all field values indicating that

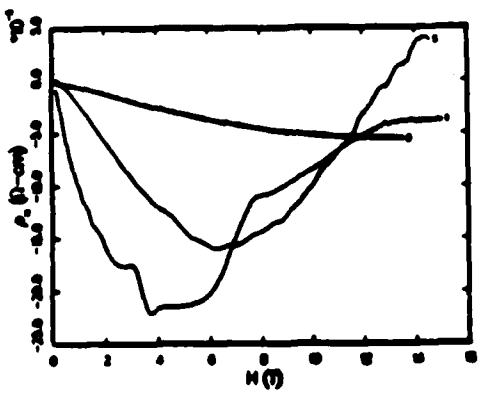

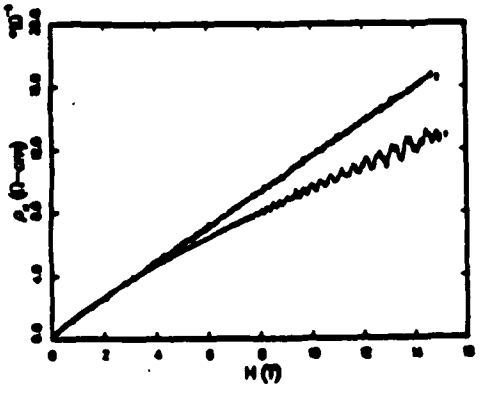

Fig.1 Hall resistivity vs. field (H) of HOPG at He(1), Ni(2) and Rm(3)temp.

Fig.2 Hall resistivity vs. field (H) of stage-2 at He(1) and Rm(2) temp.

the majority of charge carriers are electrons. This result is consistent with the low field measurements of Dillon et al [4] and Ayache [5], however at high fields our data exihibit a saturation effect. The electron and hole densities of HOPG are nearly equal, but due to the differences in their effective masses the electrons are the dominant contributors to the Hall Voltage. As the field becomes large enough to force all carriers to complete their cyclotron oscillations, the Hall Voltage saturates at a negative value. The striking result at liquid nitrogen Temperature is the reversal of the Hall Voltage which becomes positive (negative Hall Coefficient R_H) at a field of about 12T. Similar behavior was also observed at low fields ($H \leq 0.1T$) by Dillon et al [4]. The low field data were described as mobile minority hole behavior which also depends in part on the quality of the sample [6]. In the high field limit at nitrogen Temperature holes are the dominant contributors to the Hall Voltage. At helium Temperature the Hall Voltage saturates at a very small negative value similar to that at room temperature indicating a dominant electron contribution.

Our data from the Hall effect measurements of stage-2 $FeCl_3$ GIC indicate differences between stage-2 and HOPG summarized as follows:

1-In stage-2 the Hall Voltage is positive at all temperature and field values. Fig (2) shows the Hall resistivity of stage-2 at helium and room temperatures as a function of the applied field. As shown in the figure the Hall signal is smaller at lower temperature indicating a decrease in the scattering rate of the charge carriers.

2- In stage-2 the magnitude of the Hall signal is comparable to that of the magnetoresistance voltage. The Hall data of stage-2, therefore, are more reliable than those of HOPG in which the very small Hall signal is masked by a relatively large magnetoresistance voltage.

3- The Hall Voltage of stage-2 exihibits shubinkov-de Haas (SdH) quantum oscillations at low temperature and high field. In fig (3) the Hall resistivity is shown as a function of the applied field at liquid helium Temperature for both stage-2 and HOPG. As shown in the figure the oscillations occur in stage-2 in a field as low as 8T, whereas HOPG has oscillations of much lower frequencies at lower fields. The existance of the QO at low temperature excludes the interpretation of the data as a one-carrier model and therefore the Hall Coefficient must be given by the equation of the two carrier model,

$$R_H = \frac{1}{ec} \frac{P\mu_p^2 - n\mu_n^2}{(P\mu_p + n\mu_n)^2}$$

where P and n denote the hole and electron carrier densities μ_p and μ_n are the corresponding mobilities. Based on a two-carrier model the determination of the four quantities P, n, μ_p. and μ_n from the GM data is not possible,

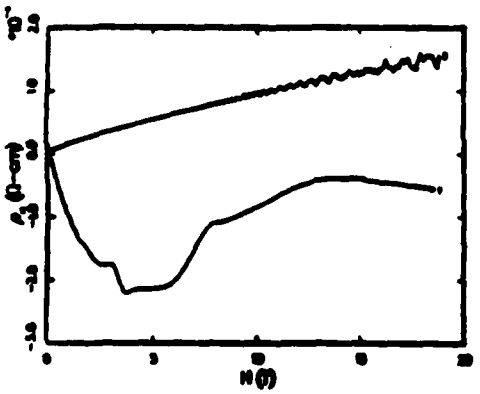

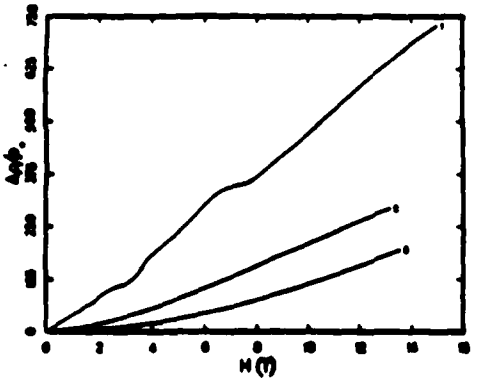

Fig. 3 Hall resistivity vs. field (H) of HOPG (1) and stage-2(2) at He temp.

Fig. 4 Magnetoresistance vs. field (H) of HOPG at He(1), Ni(2) and Rm(3) temp.

however as described above qualitative information about the charge carriers and the carrier density can be deduced.

B-MAGNETORESISTANCE DATA

The transverse magnetoresistance $\Delta\rho/\rho$ as a function of the applied field at room, Ni, and He temperatures for HOPG is presented in Fig (4). Our data qualitatively agree with the high field data of Lowrey and Spain [7] At all temperature values $\Delta\rho$ increases continuously with no sign of saturation up to a field of 20T. The magnetoresistance is large and significantly enhanced at lower temperatures indicating the dominance of impurities and imperfection scattering. The magnetoresistance data of stage-2 is shown in fig (5). In this figure the transverse component $\Delta\rho/\rho$ is plotted versus the applied field at room, Ni, and He temperatures. At room and Ni temperatures $\Delta\rho$ of stage-2 and that of HOPG, have a typical field dependent character. This similarity between the data for HOPG and stage-2 supports the two-dimensional model of the transport mechanism in these intercalated compounds. Therefore, the scattering of the charge carriers is an in-plane mechanism controlled by the graphite lattice and the density of free carriers. The increase of the number of free carriers due to the charge transfer between the graphite and the intercalant is accounted for by the decrease in the magnitude of $\Delta\rho$ of stage-2 relative to that of HOPG. At He temperature QO for stage-2 are readily observed at fields of H>8T. The comparison between the oscillations in fig (5) and those of fig (4) indicate that the SdH frequencies of stage-2 are greater by several orders of magnitudes than those of HOPG. This difference can be interpreted as an increase in the Fermi surface cross-sectional areas as a result of the charge transfer between the graphite and the intercalant. It is interesting to note, shown in fig (6), the damping of the SdH oscillations as the temperature increases. As shown in the figure the oscillations persist at temperatures as high as 33K. The existence of the oscillations at this temperature, a temperature which requires sufficient perfection to satisfy the quantum condition $\omega_c\tau>>1$, indicates that the $FeCl_3$ intercalated compound is an interesting system for further study.

*Supported in part by the Air Force Office of Scientific Research Grant AFOSR 82-0286. +Also with the Francis Bitter National Magnet Laboratory, supported by NFS.

1-I.L. Spain and J.A. Woollam, Solid State Commu. 9, 1581 (1971).
2-I.L. Spain, Chem. and Phys of Carbon 8, 1, (1973).
3-M.S. Dresselhaus, and G. Dresselhaus, Advanced in Phys 30, 139 (1981).
4-R.O. Dillon, I.L. Spain, J.A. Woollam and W.H. Lowrey, J. Phys Chem. solids, 39, 907 (1978). 5-C. Ayache, Physica 99B, 509 (1980).
6-J.D. Cooper, J. Woore, and D.A. Young, Nature 225,721 (1970).
7-W.H. Lowrey, and I.L. Spain, Solid State Commu. 22, 615 (1977).

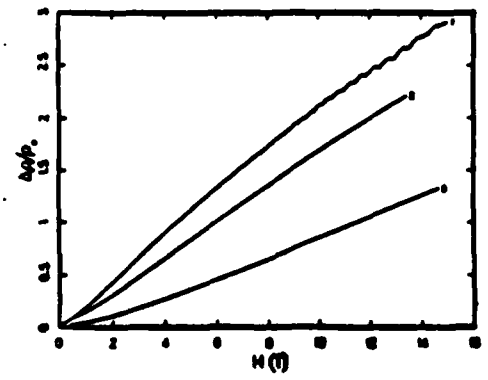

Fig. 5 Magnetores.vs. field (H) of stage-2 at He(1), Ni(2) and Rm(3) temp.

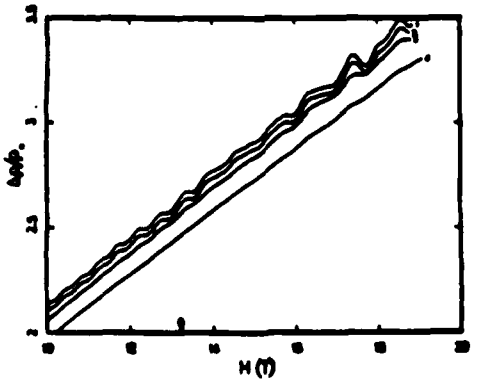

Fig. 6 Magnetores vs. field (H) of stage-2 at: 1-4k 2-6k 3-20k 4-33k

SUBMITTED FOR PUBLICATION IN THE PHYSICAL REVIEW

12/17/86

Planar Classical Dipolar System on a Honeycomb Lattice

George O. Zimmerman*, A.K. Ibrahim*

Physics Department, Boston University

Boston, Massachusetts, 02215

F.Y. Wu**

Physics Department, Northeastern University

Boston, Massachusetts, 02115.

The behavior of a system of dipoles is presented. Here we study a system of dipoles located on a honeycomb lattice under the mean-field approximation. The dipoles are confined to rotate in the plane of the lattice. It is found that in zero external field, the system has a ground state which is continuously degenerate. This degeneracy persists to $T \neq 0$ in zero field. For non-zero planar field pointing in an arbitrary direction in the plane, we compute numerically the magnetization, susceptibility, and the specific heat as functions of both temperature and field. Our results show the occurence of cusps in these quantities, indicating the onset of phase transitions. On the basis of these calculations a phase diagram for the system is then constructed.

I-Introduction

This study is motivated by recent experimental measurements [1] of the thermal and magnetic properties of the $FeCl_3$-graphite intercalated compounds. The intercalate forms monomolecular layers of $FeCl_3$ sandwiched between graphite layers with the Fe^{3+} ions arranged on a honeycomb lattice. The iron ions are in the spin-$\frac{5}{2}$ state with nearest neighbor distance of $3.5A^{\circ}$. There is also evidence that, at low enough temperatures, the Fe^{3+} dipoles are confined to rotate in the intercalate plane. It is thus reasonable to assume that dipolar interactions play a significant role in this substance, with the intercalate described by a system of planar dipoles arranged on the honeycomb lattice. In this paper we carry out the theoretical investigation of the thermal and magnetic properties of such a dipole system under the mean-field approximation. Results of experimental measurements as well as comparison of the theoretical prediction with experiments is given elsewhere [1].

The outline of this paper is as follows: The problem is described, and formulated in section II using the mean-field approximation. The solution of a special case, in which all dipole moments are of equal magnitude and interact with nearest neighbor interactions, is analyzed in section III. The ground-state in zero field is then studied, with interactions extending to all neighbors in part a) of section IV. The most general solution of the mean-field equations, for nearest neighbor interactions, are studied numerically in part b) of section IV, and in section V we discuss the resulting phase diagram.

II- Mean-Field Formulation

Consider a system of N dipoles on a honeycomb lattice in an external magnetic field $\vec{H}$. We assume the dipoles interact by means of the dipolar interaction

$$U_{ij} = J_{ij}[\hat{\mu}_i \cdot \hat{\mu}_j - 3(\hat{\mu}_i \cdot \hat{r}_{ij})(\hat{\mu}_j \cdot \hat{r}_{ij})] \tag{1}$$

with all dipole moments and the applied field $\vec{H}$ confined to the plane of the lattice, and

write the Hamiltonian as

$$\mathcal{H} = \sum_{<i,j>} U_{ij} - \vec{H} \cdot \sum_{i} \vec{\mu}_i. \tag{2}$$

Here the summation $\sum_{<i,j>}$ is taken over all pairings of dipoles, $\vec{\mu}_i$ is a dipole moment of unit magnitude at the i^{th} lattice site, and J_{ij} is the coupling constant between dipoles $\vec{\mu}_i$ and $\vec{\mu}_j$. The experimental situation corresponds to $J_{ij} > 0$.

The free energy $F(\rho)$ of the system is given by the expression

$$\beta F(\rho) = Tr\left[\rho(\beta \sum_{<i,j>} U_{ij} - \vec{h} \cdot \sum_{i} \vec{\mu}_i + ln\rho)\right] \tag{3}$$

where $\beta = 1/k_B T$, $\vec{h} = \beta \vec{H}$ and ρ is the density matrix. In the mean-field analysis we seek to minimize the free energy in the subspace

$$\rho = \prod_{i=1}^{N} \rho_i \tag{4}$$

where ρ_i is the single particle density matrix normalized to

$$Tr\rho_i = 1. \tag{5}$$

Substitution of (4) into (3) and the use of (1) leads to

$$\beta F(\rho) = \sum_{<i,j>} K_{ij}\left[\vec{m}_i \cdot \vec{m}_j - 3(\vec{m}_i \cdot \hat{r}_{ij})(\vec{m}_j \cdot \hat{r}_{ij})\right]$$

$$-\vec{h} \cdot \sum_{i} \vec{m}_i + \sum_{i} Tr(\rho_i ln\rho_i) \tag{6}$$

where $K_{ij} = \beta J_{ij}$, and

$$\vec{m}_i = Tr(\rho_i \vec{\mu}_i), \quad i = 1, 2, 3, ..., N \tag{7}$$

is the magnetization of the dipole $\vec{\mu}_i$.

It is straightforward to carry out the minimization $\partial F/\partial \rho_i = 0$ subject to the contraint (5). This procedure leads to

$$\rho_i = \frac{1}{2\pi I_0(a_i)} e^{\vec{a}_i \cdot \vec{\mu}_i} \tag{8}$$

and, consequently,

$$\vec{m}_i = m(a_i)\hat{a}_i \tag{9}$$

where

$$m(a) = \frac{I_1(a)}{I_0(a)}, \tag{10}$$

and $I_n(a)$ is the modified Bessel function of order n. Here, the vectors $\vec{a}_i$, i=1, 2, ..., N, are determined from the self consistent equations

$$\vec{a}_i = \vec{h} - \sum_j{}' K_{i,j} m(a_j)\left[\hat{a}_j - 3\hat{r}_{i,j}(\hat{a}_j \cdot \hat{r}_{i,j})\right], \tag{11}$$

where the prime over the summation sign denotes the restriction of j≠i. Our goal now is to solve for $\vec{a}_i$ from (11). Then the per-dipole magnetization is given by

$$\vec{M}(T,H) = \frac{1}{N}\sum_{i=1}^{N}\vec{m}_i \tag{12}$$

from which we can directly compute the magnetic susceptibility as

$$\chi = \frac{dM}{dH}. \tag{13}$$

The per-site entropy, given by the last term in (6), can now be obtained by combining (7) and (8) as

$$S = -k_B\sum_{i=1}^{N}\left[a_i m(a_i) - ln(2\pi I_o(a_i))\right] \tag{14}$$

from which we can compute the per-site specific heat:

$$C = T\frac{dS}{dT}. \tag{15}$$

So far we have been careful in the formulation to allow dipolar interactions between *all* pairs. For simplicity we now assume nearest-neighbor interactions. Furthermore, we look for solutions of (11) with periodic ordering. An honeycomb lattice of N sites can be decomposed into N/6 nonintersecting elementary hexagons, each of which containing

6 sites oriented and numbered as shown in Fig.1. A priori. and guided by our numerical solutions, we expect the magnetization of the six sublattices to be different. Allowing this possibility then, for periodic ordering. (11) reduces to six equations as follows:

$$\vec{a}_{\alpha} = \vec{h} - K \sum_{\beta'=1'}^{3'} m(a_{\beta'}) \left[\hat{a}_{\beta'} - 3\hat{r}_{\alpha\beta'}(\hat{a}_{\beta'} \cdot \hat{r}_{\alpha\beta'}) \right], \quad \alpha = 1, 2, 3$$

$$\vec{a}_{\alpha'} = \vec{h} - K \sum_{\beta=1}^{3} m(a_{\beta}) \left[\hat{a}_{\beta} - 3\hat{r}_{\alpha'\beta}(\hat{a}_{\beta} \cdot \hat{r}_{\alpha'\beta}) \right], \quad \alpha' = 1', 2', 3' \tag{16}$$

where $K = \beta J_{nn}$, J_{nn} being the nearest neighbor interaction, and $\hat{r}_{\alpha\beta'}$, is the unit vector pointing from site α to site β'. For fixed T and H we solve (16) for $\vec{a}_{\alpha}$ and $\vec{a}_{\alpha'}$. Then the magnetization is given by (12). In fact, using the identity

$$\sum_{\alpha=1}^{3} \hat{r}_{\alpha\beta'}(\vec{A} \cdot \hat{r}_{\alpha\beta'}) = \frac{3}{2}\vec{A}, \tag{17}$$

which is valid for any vector $\vec{A}$, we find by directly summing over (16),

$$\vec{m}_{1'} + \vec{m}_{2'} + \vec{m}_{3'} = \frac{2}{3K}(\vec{a}_1 + \vec{a}_2 + \vec{a}_3 - 3\vec{h})$$

$$\vec{m}_1 + \vec{m}_2 + \vec{m}_3 = \frac{2}{3K}(\vec{a}_{1'} + \vec{a}_{2'} + \vec{a}_{3'} - 3\vec{h}), \tag{18}$$

and, hence using (12),

$$\vec{M}(T,H) = \frac{2}{3K}\left(\frac{1}{6}\sum_{\alpha=1}^{3} \vec{a}_{\alpha} + \frac{1}{6}\sum_{\alpha'=1'}^{3'} \vec{a}_{\alpha'} - \vec{h}\right). \tag{19}$$

III- Solution of the Special Case of Equal Dipole Moments

In this and subsequent sections, we present results on numerical solutions of (16) and the resulting determination of the magnetization and susceptibility. For the purpose of illustration, however, we analyze in this section the solution of (16) when the magnetizations $\vec{m}_{\alpha}$ and $\vec{m}_{\alpha'}$ have equal magnitude. This is, we assume

$$a_{\alpha} = a_{\alpha'} = a. \tag{20}$$

While the assumption in (20) simplifies the analysis, it must be pointed out that, as will be seen in Sec. IV below, solutions other than (20) do exist and the analysis restricted to (20) is applicable only in a limited region of the phase space, including the case of $\vec{H} = 0$

Consider first the ground state for $\vec{H} = 0$. By symmetry we expect the dipoles to be arranged in a symmetric fashion, namely, the dipoles $\vec{\mu}_1, \vec{\mu}_2, \vec{\mu}_3$, and $\vec{\mu}_{1'}, \vec{\mu}_{2'}, \vec{\mu}_{3'}$, making 120° with respect to each other, although there can be relative rotations. A straightforward calculation shows that the ground state is obtained when

$$\begin{aligned} \theta_3 &= \theta_2 - 120° = \theta_1 - 240° \\ \theta_{3'} &= \theta_{2'} - 120° = \theta_{1'} - 240° \end{aligned} \tag{21}$$

where $\theta_i(\theta_i')$ is the azimuth angle of the dipole at site $i(i')$. [CF. Fig. 1]. Any other relative positioning of the two sets of dipoles yields a higher energy. When (21) is satisfied, we find the per-site energy

$$E = \frac{-9}{4} J_{nn} \cos(\theta_1 + \theta_{1'} + 120°). \tag{22}$$

clearly, the ground state is highly degenerate and is attained by setting

$$\begin{aligned} \theta_1 + \theta_{1'} &= 240°, \quad for\ J_{nn} > 0, \\ \theta_1 + \theta_{1'} &= 60°, \quad for\ J_{nn} < 0 \end{aligned} \tag{23}$$

Indeed, numerical simulations show that the conditions (21) and (23) also lead to the lowest energy when interactions are extend to all neighbors, with each dipole interacting with every other one.

For $T \neq 0$, $\vec{H} \neq 0$, and using (20) and (19), we obtain from (18) the constraint

$$\vec{a}_1 + \vec{a}_2 + \vec{a}_3 = \vec{a}_{1'} + \vec{a}_{2'} + \vec{a}_{3'} = \frac{3\vec{h}}{1 - \frac{3}{2}C(a)} \tag{24}$$

where

$$C(a) = Km(a)/a. \tag{25}$$

Note that (24) implies $\vec{a}_1 + \vec{a}_2 + \vec{a}_3 = \vec{a}_{1'} + \vec{a}_{2'} + \vec{a}_{3'} = 0$ in zero field.

We can further iterate (16) to obtain equations for $\vec{a}_\alpha$ and $\vec{a}_{\alpha'}$ individually. After some algebra and the use of identities (17) and

$$\hat{r}_{\alpha\beta'} \cdot \hat{r}_{\beta'\gamma} = \frac{1}{2}(1 - 3\delta_{\alpha\gamma}), \tag{26}$$

we arrive at the result, assuming the constraint (20),

$$A(a)\vec{a}_\alpha = B(a)\vec{h} + D(a) \sum_{\beta=1}^{3} \sum_{\beta'=1'}^{3'} \hat{r}_{\alpha\beta'}(\vec{a}_\beta \cdot \hat{r}_{\beta\beta'}) \tag{27}$$

where

$$A(a) = 1 - \left[\frac{9}{2}C(a)\right]^2$$

$$B(a) = \frac{A(a)}{1 - \frac{3}{2}C(a)}$$

$$D(a) = \frac{27}{4}[C(a)]^2, \tag{28}$$

and an equation similar to (27) for $\vec{a}_{\alpha'}$ with the primed and unprimed subscripts interchanged.

Each of these two equations represents a set of six equations containing four unknowns, e.g., the parameter a and the three directional angles of $\vec{a}_\alpha$ and, therefore, is generally a set of over-determined equations which does not possess a solution. However, when $A(a) = 0$ or, equivalently,

$$| \frac{9}{2}C(a) | = 1, \tag{29}$$

which also happens to be the characteristic equation of (27). It can be shown that (27) reduces to a set of two independent equations. While in this case (29) and (27) are insufficient to determine $\vec{a}_\alpha$ uinquely, the overall constraint (24) still holds. Thus from (29) and (24) we find

$$\begin{aligned} \vec{a}_1 + \vec{a}_2 + \vec{a}_3 = \vec{a}_{1'} + \vec{a}_{2'} + \vec{a}_{3'} &= \frac{9}{2}\vec{h}, \quad J_{nn} > 0 \\ &= \frac{9}{4}\vec{h}, \quad J_{nn} < 0. \end{aligned} \tag{30}$$

Equation (30) for either $J_{nn} > 0$ or $J_{nn} < 0$ is a set of two independent equations and is equivalent to (20). Thus, for fixed T and H, we use (29) to compute

$$a = a_0(T). \tag{31}$$

Then any set of $\vec{a}_1$ and $\vec{a}_{1'}$ whose magnitudes are $a_0(T)$ and satisfying (30) is a solution. The constraint (30) now leads to the existence of helical and nonhelical phases similar to those discussed in Ref.[3]. The critical temperature T_C is given by $a_0(T_C) = 0$ or, using (29) and (25),

$$T_C = \frac{9|J_{nn}|}{4k}. \tag{32}$$

The phase boundary between the helical and nonhelical phases is $\vec{a}_1 + \vec{a}_2 + \vec{a}_3 = \vec{a}$, or, using (30) and (31),

$$a_0(T) = \frac{9H}{2kT}, \quad J_{nn} > 0$$

$$a_0(T) = \frac{9H}{4kT}, \quad J_{nn} < 0. \tag{33}$$

The border between the paramagnetic and nonhelical phases is $\vec{a}_1 + \vec{a}_2 + \vec{a}_3 = 3\vec{a}$, or,

$$a_0(T) = \frac{3H}{2kT}, \quad J_{nn} > 0$$

$$a_0(T) = \frac{3H}{4kT}, \quad J_{nn} < 0. \tag{34}$$

Plot of the phase diagram is similar to that of Fig.2 of Ref.[2] and will not be repeated here.

IV- Results of the Numerical Solution

In this section we present results of numerical solutions of (16) without the restriction (20) of equal dipole magnitude.

a) Ground State Energy in Zero Magnetic Field

The ground state calculation for zero magnetic field was performed on a set of 72 dipoles. The dipoles were located on a rectangle which measures $9 \times 6\sqrt{3}$ where the nearest neighbor distance is taken as one. In order to eliminate effects of the boundary, this set was surrounded by 48 similar dipole arrays. The field of all the $48 \times 72 = 3456$ dipoles as well as the other 71 dipoles within the original rectangle was computed at the site of each of the 72 dipoles in the centeral rectangle.

For nearest neighbor interactions we verified that, the ground state energy is given by (22), i.e. the assumption (20) of equal magnetization magnitudes was correct. We have further computed the zero-field ground state energy for interactions extending to all neighbors. This lead to the same ground state configurations given by (21) and (23), but with a per-dipole energy -2.2269 J_{nn}, which was about 1% higher than the value of -2.25 J_{nn} implied by (22) for nearest neighbor interactions. Furthermore, our numerical results indicated that the ground state with extended-neighbor interactions was again degenerate with respect to relative rotations of the two sets of dipoles $\vec{\mu}_i$ and $\vec{\mu}_{i'}$ as long as both (21) and (23) were obeyed.

b) Mean-Field Calculation

For general $\vec{H}$ and $T \neq 0$ (16) was solved by means of a numerical iterative method starting from states specified by (21) and (23), with some chosen initial values of a_α. Random initial orientations were also tried but they did not lead to new solutions. It turns out that there exist solutions to (16) with different final dipole configurations and slightly

different free energies, typically one tenth of $k_B T$. We identify the one associated with the lowest free energy as the true dipole configuration. The condition for self-consistency was that successive values of $\vec{a}_\alpha$ be within 0.1% of each other. An accuracy of 0.01% was also tried with no significant change in the values except for a longer computational time. For low temperature and low field, convergence was achieved after as few as 5 iterations, while near the phase boundaries, (see later discussion) it took up to 900 iterations to converge.

For H=0, our numerical solution again verified that assumption (20) of equal magnetization magnitude is correct for $T \neq 0$ and reproduced the solution given in section III. Particularly we verified that $a_\alpha(T) = 0$ and $a_{\alpha'}(T) = 0$ for $T \geq T_c$. However, for $\vec{H} \neq 0$, the numerical solutions yielded unequal magnetizations a_α and $a_{\alpha'}$. In general, magnetic fields applied along an axis of symmetry tended to pair up the dipole magnetization values. This pairing is shown in Table I. By symmetry, the behavior is identical modulo 60°, although the pairing will vary. We thus show only the pairing at 0° and 90°. The pair of dipoles with equal magnitude orient themselves with positive and negative angles with respect to the field. This pairing was broken if $\vec{H}$ was not along a direction of symmetry.

The dipole configurations corresponding to the lowest free energy are shown in figures 2 and 3 for various temperatures, and fields along the horizontal and vertical directions, respectively. In these and subsequent figures, T* is the temperature given in units of $k_B T/J_{nn}$ and h* is the field in units of H/J_{nn}. One observes that at low temperature, i.e. frame "a" of each figure, the dipole pattern resembles one of the zero field ground-state patterns specified by (21) and (23). Thus the application of the magnetic field lifts the degeneracy. Moreover, the configuration with the lowest free energy depends on the direction of the magnetic field. Although the difference in the temperature between the last two frames in Figs.2 and 3 is small, the patterns change drastically. This change is due to the 180° rotation of dipoles which previously were antiparallel to the field and signifies the occurance of a new phase.

Once a self-consistent solution for (16) was obtained, the magnetization was calculated by means of (12). This magnetization is shown, normalized to M_s, the saturation magnetization, in Fig.4 as a function of the magnetic field at fixed temperature, and in Fig.5 as a function of temperature at fixed magnetic field. The values plotted are those for the field in the horizontal direction. Magnetization values with fields applied in other directions were also calculated. The values thus obtained differed from each other by only 4%. As seen in Fig.5, the magnetization possesses a distinct cusps at low field. At higher field the cusp is replaced by an inflection point.

The susceptibility computed from the magnetization by using (13) as a function of the applied magnetic field at fixed temperatures is shown in Fig. 6, and as a function of the temperature at fixed field in Fig.7. One again observes in Fig.7 the occurrence of a distinct cusp for low field, while at higher field the cusp becomes a gradual maximum.

The entropy computed by means of (14) is shown as a function of temperature at fixed field in Fig.8, while the specific heat computed from the entropy by use of (15) is shown in Fig.9. Figure 9 again exhibits sharp cusps in the specific heat at the same temperatures as the cusps in the magnetization and magnetic susceptibility. There are no distinct features in the specific heat which can be associated with the inflection points in the magnetization shown in Fig.5 or the gradual maxima in the susceptibility shown in Fig.7.

V-The Phase Diagram

On the basis of the above results, one can now construct a phase diagram in the $T^* - h^*$ plane by plotting the locus of the susceptibility maxima. This is shown in Fig.10 for the field applied along the horizontal direction. This diagram is also valid to within 4% in h^* for fields applied in other directions in the plane.

The diagram shows three distinct phases. Phase I is the ordered phase where in-

teractions between the dipoles dominate. Phase II is a paramagnetic phase where the susceptibility obeys Curie's law. The transition between phase I and phase II is marked by the occurrence of distinct cusps in the magnetization, magnetic susceptibility and the specific heat. In a field applied along an axis of symmetry, that transition is also marked by an flipping of dipoles which are at an angle of 180° with the field in phase I, to a parallel orientation with the field in phase II. This is seen in the change in configuration between frames b and c in figures 2 and 3. In these figures frame b is in the ordered phase, while frame c is in the paramagnetic phase. Phase III represents a magnetic field induced ferromagnetic phase. In this phase the dipoles are completely lined up with the field. Starting in phase III, as one increases the temperature at a fixed field, there is an abrupt change in the alignment of the dipoles with the field. This change is at the transition to phase II. In phase II the average angle a dipole makes with the applied field is greater than 1° near the transition. The transition between phase III and phase II is marked by the inflection points in the magnetization of Fig.5 and the maxima in the susceptibility of Fig.7.

VI-Summary

A system of dipoles which are confined to a plane exhibits many properties of a physical system with long range interactions and an intrinsic anisotropy. For any particular configuration at zero field and temperature, the energy of the system can be computed exactly for extended neighbor interactions. Here we have computed the ground-state energy of such an extended system on a honeycomb lattice and found its value to be within 1% of that determined for nearest neighbor interactions only. Moreover, we found that the ground-state degeneracy specified by (21) and (23), which was derived for only nearest neighbor interactions, also holds for extended neighbor interactions.

We have also studied the behavior of the system at finite temperature and non-zero field applied in an arbitrary direction in the plane, under the mean-field approximation. In

this approximation only nearest neighbor interactions were taken into account. We found that in zero field the degeneracy persists. In non-zero field, the magnetic field selects a particular dipole configuration which in low fields resembles one of the patterns described by (21) and (23). Two such configurations, for fields along the horizontal and vertical directions, are shown in figures 2 and 3. A set of states of minimum free-energy was then selected from which measurable quantities, such as the magnetization, susceptibility and the specific heat were computed. These quantities show distinct maxima which denote phase transitions.

The phase diagram is shown in Fig.10. The nature of the phases was established by the examination of the dipole configuration in each phase, the values of the mean field parameters, and the values of the free energy and the measurable quantities mentioned above. The phases are shown in Fig.10. Phase I is the low temperature low field phase where the dipole pattern resembles one of the ground states. In this phase the interaction between the dipoles predominates. If the field is applied along an axis of symmetry, one set of dipoles will line up at 180° to the field. The transition from phase I to phase II is marked by the flipping of the antialigned dipoles by 180° so that they are now parallel to the field. Phase II is the high temperature phase and is identified as the paramagnetic phase. Phase III, the high field phase, is the field induced ferromagnetic phase. In this phase the dipoles are completely lined up with the field, the dipole-magnetic field interaction dominates, and the mean field adds to the magnetization of the system.

Acknowledgements

We would like to thank Dr. F.Leyvraz, Dr. M.S.Dresselhaus, Dr. G.Dresselhaus and Dr. C.Henley for extremely useful discussions.

*Supported by the Air Force Office of Scientific Research Grant AFOSR 82-0286

**Supported by the National Science Foundation Grant DMR 8219254

References

1 - A.K. Ibrahim and G.O. Zimmerman, To be published in The Phys. Rev. B35, (1987)

2 - D.H. Lee, R.G. Caflisch, J.D. Joannopoulos and F.Y. Wu, Phys. Rev. B29, 2680, (1984)

Table I

Pairing of Dipoles as a Function of the

Direction of Field.

Field direction	0°	90°
Pairing	1-3'	1-3
	2-3	1'-3'
	1'-2'	2-2'

Field direction refers to the angle the field makes with the horizontal as referred to Fig.1

Figure Captions

Figure 1. The honeycomb lattice with the sublattice points numbered on one of the elementary hexagons.

Figure 2. Dipolar configuration for a field $h^* = 0.84$ applied in the horizontal direction with a- $T^* = 0.68$, b- $T^* = 1.82$ and c- $T^* = 2.00$. a- and b- are in the ordered phase, phase I. c- is in the paramagnetic phase, phase II, discussed in the text.

Figure 3. Dipolar configuration for a field $h^* = 0.84$ applied in the vertical direction with a- $T^* = 0.68$, b- $T^* = 1.82$ and c- $T^* = 2.00$. a- and b- are in the ordered phase, phase I. c- is in the paramagnetic phase, phase II, discussed in the text.

Figure 4. Magnetization as a function of the applied external magnetic field, h* at fixed temperature. The magnetization is normalized to M_s, the saturation magnetization.The magnetization curves in increasing order of magnetization referred to the right hand side of the graph are at T^*=3.41, 2.05, 1.59, and 0.68 respectively.

Figure 5. Magnetization as a function of temperature at fixed magnetic fields. The magnetization is given in units of M_s, the saturation magnetization. The magnetization curves in increasing order of magnetization referred to the right hand side of the graph are at h^*=0.084, 0.840, 1.680, 1.932, 2.352, and 2.520 respectively.

Figure 6. The magnetic susceptibility for the temperatures of Fig.4 as a function of an externally applied magnetic field. The three cusps which occur at increasing field are at T*=2.05, 1.59 and 0.68. The line is at T*=3.41.

Figure 7. The magnetic susceptibility as a function of temperature at fixed magnetic field. In order of increasing susceptibility as referred to the right hand side of the figure the curves are at h*=2.520, 2.352, 1.932, 1.680, 0.840 and 0.084.

Figure 8. The entropy at constant applied magnetic field as a function of temperature. In order of decreasing entropy as referred to the right hand side of the graph the values are at $h^*=8.41\times10^{-5}$, 0.841, and 1.68, respectively.

Figure 9. The specific heat as a function of temperature at constant applied magnetic field. The fields are those of Fig.8 with the addition of $h^*=1.26$. Above $T^*=3$ the specific heat is a monotonically increasing function of the field.

Figure 10. The phase diagram of the system in the T^*-h^* plane. Phase I is the ordered phase, phase II is the paramagnetic phase, and phase III is a field induced ferromagnetic phase.

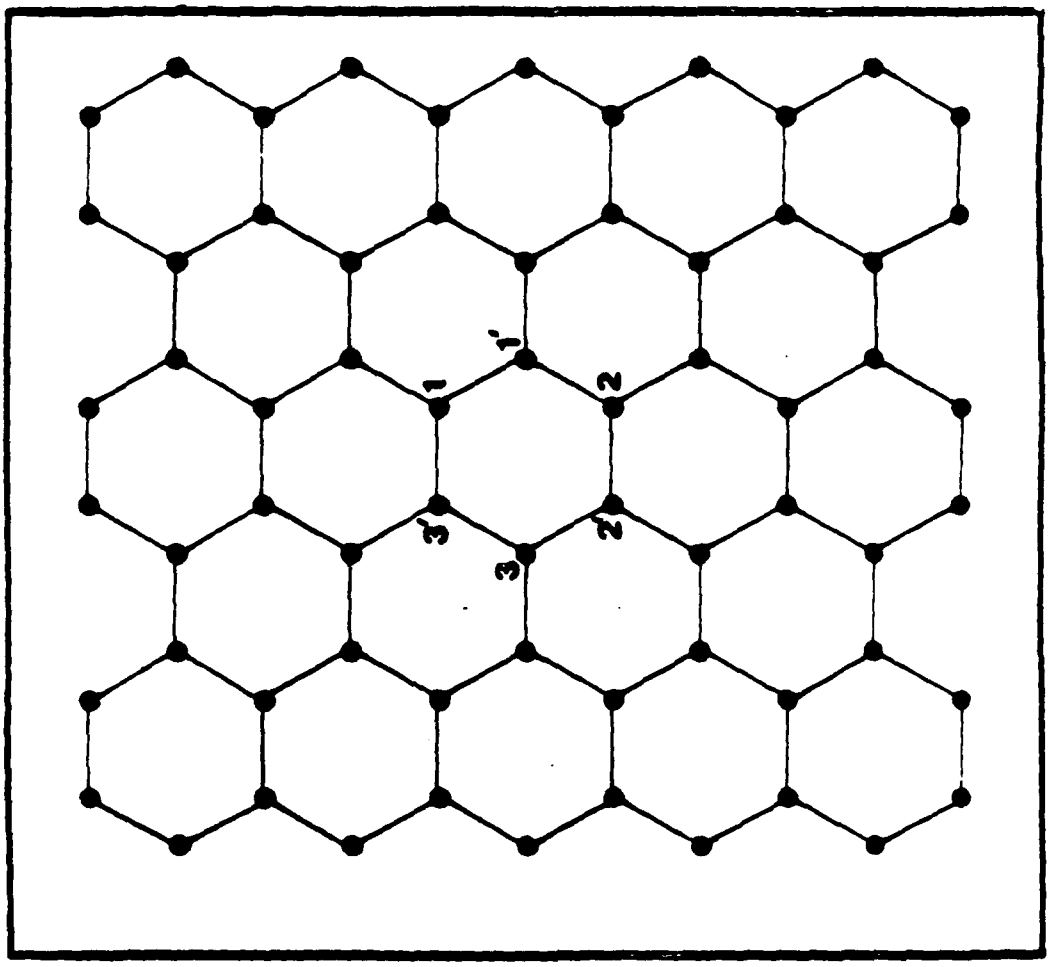

FIG 1

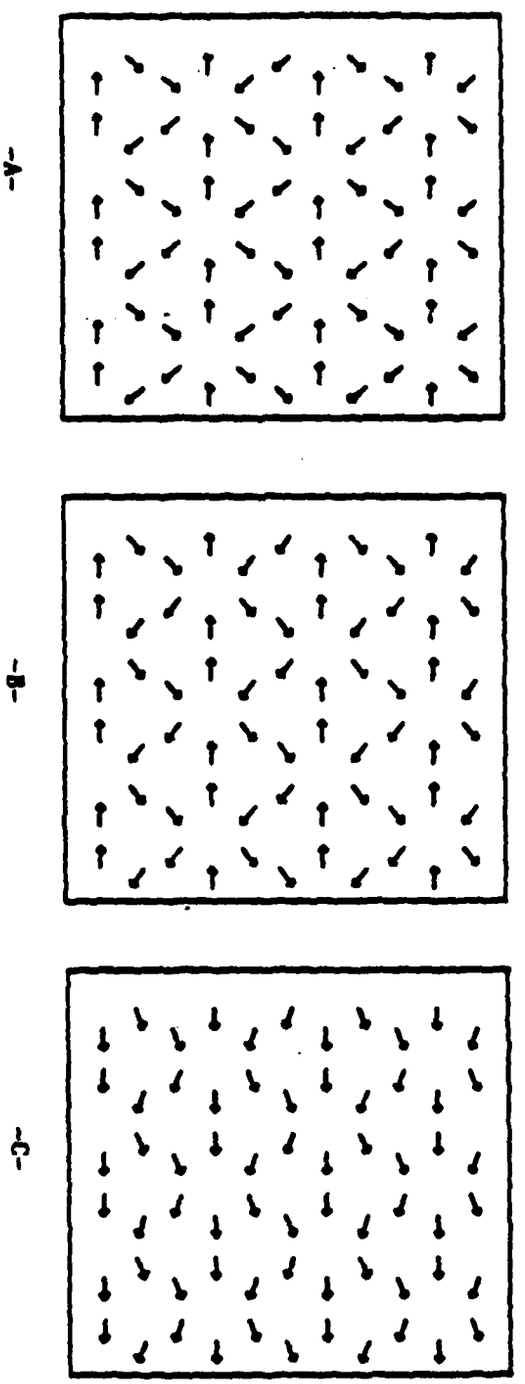

FIG 2

FIG. 3

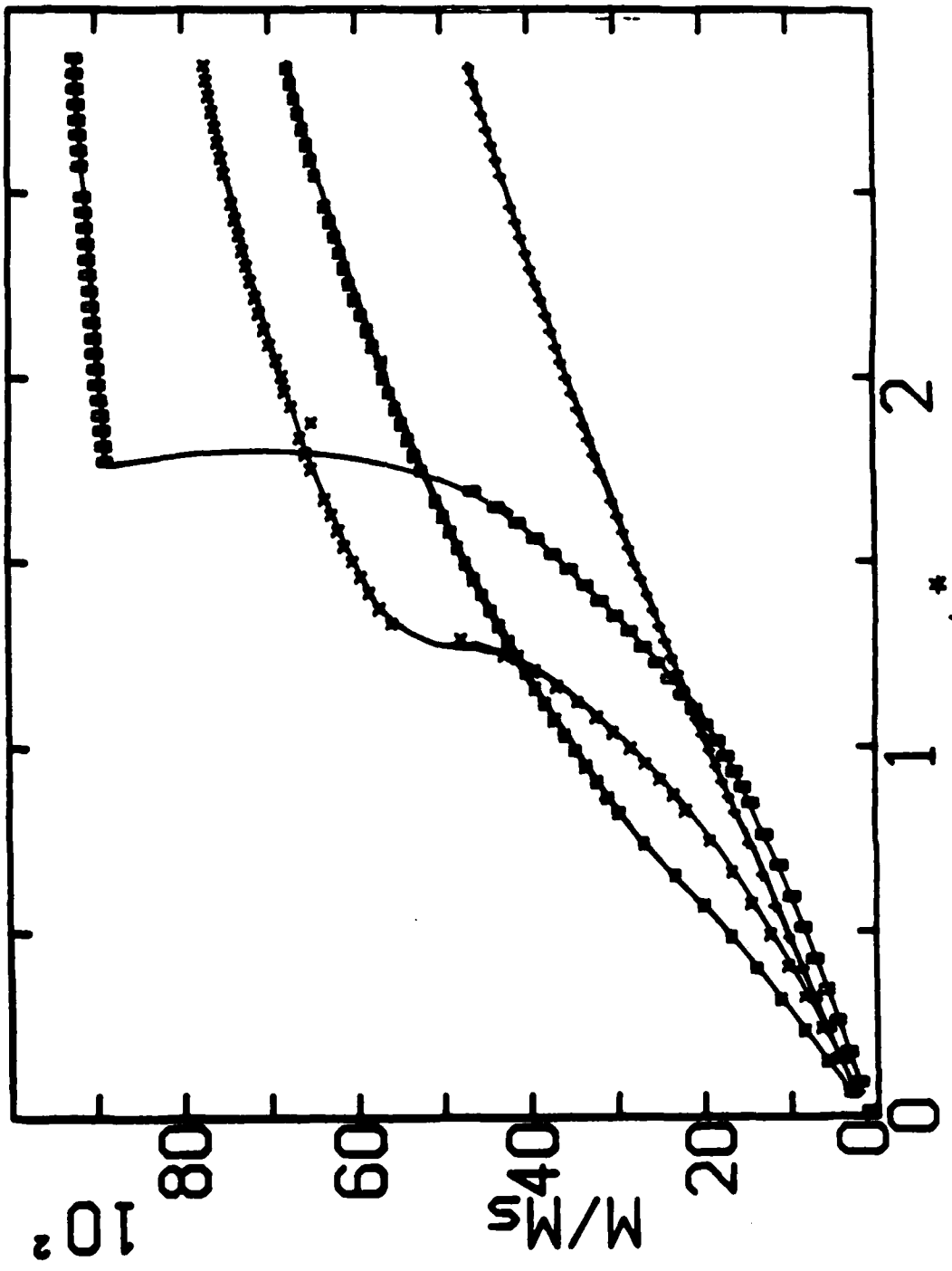

Fig 4

Fig. 5

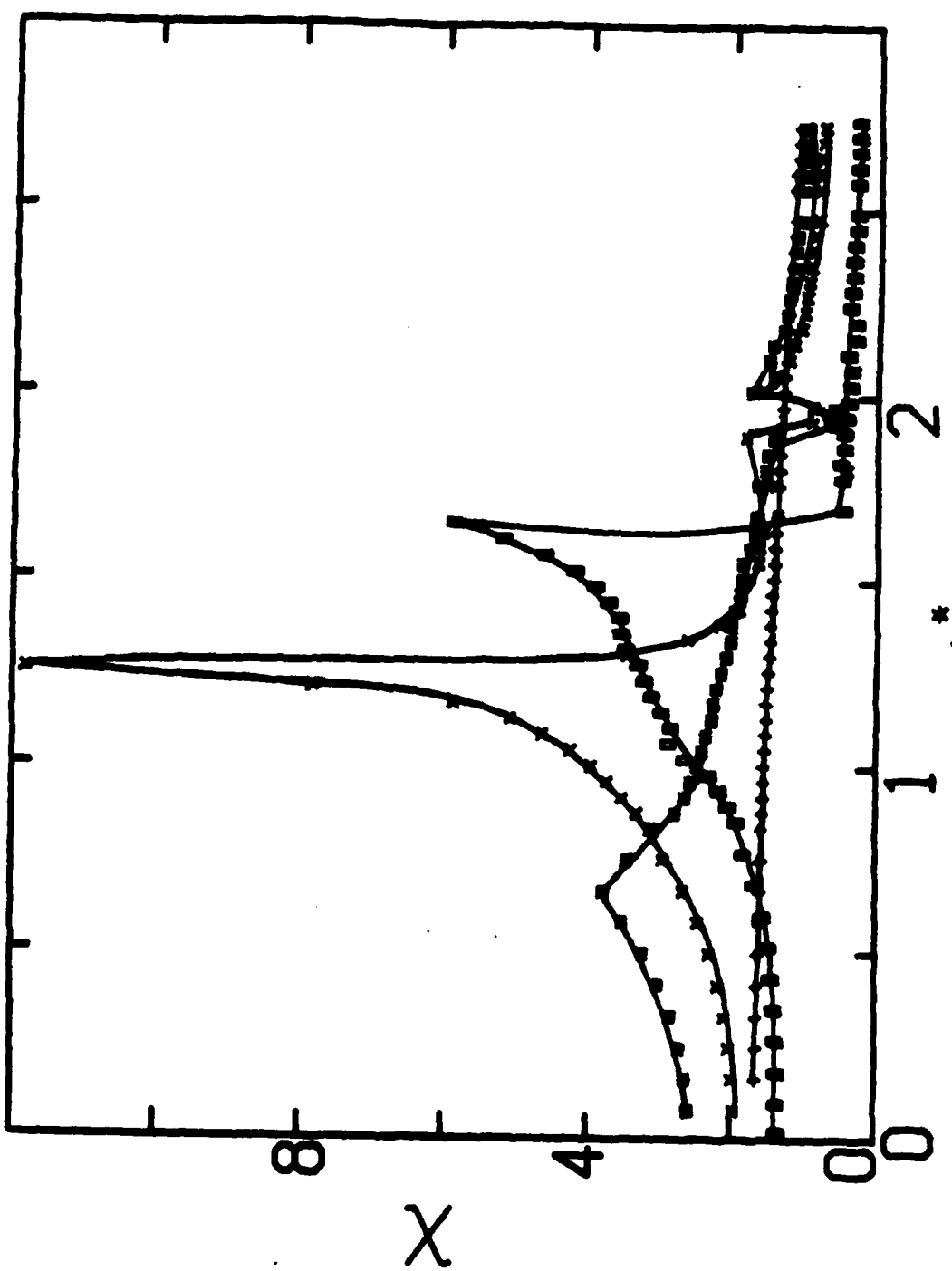

FIG 6

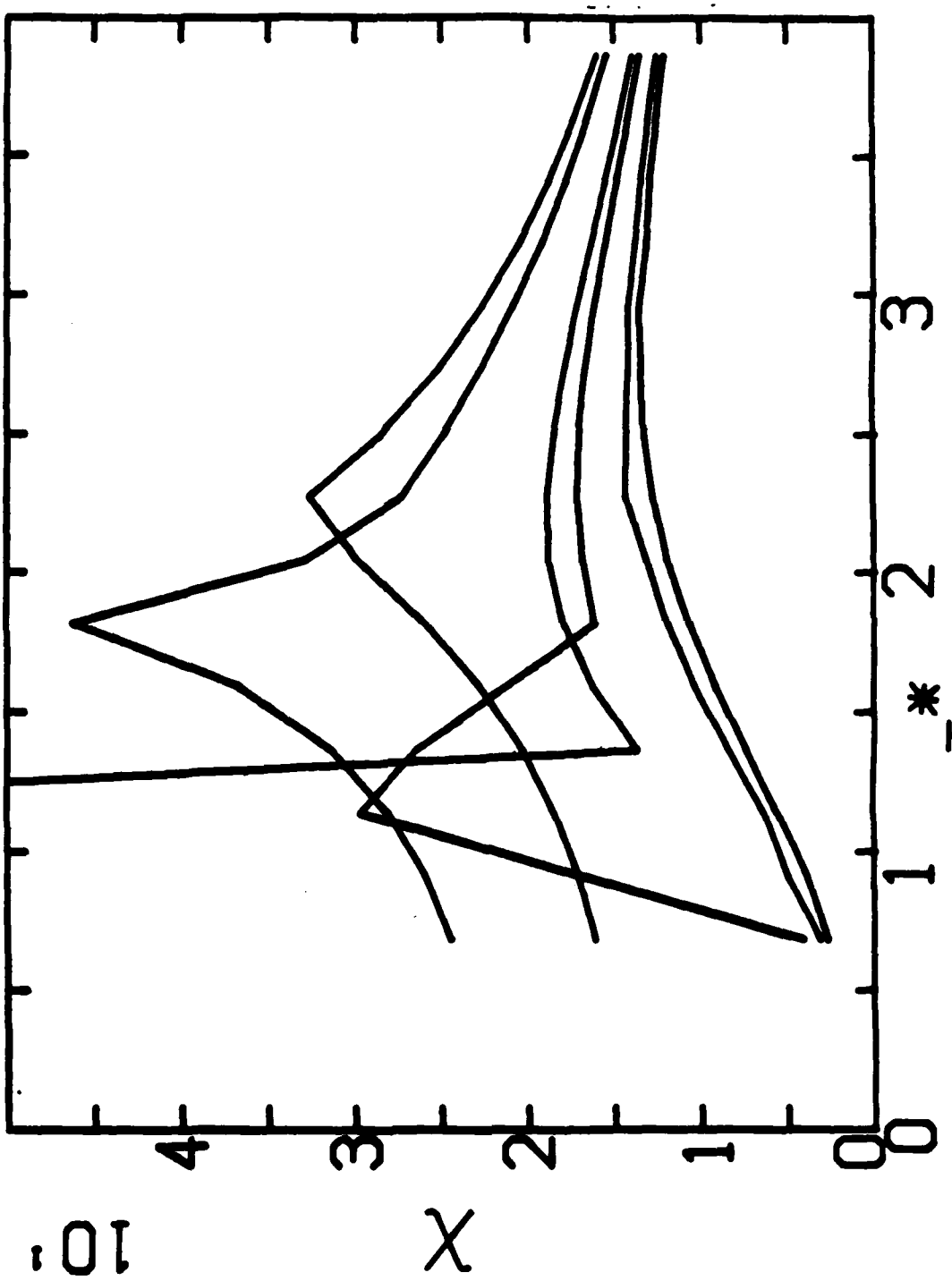

FIG. 7

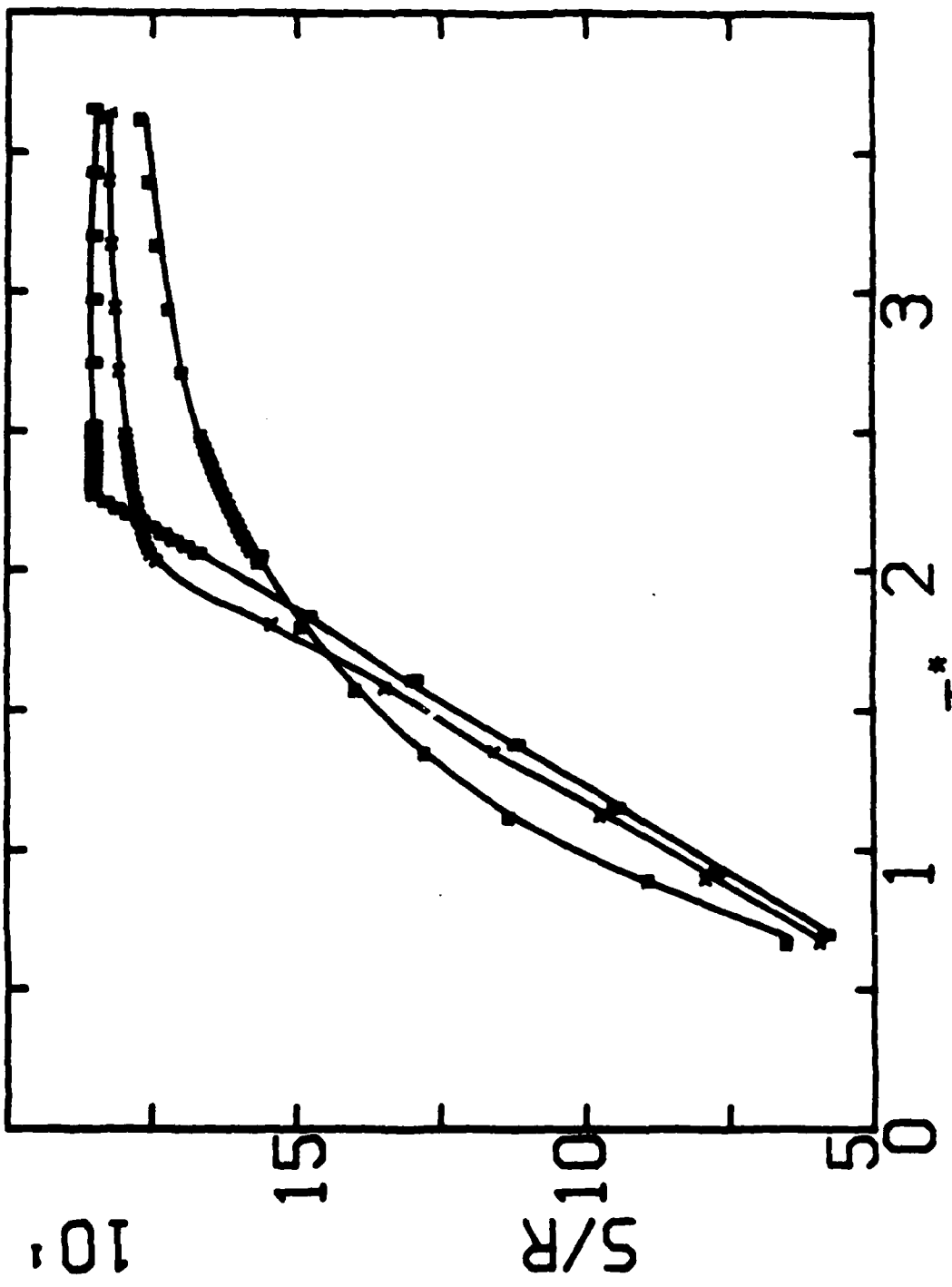

FIG 8

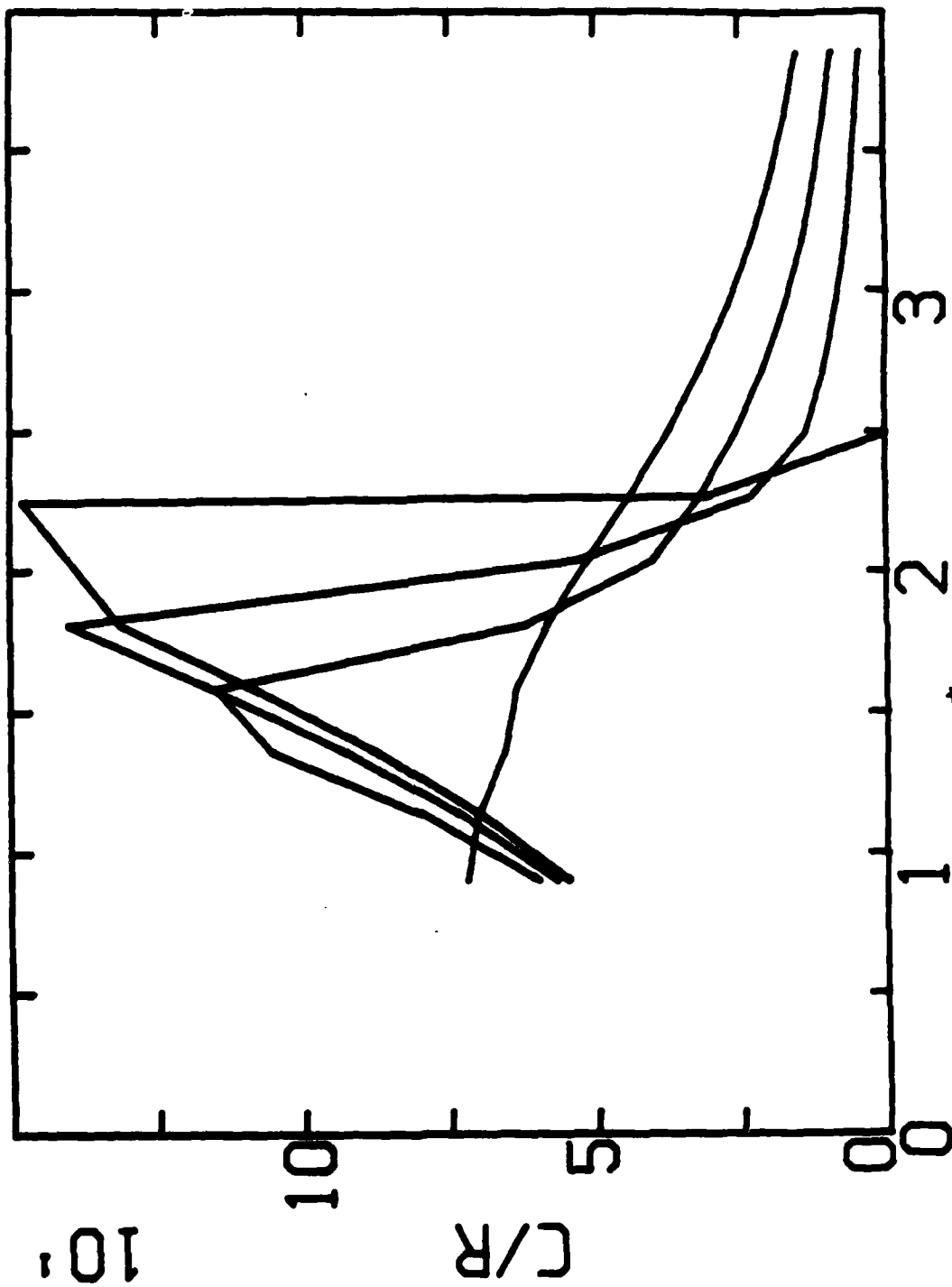

FIG. 9

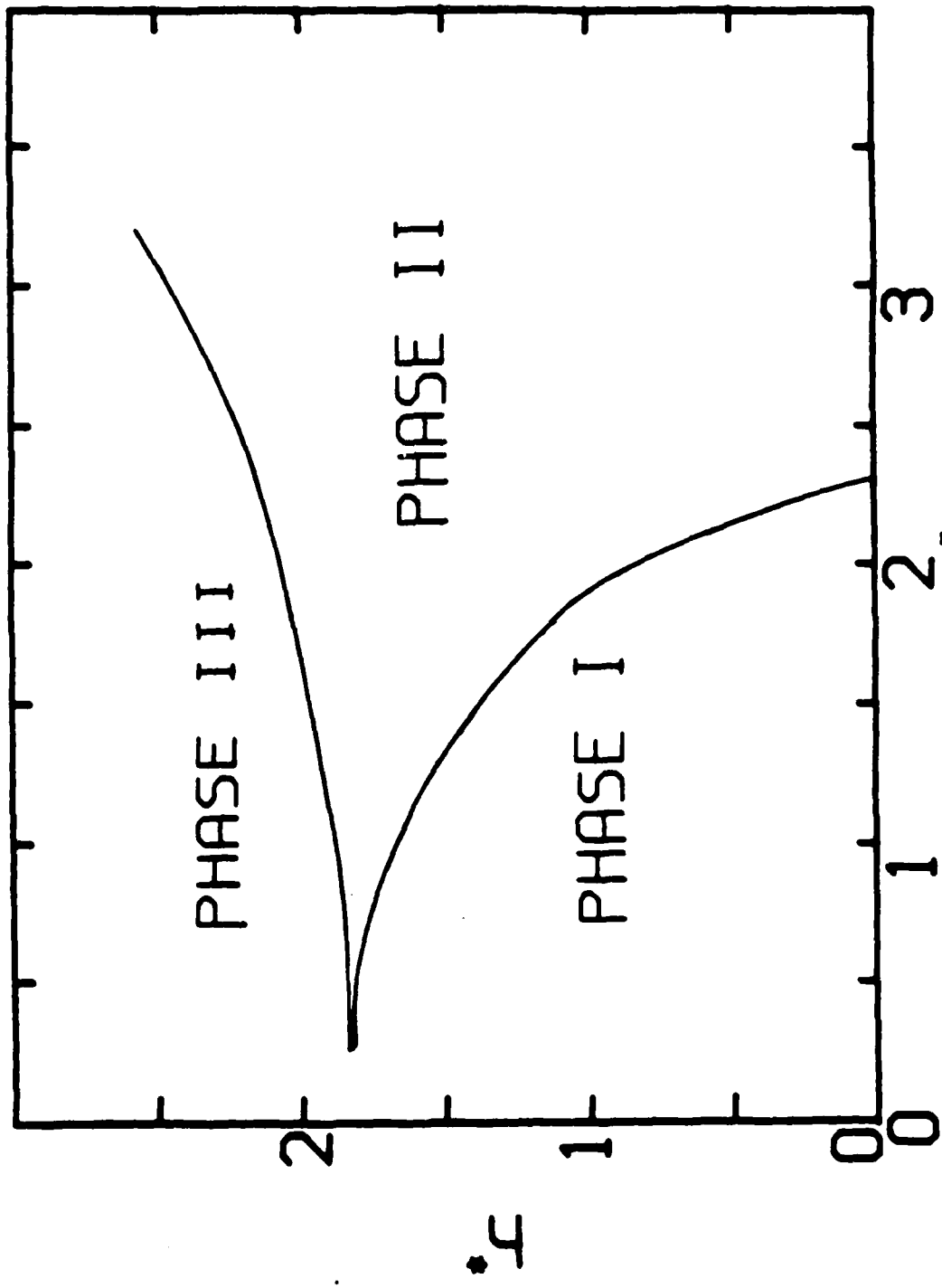

Fig 10

APPENDIX IX

To be published in Journal of Applied Physics, April 1987

The Effect of Defects on a Two Dimensional Dipolar System on a Honeycomb Lattice

George O. Zimmerman* and A.K. Ibrahim*
Physics Department, Boston University, Boston MA. 02215
F.Y. Wu**
Physics Dapartment, Northeastern University, Boston MA. 02115

Abstract

A theoretical investigation of a planar dipolar system on a honeycomb lattice reveals that the ground state energy is increased for finite systems over that of an infinite system. The infinite system has a ground state degeneracy with respect to dipole orientations. This degeneracy is lifted for finite systems. A mean field calculation including nearest, second and third neighbors shows that there are three phases, an ordered phase, a quasiparamagnetic one which goes over to a paramagnetic one at high temperature and a magnetic field induced ferromagnetic phase. A defect in the second nearest neighbor has the effect of introducing a finite magnetization at zero field at low temperatures.

Introduction

The attraction of a dipolar system lies in the fact that the interaction between any two dipoles can be easily and exactly calculated. Dipolar forces are long range, and there is an inherent anisotropy built into the interaction because it depends not only on the relative orientation of the dipoles but also on their location. Much work was done in the 1930's on the mathematics of three dimensional dipole lattices [1] and later dipolar interactions were used to explain the magnetic transition of Cerium Magnesium nitrate, a paramagnetic salt which undergoes an antiferromagnetic transition in the millidegree range [2,3]. The shape correction due to dipolar interactions was also explored [4-6]. In this paper we will confine ourselves to the two dimensional system of dipoles. By that we mean that the dipoles are located in a plane and their rotation is such that they always point parallel to the plane and rotate about an axis normal to it. The magnetic field, however, is three dimensional.

One can show that in a perfect dipolar honeycomb lattice, of infinite extent and at zero temperature, the ground state is infinitely degenerate [7]. Fig. 1 shows one of a degenerate configurations from which all the others can be derived. One can decompose the lattice into elementary hexagons, with the six dipoles numbered 1 ,1',2 ,2',3 and 3'

constituting one of those. Those with "N" denote the next, second and third nearest neighbor to the initial hexagon. Dipoles with the same number have the same orientation. From this configuration one obtains all the other states with identical energies by rotating the unprimed dipoles by the same arbitrary angle clockwise while the primed dipoles are rotated by the same angle in the counterclockwise direction, or vice versa. It is thus of interest to explore if defects or boundaries favor one of the ground states over another [8]. In the same paper [8], a mean field calculation was performed which extended the behavior of the system to finite temperatures and finite magnetic fields. That calculation, which was confined to the first nearest neighbors only, showed that the system has a critical point at zero field where it undergoes a transition from an ordered to a disordered state, and that transition can be traced as a function of an applied magnetic field. The change of phase is marked by susceptibility and specific heat maxima.

Section 2 of this paper describes briefly the calculation method. In section 3 we extend our calculations of the ground state to finite lattices of two shapes and examine the total energy as a function of dipole orientation. In section 4 the mean field calculation is extended to the second and third nearest neighbors. This calculation is also performed for the lattice having a vacancy in a second or third neighbor. Section 5 presents a discussion of the results.

Method of Calculation

The ground state energy calculations of an infinite and the finite systems was performed by summing the interactions of each dipole with all the others in the lattice. in these calculations we used the usual expression for the dipolar energy which is given in Eq.(1)

$$U_{ij} = \frac{\vec{\mu}_i \cdot \vec{\mu}_j}{r_{ij}^3} - \frac{3(\vec{\mu}_i \cdot \vec{r}_{ij})(\vec{\mu}_j \cdot \vec{r}_{ij})}{r_{ij}^5} \qquad (1)$$

In this expression i and j denote the two interacting dipoles, μ is the magnetic moment and r is the distance between the two dipoles. If the dipoles are identical, one can rewrite (1) in terms of unit vectors as shown in Eq.(2).

$$U_{ij} = J[\hat{\mu}_i \cdot \hat{\mu}_j - 3(\hat{\mu}_i \cdot \hat{r}_{ij})(\hat{\mu}_j \cdot \hat{r}_{ij})] \qquad (2)$$

From now on we use dimensionless units where J=1, the temperature is given in units of J, the distance between two nearest neighbors, (ND), will be taken as one and the magnetic field will be in units of $(\mu H/J)$.

An infinite lattice was simulated by taking into account the interaction of 3528 dipoles on a rectangle of 72.8 ND by 62.8 ND and taking the energy of only the central 72 dipoles. Extending the boundary further had no effect on the central dipoles thus providing a natural cutoff. The ground state energy per dipole was thus computed as E=-4.450 .

The mean field calculation was performed by selfconsistently solving the equations of Lee et al [9] modified for dipolar interactions. In that method, the free energy, given in Eq.3 is minimized.

$$F(\rho) = k_B T Tr\left[\rho(K\sum_{i,j} U_{i,j} - \vec{h}^* \cdot \sum_i \vec{\mu}_i + ln\rho)\right] \tag{3}$$

In this equation F denotes the free energy, ρ is the density matrix, $K=J/k_BT$ and $h^*=H\mu/k_BT$. This minimization gives an expression for the magnetization of a dipole given by Eq.(4).

$$\vec{m}_i = m(a_i)\hat{a}_i \tag{4}$$

where

$$m(a) = \frac{I_1(a)}{I_0(a)}, \tag{5}$$

and $I_n(a)$ is the modified Bessel function of order n. The vectors $\vec{a}_i$ are mean field parameters which are determined from the self consistent equations

$$\vec{a}_i = \vec{h} - K\sum_j{}' m(a_j)\left[\hat{a}_j - 3\hat{r}_{i,j}(\hat{a}_j \cdot \hat{r}_{i,j})\right], \tag{6}$$

where the prime over the summation sign denotes the restriction that $i \neq j$. An iterative solution of Eq.(6) provides self consistent values of a_i from which F, the free energy, M, the magnetization and S, the entropy, can be obtained for any temperature and applied magnetic field. The magnetic susceptibility and the specific heat can then be obtained by simple differentiation.

The Ground State

The calculation of the energy per dipole was carried out as described in the previous section. For an infinite lattice, the energy per dipole is E=-4.450. As pointed out in the introduction, that value is invariant under the rotation of the unprimed dipoles by an

arbitrary angle in the counterclockwise direction with a corresponding rotation of the primed dipoles in the clockwise direction or vice versa.

A finite array raises the energy of the system. Moreover, that energy is, to a small degree, dependent on the orientation of the dipoles. As an example we calculated the energies of two such arrays. The first was 170 dipoles arranged on a square with a side length of 15.5 ND, the other was an array of 180 dipoles contained within a circle of 17 ND. In both of these arrays 20% of the dipoles were on the boundary, where the boundary dipoles were defined as those which were missing at least one nearest neighbor. The average energy per dipole, E, is shown in Fig.2 for both arrays as a function of spin orientation. In this simulation the ground state was preserved by rotating the dipoles as previously described, such rotation also applied to the dipoles on the boundary. Since the dipoles numbered "2" in Fig.1 start with a zero angle with respect to the horizontal axis, we took that dipole as an indicator, and thus the angle, in degrees, denotes the "2" dipole orientation.

For the square the average minimum energy per dipole was -4.169 while the maximum was -4.072, for the circle the values were -4.151 and -3.978 respectively. The overall change in energy due to orientation is about 2.5% for the square and 4.3% for the circle. Both have the expected 180° symmetry. For the finite size of the array the average energy was raised from an average of -4.450 to -4.120 for the square and -4.064 for the circle. Although there is an overlap in the energies as shown in Fig.2 it is somewhat surprising that the square has a lower energy than the circle.

Mean Field Calculation

In reference 7 we calculated the behavior of the system taking into account only the nearest neighbor interactions. Thus the interactions of the central hexagon containing the dipoles numbered 1, 1', 2, 2', 3 and 3' and the nearest neighbors of each of them were taken into account. In this approximation, a primed dipole, as shown in Fig.1, interacted only with an unprimed one, and vice versa. Since in a honeycomb lattice, with nearest neighbor distance 1 ND the second nearest neighbors are $\sqrt{3}$ ND away while the third neighbors are 2 ND away, they contribute significantly to the interaction. The calculation was thus extended to also include second and third nearest neighbors. The magnetization calculated in this manner is shown in Fig.3 for a temperature of 2 and as a function of the applied magnetic field. This figure shows our present calculation,

squares, as well as our previous results which contained only the nearest neighbors, "+", for comparison.

One notes that the nearest neighbor calculations (nn) give a lower magnetization than those including second and third nearest ones (nnn). Fig.4 shows the magnetic susceptibility as a functon of the applied field which was obtained by differentiation of the data shown in the previous figure. As the field increases, one sees a sharp and large maximum in the susceptibility, here seen at h=0.7 and then a less pronounced peak near h=1.6. Those peaks indicate transitions from phase I to phase II, low field high magnitude maximum, and from phase II to phase III, high field low magnitude peak.

If one maps those phases on the temperature-magnetic field plane one obtains Fig.5. Here the boxes denote the phase I to II transition, while the stars denote the phase II to III transition, as calculated for nearest neighbors only. The "x" and the "+", respectively, denote the same transition for the nnn calculation. One notes that at low fields the nnn results raise the I to II transition to higher temperatures, while lowering it for fields above 0.75 with respect to the nn results. The II to III transition comes at a lower field for nnn at any particular temperature as long as the temperature is above 0.5.

Phase I is the ordered phase where dipolar interactions dominate. Phase II has the character of a paramagnetic phase, however, one can still detect the results of dipolar interactions. Because of that we will call it the quasiparamagnetic phase. At zero external magnetic field there are no solutions of Eq.(6) in phase II other than $a_i = 0$, however, if a field is applied, the dipoles align making an angle with the field between 3° and 10° with alternate dipoles having a positive and negative angle. Those angles, of course, become smaller as the temperature and field are increased. In phase III the dipoles are fully alligned with the magnetic field. This may be a field induced ferromagnetic phase.

The nnn calculation was repeated with one of the second nearest neighbors to the central hexagon eliminated. The eliminated dipole is indicated in Fig.1 by the small box. Thus of the 18 neighbors of the central hexagon one is missing. One thus introduces a defect in the lattice; we shall call this calculation nnd. The magnetization and susceptibility given by this calculation are shown in Fig.3 and 4 respectively and are denoted by "x". Both the overall magnetization and the susceptibility of this calculation are similar to the nnn results. However, the magnetization of the nnd is generally greater in phase I,the same in phase II, and smaller in phase III as compared to that of nnn. The phase boundaries appear to be unaffected by the defect.

In nnd there is a finite magnetization at zero and low fields. Once the defect is introduced it provides a focus for polarization. Thus at low fields the the defects enhance the magnetization. As the field and temperature are raised, the influence of the defect becomes insignificant and thus the equality between the nnn and nnd results in phase II. In phase III the defect provides a disturbance in the lattice regularity and acts as a cavity in a ferromagnetic system, decreasing the overall magnetization. Thus the lower magnetization in phase III. Figures 6 and 7 show this effect in greater detail for the low field region where both the susceptibility and magnetization are plotted for the nnn, box and nnd, "x", calculations. Fig.6 shows that in nnn the magnetization goes to zero in zero field while it is finite in the nnd case. Fig.7, which shows the susceptibility with 0.3 subtracted from the actual value, indicates that in nnd the susceptibility has a small minimum at low fields, while in nnn it is a monotonically increasing function in the low field region.

Conclusions

The inclusion of boundaries in a system of dipoles confined to rotate in a plane and located on a honeycomb lattice raises the average ground state energy. Moreover, depending on the shape of the boundaries, the average ground state energy depends on the dipole orientation.

The inclusion of second and third nearest neighbors in the interaction alters the phase boundaries of the system. Defects introduce a finite magnetization at low temperature, even at zero field. In low fields, the susceptibility appears to have a minimum with the temperature held constant for calculations including defects, while it is a monotonically increasing function of the field when no defects are included.

The system studied, might be applicable to some two dimensional systems where dipolar interactions play an important role. For one, such systems migh be found in graphite intercalated compounds where a magnetic subetance is the intercalant. The graphite layers thus reduce the interaction between the intercalant layers creating a magnetic two dimensional array within each intercalant layer.

References

1. L.W. McKeehan, Phys.Rev. 43, 1022, (1933)

2. Th. Niemeyer, Physica 57, 291, (1972)

3. P.H.E. Meijer and D.J. O'Keeffe, Phys.Rev. 31, 3786.(1970)

4. B.R.A. Nijboer and F.W. DeWette, Physica 24, 422, (1958)

5. H. Horner, Phys.Rev. 172, 535, (1968)

6. P.M. Levy and D.P. Landau, J.Appl.Phys. 39, 1128, (1968)

7. G.O. Zimmerman, A.K. Ibrahim and F.Y. Wu, submitted for publication

8. C.L. Henley, Preprint

9. D.H. Lee, R.G. Caflisch, J.D. Joannopoulos and F.Y. Wu, Phys.Rev. B29, 2680, (1984)

* Supported by the Air Force Office of Scientific Research Grant AFOSR-82-0286

** Supported by the National Science Foundation Grant DMR-8219254

Figure Captions

Fig.1 The lattice with ground state dipole directions. N denotes neighbors of the main hexagon taken into account in the mean field calculation.

Fig.2 The energy per dipole of the square,"x", and the circular, box, array of dipoles, as a function of the angle of dipole #2.

Fig.3 Magnetization at T=2 as a function of the applied field showing nn, "*", nnn, box, and nnd, "x", results.

Fig.4 The Magnetic susceptibility at T=2 as a function of the applied field with symbols as in Fig.3.

Fig.5 The phase diagram of the system with the phases described in the text. The boxes and the "*" denote the nn calculation while "x" and "+" show the nnn and nnd results.

Fig.6 The low field behavior of the magnetization at T=2. The box denotes the nnn calculation while "x" denotes nnd.

Fig.7 The low field susceptibility at T=2 with 0.3 subtracted from the actual value. Symbols are the same as in Fig.6.

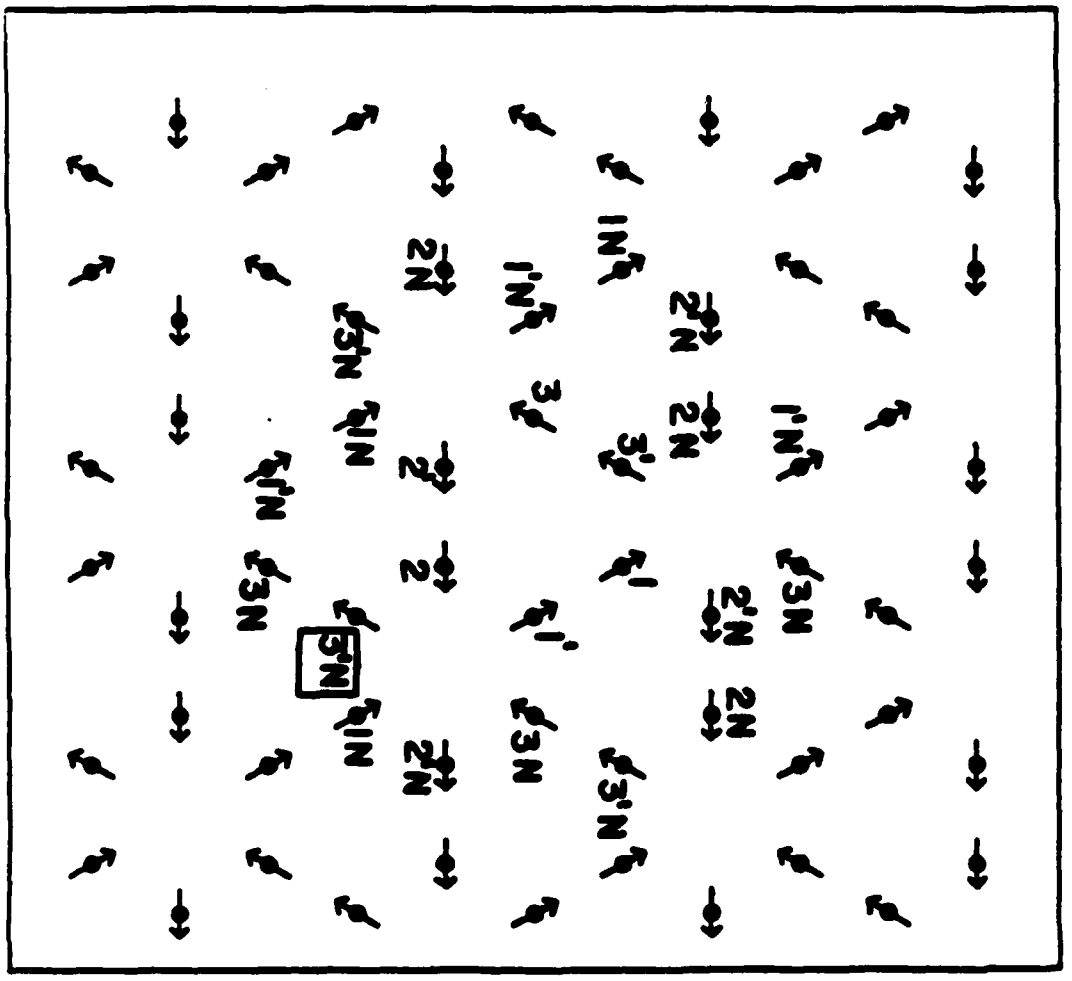

Fig. 1

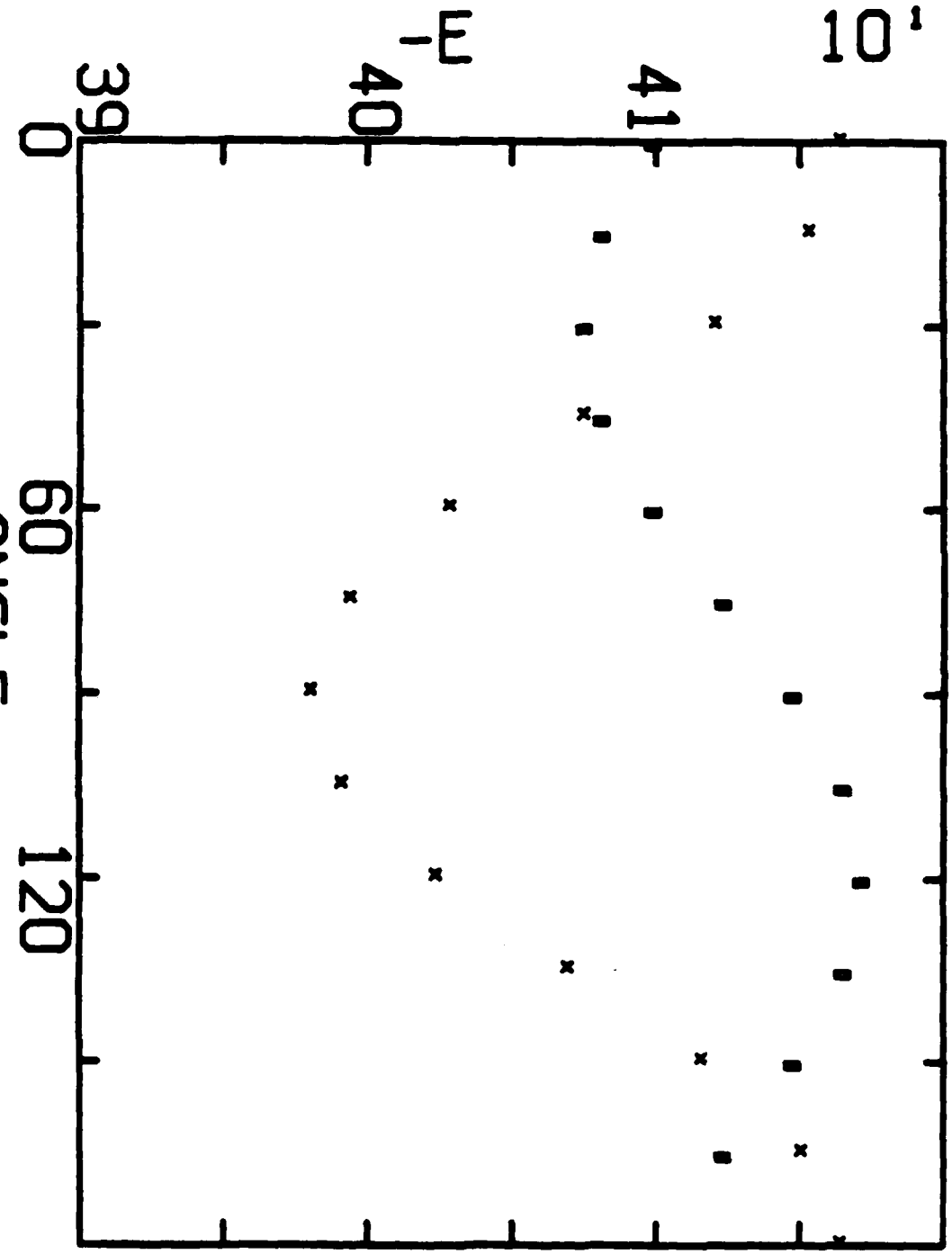

Fig. 2

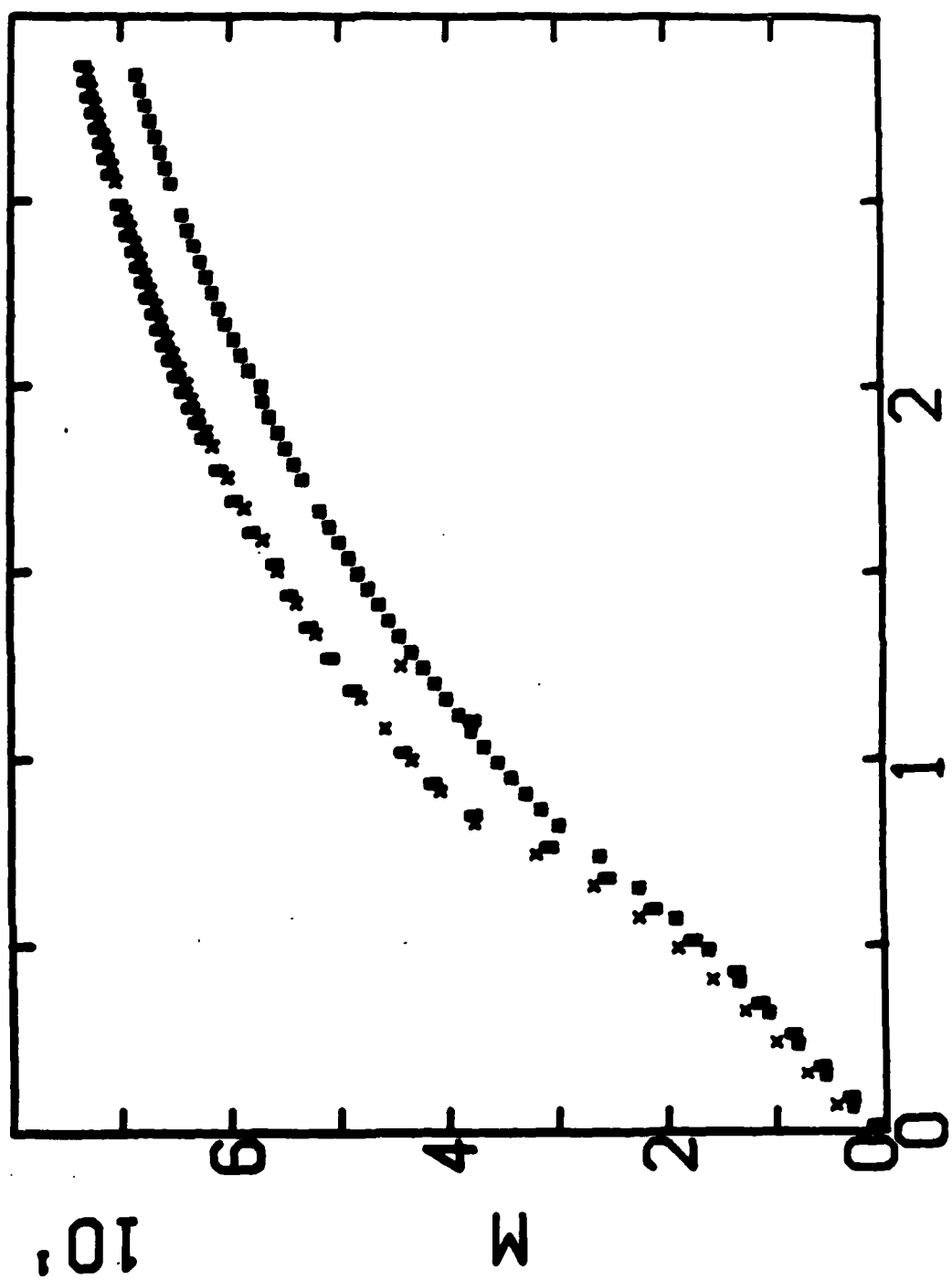

Fig. 2

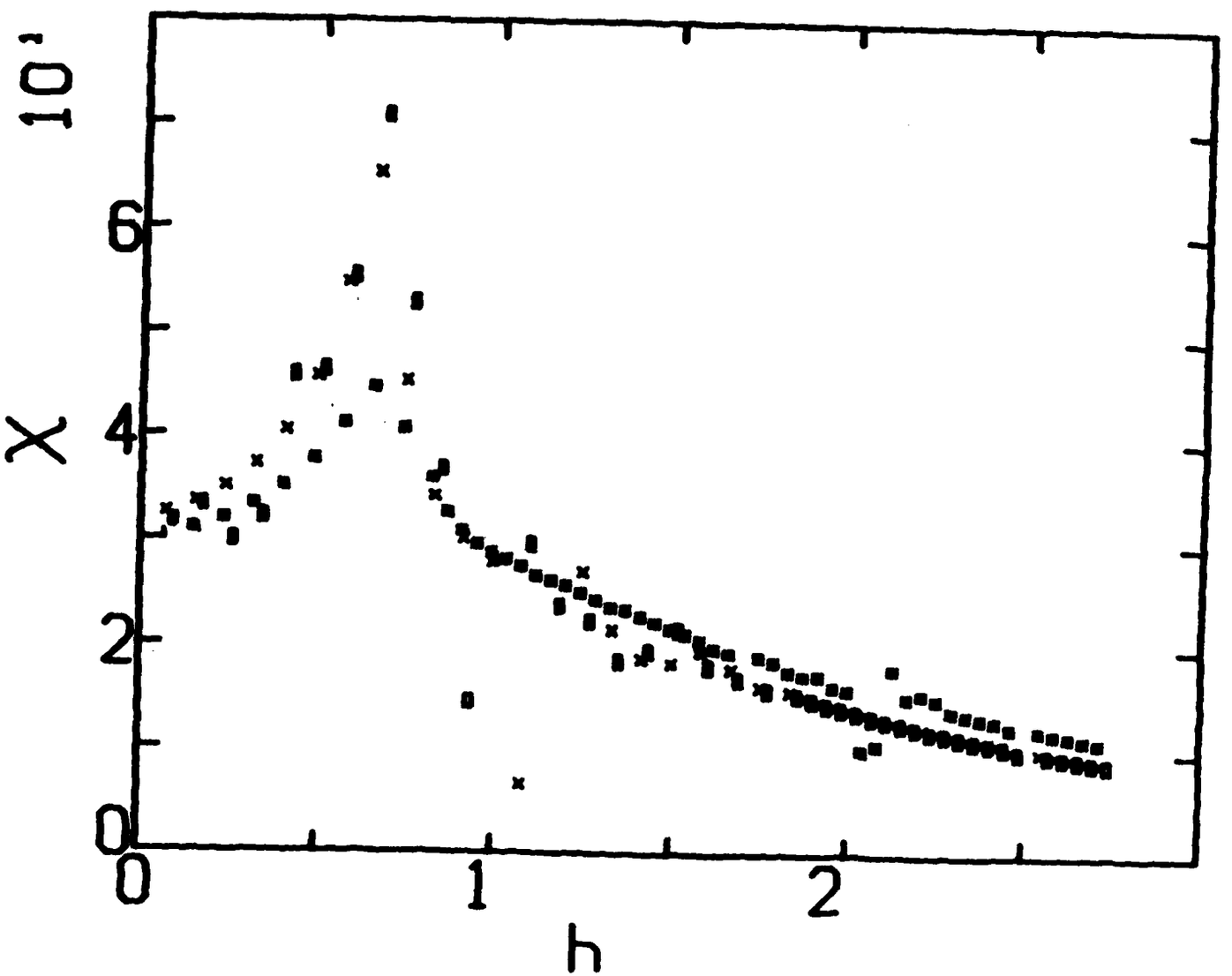

Fig. 4

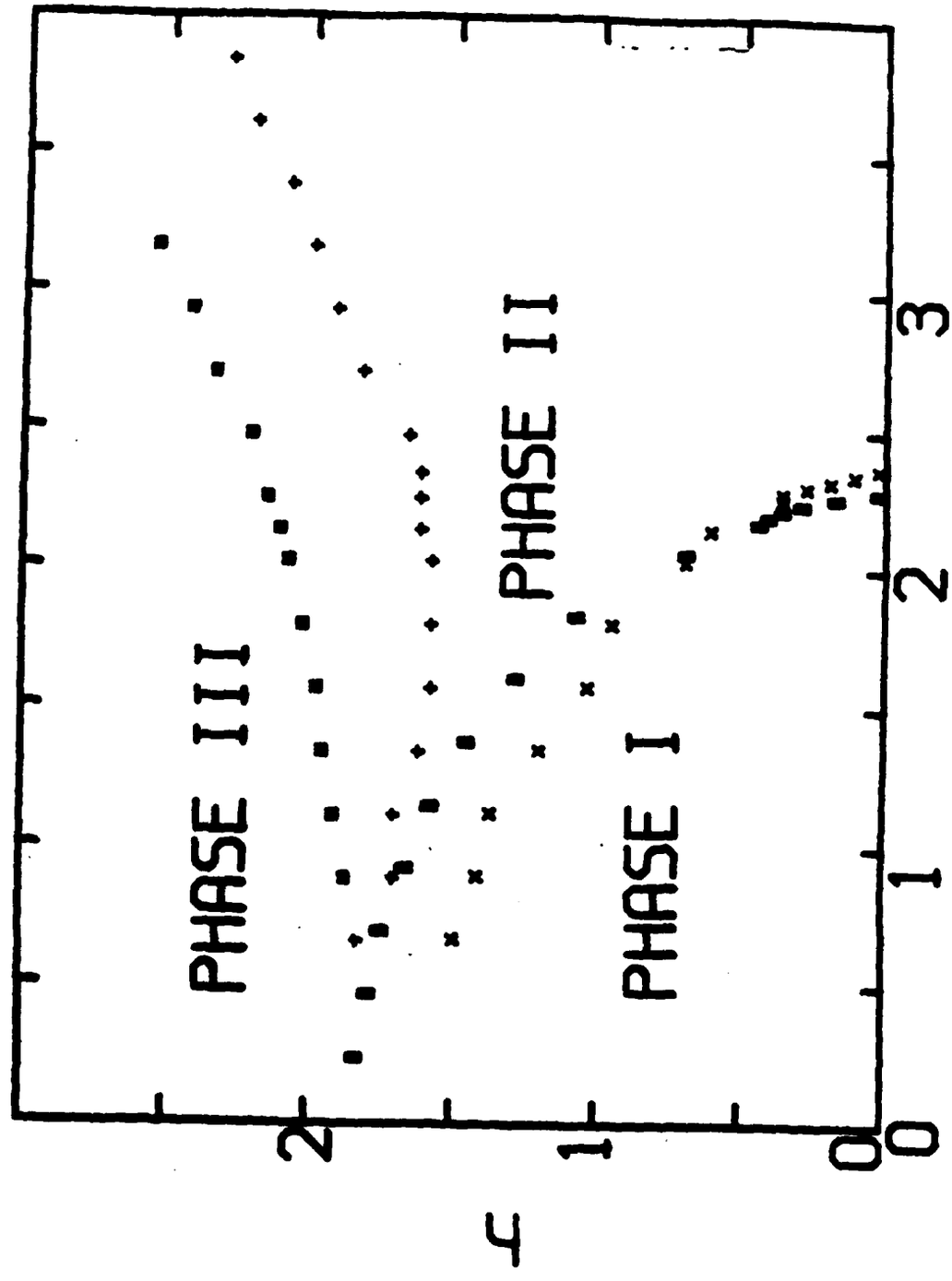

Fig. 5

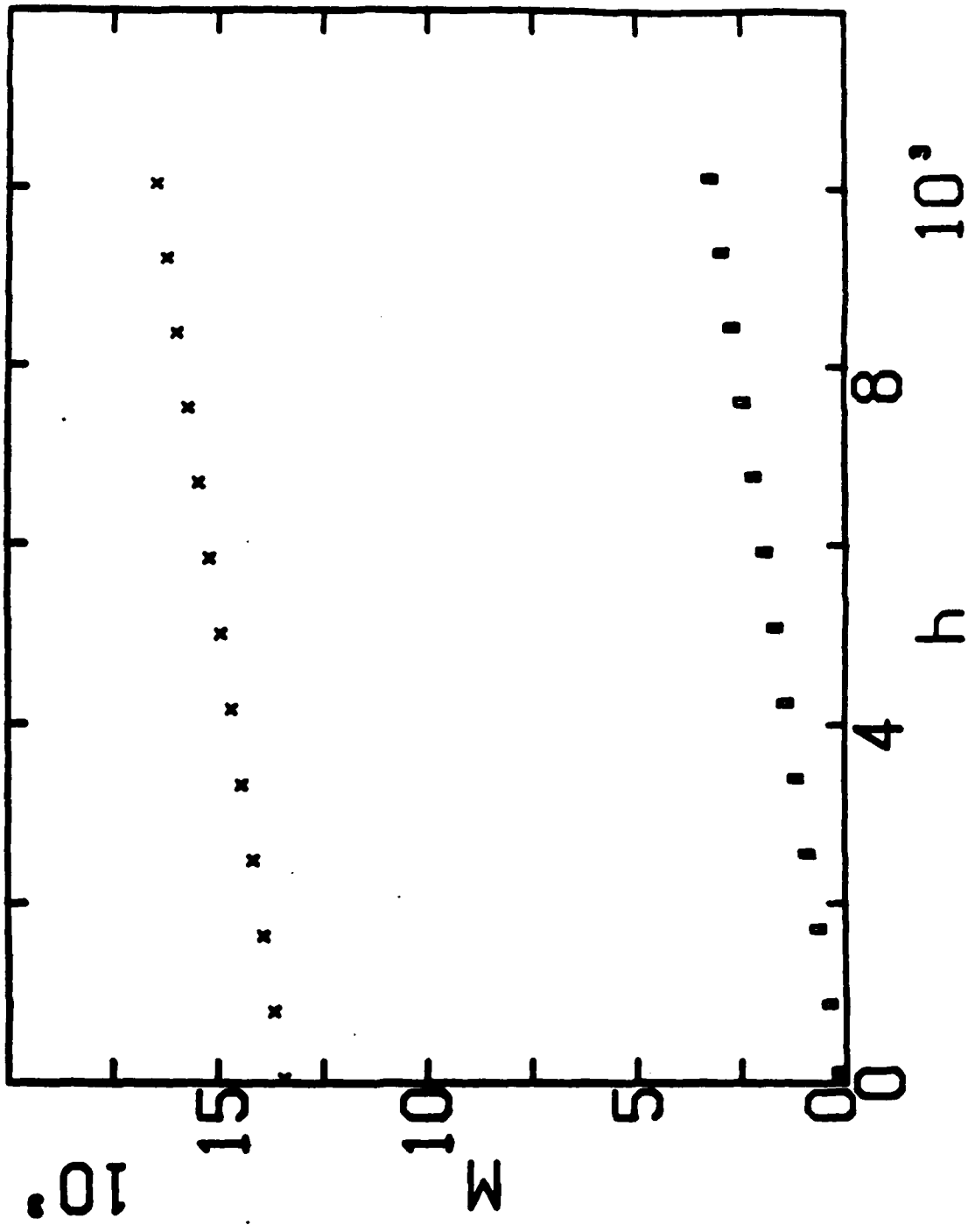
10³
M
15
10
5
0
4
h
8
10³

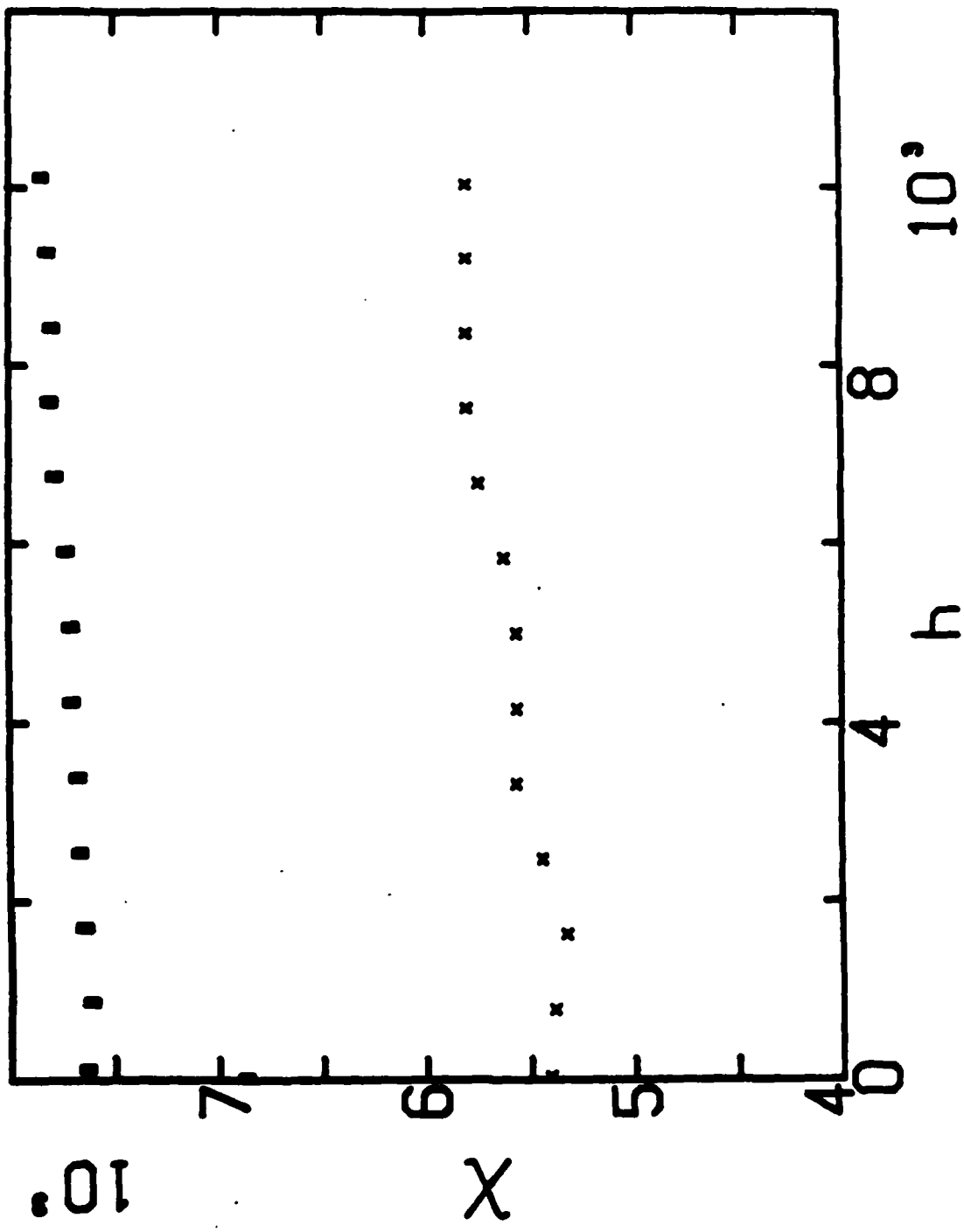

FIG. 7

Self-balancing resistance bridge

Alvaro Kaplan, George O. Zimmerman, and Dean S. Edmonds, Jr.

Department of Physics, Boston University, Boston, Massachusetts 02215

(Received 27 May 1986; accepted for publication 28 July 1986)

An automatically balanced resistance bridge with below-picowatt dissipation in the measured resistance has been developed. The bridge, capable of measuring resistances between 20 Ω and 10 kΩ with an accuracy of 5%, was specifically designed to allow resistance measurements to be made at low temperatures without introducing an appreciable heat source to the cryostat. It consists of a Wheatstone bridge having a photoresistor as one of its arms. The feedback balance is accomplished by means of light-emitting diodes which control the photoresistor. A novel feedback principle used in the bridge is described.

In measurements of resistance of materials at temperatures below the boiling point of He^4 (below 4.2 K), it is important that the power dissipated in the material whose resistance is being measured be small. This is necessitated by the fact that at those low temperatures, the specific heats of substances become small, and the thermal contact between substances and helium is limited by the various thermal "resistances," the one most considered being the Kapitza resistance.[1] Thus if too much power is dissipated in the resistive element during the measurement process, the temperature of the substance whose resistance is being measured may bear little relation to the temperature of its surroundings. This point is crucial if the substance in question is serving as a thermometer.

Carbon resistors, carbon glass resistors, phosphor bronze resistors, and other resistive elements have had a venerable tradition as secondary thermometers in low-temperature physics,[2] and are even now being used in ultralow-temperature applications. We have developed a self-contained, self-balancing resistance bridge whose power dissipation is less than 1 pW. It is basically a Wheatstone bridge with a lightsensitive resistance as one arm. This resistance is packaged with seven LED's which shine on it and are driven by the control circuit output so that at balance the unknown resistance R_3 is given as a function of the control circuit output voltage V_0 by a relation of the form

$$V_0 = A + B(R_3)^{-1/2}. \tag{1}$$

Figure 1 is a graph of the actual results obtained with our setup and allows values for the constants A and B to be determined. Individual operating conditions will affect these values, but the form of Eq. (1) should hold in any case

Rev. Sci. Instrum. 57 (11), November 1986 0034-6748/86/11[illegible]-03$01.30

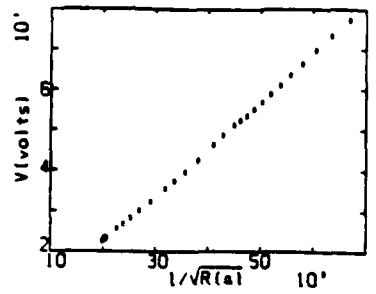

FIG. 1. Output voltage V_0 plotted against sense resistance R_1. A linear plot is obtained by plotting V_0 against $R_1^{-1/2}$.

The complete circuit of the self-balancing bridge is given in Fig. 2. The ac excitation for the bridge is a 340-Hz sine wave obtained from the type 8038 oscillator chip.[3] The frequency of this oscillator is given by

$$RC_2 f \approx 0.309, \qquad (2)$$

where $R = R_7 = R_8$ is in ohms, C_2 is in farads, and f is in hertz. R_7 and R_8 are made equal when a symmetrical square wave is desired, and Eq. (2) applies when pins 7 and 8 of the 8038 are connected together. In the circuit of Fig. 2 a frequency control voltage is introduced at pin 8 to allow fine tuning the 8038 to the exact frequency of the tuned error-signal amplifier. The values shown give a 340-Hz output signal with R_{10} set near midrange.

The output signal from the bridge, when not balanced, is amplified by a narrow-band twin-T push–pull amplifier built for us by the White Instrument Company under model number 4529.[4] The amplified 340-Hz sine wave is then detected by a full-wave synchronous rectifier, a phase-sensitive detector using a type 4066 quadruple gate chip, whose output is further amplified but not filtered, so that we have at this point a rectified sine wave, either positive-going or negative-going depending on which way the bridge is out of balance. The distinguishing feature of our arrangement is that this signal is not used directly to control the balancing of the bridge, but is instead applied to an operational amplifier having no feedback and, therefore, functioning as a flip–flop with two stable states. When the signal is positive going, the flip-flop spends most of its time in the state giving full positive output, and capacitor C_1 charges through resistor R_1 accordingly. The resulting dc voltage is amplified by the μpc2002 power amplifier which drives the LED's already mentioned and provides output voltage V_0 across the current-sensing resistor R_2. When the amplified error signal is negative going, C_1 discharges through R_1 but, at balance, flip–flop A_3 flips back and forth randomly, spending, on the average, as much time in one state as in the other, so that the charge on C_1 remains constant. Thus the correct LED current is maintained with zero error signal, giving the system the characteristics of a first-order servomechanism rather than a simple regulator. Zener diode CR_1 and offset control

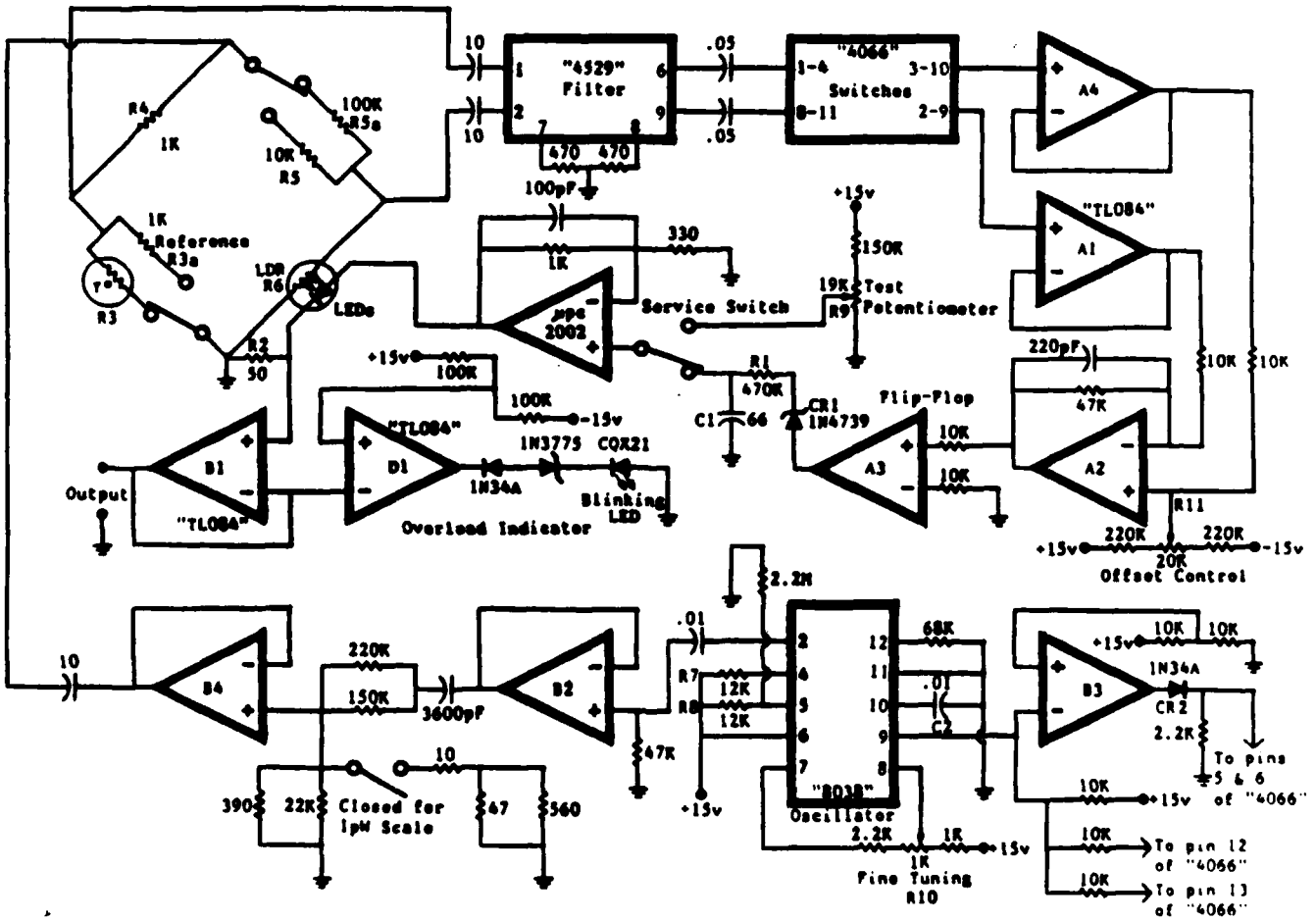

FIG. 2. Circuit of the self-balancing bridge.

R_{11} serve to asymmetrize the system so that the output of the μpc2002 will not go negative.

The system comes to balance in a reasonable time after a change occurs in R_3 and has been used to make temperature measurements to 1 mK in the helium temperature range (1–4 K). The system thus provides an inexpensive, automated, accurate alternative to the traditional manually balanced Wheatstone bridge.

This work was supported in part by Air Force of Scientific Research under Grant No. AFOSR 82-0286.

[1] O. V. Lounasmaa, *Experimental Principles and Methods Below 1 °K* (Academic, New York, 1974), p. 263.
[2] G. K. White, *Experimental Techniques in Low Temperature Physics* (Clarendon, Oxford, 1968).
[3] See *Semiconductor Reference Guide*, The Radio Shack, a division of Tandy Corporation, Fort Worth, TX, 1983.
[4] White Instruments, a division of C. van R., Inc., Austin, TX.

END

7-87

DTIC